Dissection of the molecular function of the zinc finger transcription factor Sp8 during development of the murine forebrain and olfactory system

Von der Fakultät für Lebenswissenschaften der
Technischen Universität Carolo-Wilhelmina zu Braunschweig

zur Erlangung des Grades eines Doktors der Naturwissenschaften
(Dr. rer. nat.)

genehmigte
D i s s e r t a t i o n

von Andreas Bernd Zembrzycki
aus Gelsenkirchen

1. Referent:	Prof. Dr. Hans-Henning Arnold
2. Referent:	Prof. Dr. Ahmed Mansouri
Eingereicht am:	18. 04. 2007
Mündliche Prüfung (Disputation):	04. 07. 2007
Druckjahr:	2007

Vorveröffentlichungen der Dissertation

Teile aus dieser Arbeit wurden mit Genehmigung des Fachbereichs für Biowissenschaften und Psychologie, vertreten durch den Mentor der Arbeit, in folgendem Beitrag vorab veröffentlicht:

Publikation:

Zembrzycki, A., Griesel, G., Stoykova, A., & Mansouri, A. Genetic interplay between the transcription factors Sp8 and Emx2 in the patterning of the telencephalon. *Neural Development* 2007, **2**:8.

Diese Arbeit wurde am Max Planck Institut für Biophysikalische Chemie
– Karl-Friedrich-Bonhoeffer-Institut –
in Göttingen
in der Abteilung Molekulare Zellbiologie (Direktor: Prof. Dr. Peter Gruss),
Arbeitsgruppe Molekulare Zelldifferenzierung (Prof. Dr. Ahmed Mansouri)
durchgeführt.

TABLE OF CONTENTS

1 INTRODUCTION

"…die Embryonalentwicklung der
Maus ist seltsam und
nicht leicht zu verstehen…"

Müller Hassel;
Entwicklungsbiologie;
Seite 150.

The evolution and the development of the forebrain is linked to the improvements of cognitive functions of higher vertebrate species (reviewed by Molnar et al., 2006). Therefore, the forebrain (and especially the cerebral cortex) is the part of the central nervous system (CNS), which has developed most excessively during the evolution of mammals. The developing forebrain of the mouse consists of two major compartments, pallium and subpallium. An additional third sub compartment, which is generated in part by neurons originating within the ventral and dorsal telencephalon, is the olfactory bulb (OB) (reviewed by Mallamaci and Stoykova 2006, Fig. 1). Developmental biology serves as a potent tool for studying the molecular mechanisms controlling CNS development and therefore provides new insights to understand a variety of human developmental disorders like Lissencephaly, Childhood Epilepsy or Microcephaly (reviewed by Molnar et al., 2006).

1.1.1 The basic organization of the embryonic mouse forebrain

The subpallium reflects the ventral part of the murine forebrain and consists of the medial and lateral ganglionic eminences (MGE, LGE), also called the basal ganglia (BG) and medially the septum (SE). During embryonic development, the basal ganglia are the main progenitor source of inhibitory (GABAergic) interneurons, which will later migrate tangentially into the cerebral cortex. Postnatally, the basal ganglia will form the striatum, a major target area in which a variety of subtelencephalic afferents will terminate, including some dopaminergic neurons of the midbrain. Septal neurons control distinct aspects of hormone homeostasis. Additionally, the septum is necessary for the proper formation of the corpus callosum (CC, see below) (Fig. 1, reviewed by Molnar et al., 2006).

A prominent compartment of the mouse telencephalon is its dorsal part, which will form the cerebral cortex. It hosts and enables all sophisticated cognitive functions of higher, evolutionary young species including man and is therefore also called neocortex. The cortex is a heterogeneous structure, comprising several distinct cell types.

The predominant neurotransmitter phenotype of projection neurons, born within the pallium, is glutamatergic. The development of cortical layers proceeds in an inside-first outside-last pattern, meaning that cells, born early during development, will populate deep cortical laminae. Conversely, later born neurons will migrate through these deep

cortical layers and settle within layers, superficial to those, born earlier. Therefore, the mature dorso-ventral (D/V) organization of the cortex can be described as a six-layered column of differentially fated and functionally distinct neurons (Fig. 1, reviewed by Guillemot et al., 2006, Fig. 2).

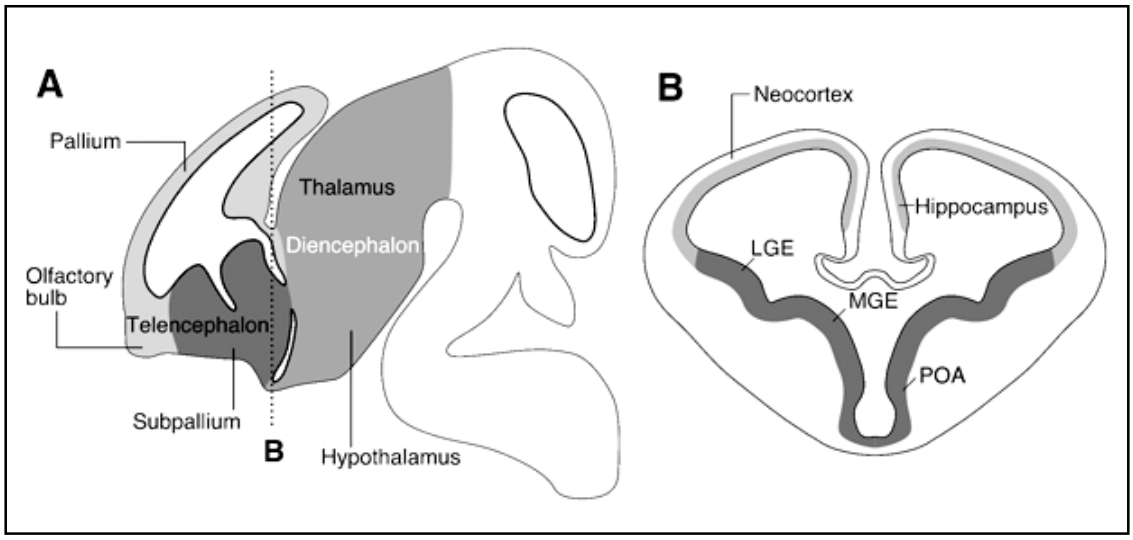

Figure 1: Organization of the murine telencephalon. Schematic drawing of major subdivisions of the embryonic mouse telencephalon. (A): Sagittal view of the telencephalon. Dashed line in (A) indicates the coronal plane of section in (B). LGE: Lateral Ganglionic Eminence, MGE: Medial Ganglionic Eminence, POA: Preoptic Area. (adapted from Marin, 2003)

1.1.2 Key events during embryonic development of the murine forebrain

To achieve a sophisticated degree of cellular and thereby functional heterogeneity, numerous events have to take place in a highly controlled fashion, starting during development. All these processes are under the control of gene activity, which will be in the focus later on.

The first step during murine cortical development is the expansion of an early progenitor pool. In parallel, few differentiated neurons arise form the preplate (PPL), around stage E10 to E11.5. Preplate cells are defined to be the sum of the first post mitotic progeny of pallial progenitors. The preplate itself contains mainly two different cell types, Cajal-Retzius cells (CR cells) and subplate cells. Neurons born after E11.5 will form the cortical plate (CP) and do not have a “preplate fate”. By migrating radially and positioning within the preplate (between CR cells and subplate), they will

progressively separate CR cells from subplate cells. During subsequent cortical maturation, CR cells lie on top of the cortical plate, generating the marginal zone (MZ) or layer I, the apical edge of the cortex. Subplate cells lie beneath the cortical plate, outside the six-layered cortex architecture (Fig. 2). MZ and subplate seem to function mostly during embryonic and early postnatal stages of mammalian development. After cortical layering and connectivity are achieved, most CR cells will be eliminated from layer I by apoptosis, leaving a widely acellular mantle zone. The subplate is a transient structure as well. After birth, the subplate disappears completely. While some subplate neurons will integrate into cortical layer VI b, most of them will be eliminated through programmed cell death (reviewed by Guillemot et al., 2006).

Early born neurons (including the preplate) are the progeny of neuronal stem cells within a proliferating compartment, contacting the lateral ventricle. Radial glia cells in the so-called ventricular zone (VZ) generate postmitotic deep layer neurons of layer V and VI and additionally give rise to proliferative active intermediate progenitors. These late progenitors will detach from the ventricle and migrate radially upwards to settle apically, on top of the VZ. These precursors will build up the second neurogenic region of the cortex, the subventricular zone (SVZ). The descendants of SVZ progenitors will exclusively form upper layer cortex neurons, populating layer II, III and IV (Noctor et al., 2004, reviewed by Mallamaci and Stoykova, 2006).

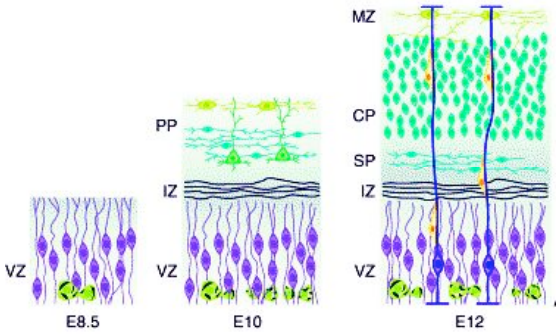

Figure 2: Corticogenesis. At E8.5, the VZ mostly contains neuronal precursors. The first postmitotic neurons generate the PPL at E10. Further the PPL begins to split into the MZ and SP at E12. Between those compartments, the CP arises. Neurons use glia cell processes as a substrate for their migration. VZ: Ventricular Zone, IZ: Intermediate Zone, PPL: Preplate, CP: Cortical Plate, MZ: Marginal Zone. (adapted from Campbell and Gotz, 2002)

The olfactory bulb is a structural forebrain unit, synergistically composed of pallial and subpallial cell types, namely subpallial/inhibitory interneurons and pallial/excitatory projection neurons. Its development starts morphologically with a budding at the anterior tip of the ventral telencephalon around E12. The initial appearance of the olfactory bulb-anlage is triggered by the invasion of olfactory sensory neuron (OSN) processes from the olfactory epithelium of the nose. This event seems to influence cell cycle parameters in the

target region. During OB genesis most of the OB interneurons are produced within the lateral embryonic LGE, called the dorsal LGE (dLGE). This region retains its neurogenic potency throughout life, bearing interesting aspects for stem cell research.

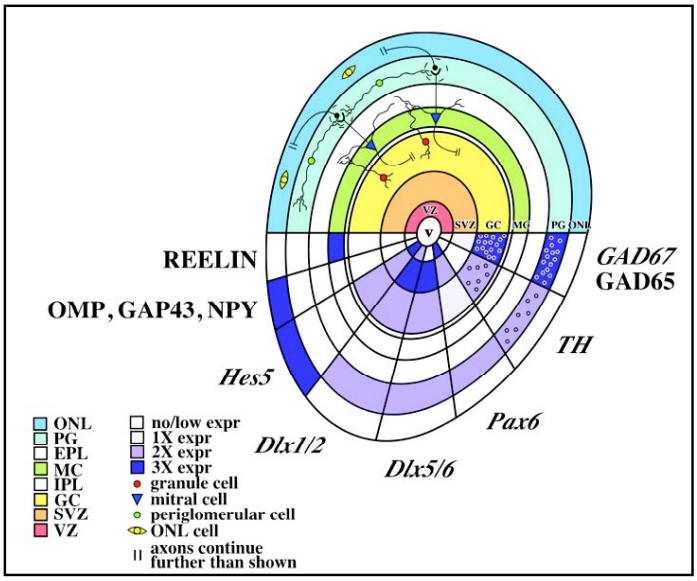

Figure 3: Laminar organization of the OB. The mature OB consists of multiple layers. Characteristic marker genes and neuronal connections are indicated. ONL: Outer Neuronal Layer, PG: Periglomerular Layer, EPL: External Plexiform Layer, MC: Mitral Cell Layer, IPL: Internal Plexiform Layer, GC: Glomerular Layer, SVZ: Subventricular Zone. (adapted from Long et al., 2003)

In rodents undifferentiated and still cycling olfactory bulb neuroblasts find their way to the OB on a stereotypic route, through chain migration within the so-called rostral migratory stream (RMS). This area lies between the basal ganglia and the lateral pallium. The RMS terminates in the ventricular zone of the olfactory bulb. The fasciculation of the RMS relies on differences in adhesive cell surface properties of differentially fated cells within the lateral pallial-subpallial boundary (PSB). These differences enable proper sorting and migration of neuroblasts towards the pallium or olfactory bulb. This area is also known as the radial glia fascicle (RGF, Fig. 4). After neuroblasts have reached the olfactory bulb, the mature structural organization is established through terminal differentiation and radial migration of precursor cells. Finally, these events establish laminar architecture of the OB, creating defined columns and local networks of functionally related neuronal subtypes (Fig. 3, reviewed by Lopez-Mascaraque and Castro, 2002).

One common feature during genesis and developmental maturation of the brain is the migration of neurons or neuroblasts from their place of birth to their final destination. Apart from chain migration, two principally different migration mechanisms occur in the developing embryonic forebrain: Tangential migration and radial migration. The mixing of cell types via migration mechanisms massively produces cellular heterogeneity and the diversification of neuronal functions.

Tangential migration is the predominant mode of movement of subpallial interneurons, on their way into the cortex. The detailed cellular mechanisms, underlying tangential migration locomotion, are still largely obscure. Radial migration within the dorsal cortex was shown to rely on two crucial and interconnected pathways: The Reelin signaling pathway and radial glia coupled translocation of neurons (reviewed by Marin and Rubenstein, 2003). CR cells in the MZ of the embryonic cortex secret the glycoprotein Reelin. Postmitotic pallial neurons are able to bind Reelin with extracellular receptors. The intracellular response upon Reelin stimulation is phosphorylation of the Dab1 protein, which triggers an intracellular response and proper positioning of neurons into laminae, corresponding to their time of birth (reviewed by Tissir and Goffinet, 2003).

Radial glia cells (RGC) are not only the main population of pallial progenitors. Additionally, they enable correct migration of their progeny into the correct position of the cortical plate. The cell bodies of RGC are located in the proliferative VZ. They extend processes radially, spanning the whole diameter of the developing cortex up to the apical surface. It is now a widely accepted model that newly born neurons attach to the processes of the mother RGC or neighboring glia process, using them as a substrate for radial migration. Once they have reached their final laminar position, they detach from the glia processes and begin to integrate into the developing cortical circuitry. Radial migration of postmitotic projection neurons generates a clonal organization of the cortical neuroepithelium and contributes to the manifestation of regional differences in gene expression of topologically different positions along the anterior-posterior axis. Tangential migration does not seem to occur (reviewed by Campbell and Gotz, 2002).

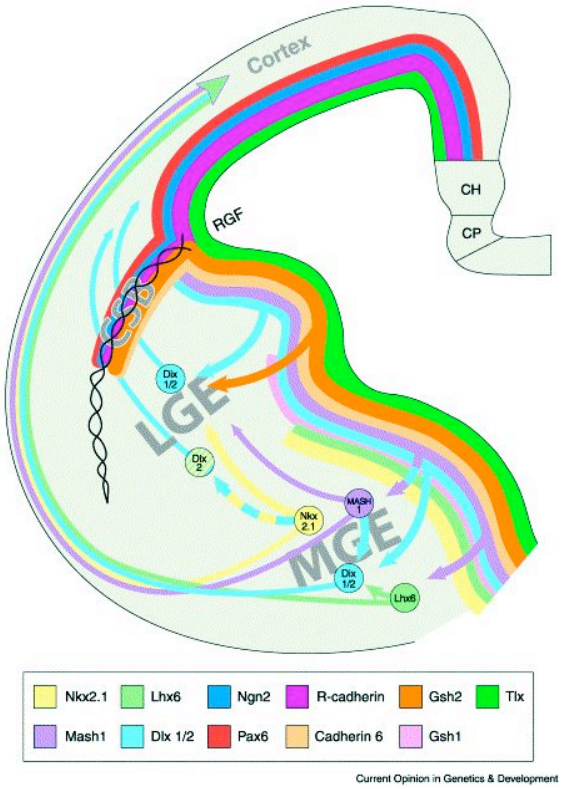

Figure 4: D/V patterning and tangential migration in the forebrain. Image shows the expression domains of important marker genes and the migratory routes of ventral neuronal populations. RGF: Radial Glia Fascicle, CSB: Corticostriatal Boundary (or PSB). CP: Choroid Plexus, CH Cortical Hem. (adapted from Zaki et al., 2003)

Migration defects of neurons highlight a variety of diseases. The Reeler mouse is the most prominent model for studies of corticogenesis, under the condition of disrupted Reelin signaling. Those mice develop a cerebral cortex, in which the laminar organization is mainly inverted, revealing the crucial role of Reelin signaling for the development of cortical layers. Mutations in genes, affecting RGC function or morphology, disturb radial migration in a similar way. Small-eye (Sey) mice, which suffer from a natural mutation of the Pax6 gene, became an important model for the analysis of disturbed radial glia functioning. Mutant animals are characterized by severe abnormalities of radial glia specification, survival and morphology. In Sey mutants, postmitotic neurons largely fail to migrate into the CP correctly. This defect produces neuronal aggregates in certain compartments of the developing cortex (reviewed by Campbell and Gotz, 2002, Tissir and Goffinet, 2003, Mallamaci and Stoykova, 2006).

1.2 Molecular events during murine forebrain development

The earliest appearance of the forebrain is linked to the activation of the genes Six3, Otx1/2 and Foxg1 at the anterior tip of the developing neural tube. Those factors establish early molecular forebrain fate and separate the rostral most part of the CNS from more posterior brain regions (reviewed by Mallamaci and Stoykova, 2006).

1.2.1 Early establishment of A/P and D/V polarization of the forebrain

Once early forebrain fate is established, additional factors begin to be expressed in distinct regions of the forebrain vesicle.

Shh, Foxg1 and Nkx2.1 are expressed in the basal telencephalon and act as fate-determinants of the future subpallium (Chiang et al., 1996, Dou et al., 1999, Sussel et al., 1999 reviewed by Mallamaci and Stoykova, 2006). Dorsal activity of Emx2 and Pax6 will set up pallial fate (Muzio et al., 2002). The anterior-posterior (A/P) axis of the forebrain is prepatterned by the activity of two crucial signaling centers. At the rostral midline of the forebrain vesicle, the anterior neural ridge (ANR) or commissural plate expresses secreted factors of the fibroblast growth factor family (FGF). Fgf8 has multiple roles during early and late genesis of the developing embryo, including the forebrain (reviewed by Rubenstein et al., 1998, Fig. 5). At early stages, Fgf8 is a crucial determinant of rostroventral cell fates. A second signaling center, the cortical hem, is much more caudally localized and expresses factors that are members of the WNT- and BMP families. They antagonize rostral FGF signaling activity and establish caudodorsal cell identity as well as the roof plate of the forebrain anlage (Fig. 5, Sur and Rubenstein, 2005, reviewed by Mallamaci and Stoykova, 2006).

This genetic network establishes the major subdivisions of the forebrain along the dorso-ventral (D/V) and A/P axis. By subsequent activation of numerous other (mostly gradually-expressed) genes, the prepatterned forebrain is specified into further subtle subdivisions and compartmentations towards very distinct functional areas.

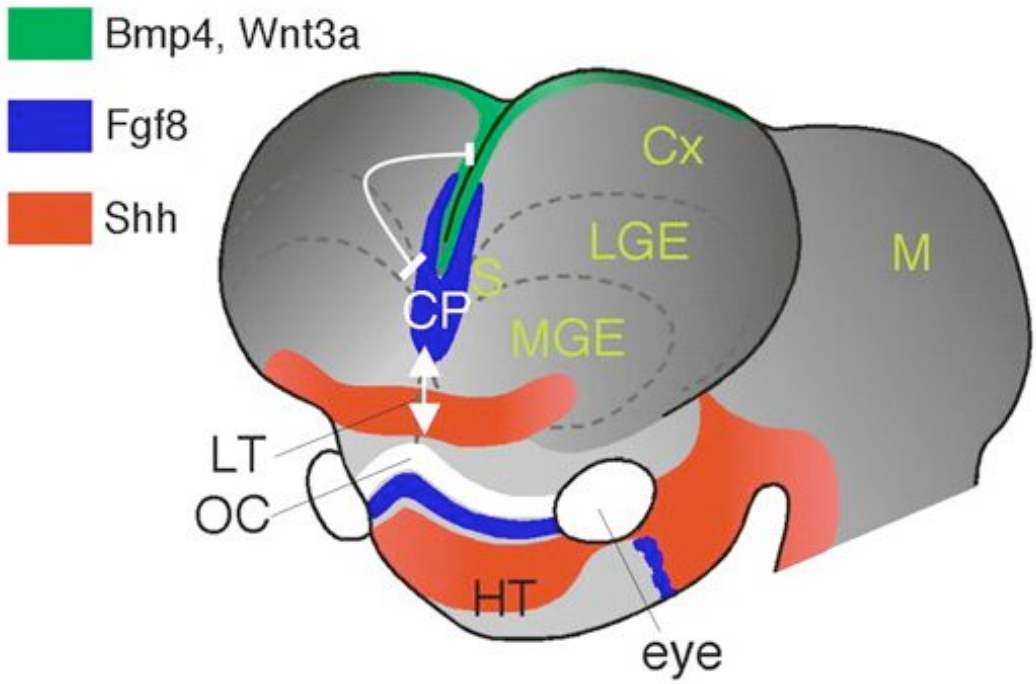

Figure 5: Important secreted molecules in the early telencephalon. Secreted molecules are released from the signaling centers of the early forebrain. Predicted interactions among these molecules and transcription factors are indicated below. CP: Commissural Plate, CX: Cortex, M: Midbrain, LT: Lamina Terminalis, OC: Optic Chiasm, HT: Hypothalamus. (adapted from Storm et al., 2006)

1.2.2 D/V patterning at the pallial-subpallial boundary

Boundaries of gene activity (e.g. dorsal/ventral) are extremely important for the subdivision of evolving brain areas and called secondary organizers or secondary signaling centers. One of those important expression interfaces is located at the lateral edge of the murine forebrain. There, typically dorsal gene activity of Pax6 and Ngn2 rapidly switches towards typical ventral gene activity of Gsh2, Mash1 and Dlx1. This fundamental change in the expression characteristics of progenitor cells occurs in a distance of two to three cell diameters. This region is termed pallial-subpallial boundary (PSB). The PSB is the prospective boundary of the forebrain, where dorsally the future cortex will develop and ventrally the basal ganglia will arise (Fig. 4, reviewed by Mallamaci and Stoykova, 2006).

After the instructive ventralizing activity of Shh (Chiang et al., 1996) and Foxg1 (Martynoga et al., 2005) is established, the basal parts of the telencephalon achieve further subdivisions through synergistic activity of Gsh2, Gsh1 and Nkx2.1. Gsh2 is expressed in a lateral/high to medial/low gradient from the PSB up to the ventral midline. Pax6- and Gsh2 activity exerts cross repression towards each other and

therefore contributes to the correct positioning of the PSB expression interface (Torreson et al., 2000). Gsh1 is strongly expressed within the medial part of the ventral telencephalon. The Gsh1+ domain overlaps with gene activity of Nkx2.1 (Corbin et al., 2003). This factor is functionally the most important fate determinant of the medial ganglionic eminence (MGE) territory, the medial component of the basal ganglia and the origin of the majority of GABAergic interneurons (Sussel et al., 1999). The neuroepithelial area, laterally from Nkx2.1+ cells, expresses high levels of Gsh2 and represents the territory of the lateral ganglionic eminence (LGE), the future striatum (Torreson et al., 2000, Corbin et al., 2003). Other factors, like genes of the Distalles (Dlx1-5) family or the bHLH transcription factors (Eisenstat et al., 1999) Mash1 (Casarosa et al., 1999) and Arx (Yoshihara et al., 2005) have a non-graded expression domain throughout the ventral telencephalon and do not primarily account to the patterning of the brain, but have fundamental functions in cell type generation, specification, neurogenesis and migration (Fig. 4, reviewed by Panganiban and Rubenstein, 2002, Guillemot et al., 2006, Friocourt et al., 2006).

1.2.3 Cortical patterning along the A/P axis

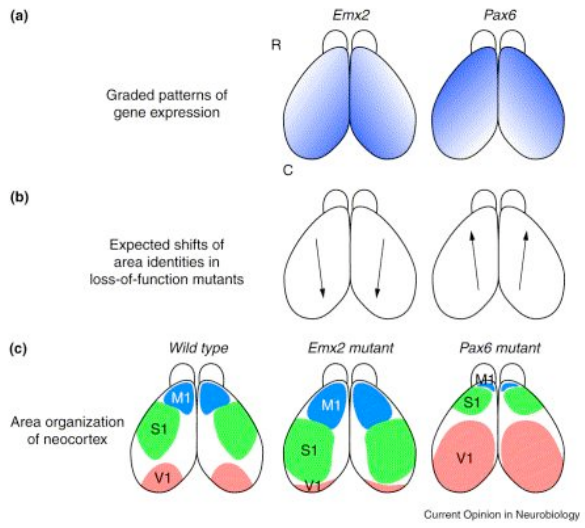

Figure 6: Graded expression of transcription factors. (a): Opposing gradients of Pax6 and Emx2 in cortical progenitors. Expected (b) and the occurring shift of the cortical area identity in Pax6KO and Emx2KO cortices (c). M1: Motor Cortex, S1: Somatosensory Cortex, V1: Visual Cortex. (adapted from O'Leary and Nakagawa, 2002)

As already mentioned briefly, proper positioning of the PSB is crucial for D/V patterning of the telencephalon. The A/P patterning of the pallium (future cortex) is greatly established through the opposing activity of two gradually expressed transcription factors Emx2 and Pax6 (Muzio et al., 2002a). The characteristic gradient of Pax6 is high in the rostrolateral pallium and low in ventromedial parts. Conversely, Emx2 is highly expressed in medial parts of the caudal forebrain and downregulated rostrolaterally.

It is accepted now that Emx2 and Pax6 mutually influence their normal graded expression characteristics in neuronal progenitors of the forebrain (Muzio et al., 2002b). Therefore, the expression of Emx2 in Pax6KO mice and vice versa the expression of Pax6 in Emx2KO mice appears upregulated (reviewed by O'Leary and Nakagawa, 2002). As a consequence of the changed gene activity in progenitors, caudomedial areas are enlarged or will shift rostrally in Pax6KO mice. Without functional Emx2 protein, rostral cortical areas will enlarge to the expense of caudomedial ones (Bishop et al., 2000, Muzio et al., 2002b, Fig. 6). These fundamental findings (achieved by analyzing these opposing expression gradients and functions of Emx2 and Pax6) led to an initial understanding, about how primary cortical motor-, somatosensory- and visual areas will be established on the genetic level. However, in Pax6 mutants, area identity does not shift at all, because distinct projections from thalamic nuclei do not show targeting defects. Emx2, on the other hand, in deed has a fundamental role for the establishment of functional cortical area identity. Both, gain and loss of function approaches could highlight that Emx2 is able to alter the identity and size of the somatosensory and visual areas, including the mistargeting of thalamic axons in a dose-dependant manner (Fig. 6, Bishop et al., 2002, reviewed by O'Leary and Nakagawa, 2002, Sur and Rubenstein, 2005).

However, the establishment of functional cortical areas is currently not fully understood. Two different models are highly debated. One model favors the genesis of cortical areas as a consequence of early genetic prepatterning of the cortical primordium along the A/P axis. This hypothesis links the activity of regionally enriched gene activity to the subdivision of the cortex into different areas/identities (protomap model). The second model underlines that the input from thalamic axons establishes area

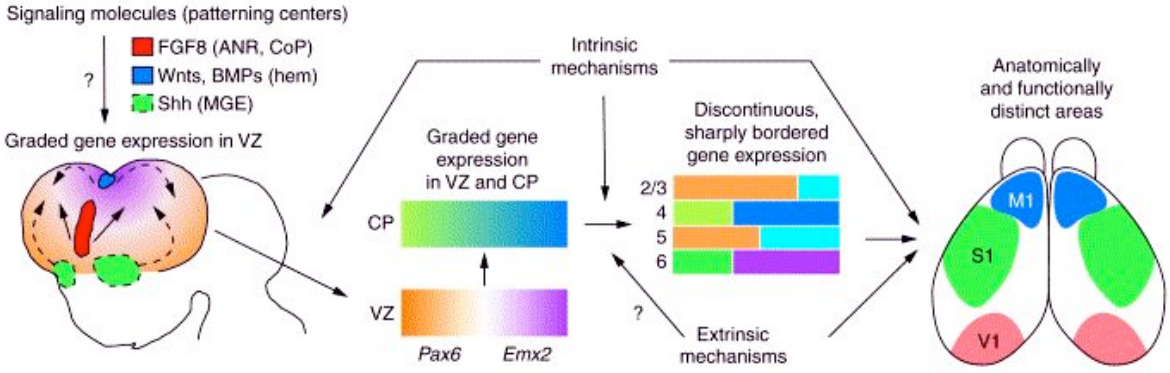

Figure 7: Extrinsic and Intrinsic A/P patterning of the cortex. The early patterning by secreted molecules induces the graded expression of transcription factors in the VZ. Further, the induction of graded and demarcating gene activity in the CP establishes different cortical areas genetically. The extrinsic invasion of thalamic afferents into the cortex establishes the area-specific connectivity and the functioning of the different areas. (adapted from O'Leary and Nakagawa, 2002).

identity. In this model, thalamic input dictates areal commitment to the cortical primordium, like writing on a clean table (protocortex model). Both models are supported by experimental data (Fig. 7, reviewed by O'Leary and Nakagawa, 2002, Sur and Rubenstein, 2005, Mallamaci and Stoykova, 2006). Therefore, further studies are needed to fully reconcile both mechanisms.

1.2.4 Major M/L subdivisions within the dorsal pallium

The medial to lateral (M/L) axis of the dorsal telencephalon is established by the activity of a variety of factors. The medial most component of the dorsal pallium is the non-neuronal choroid plexus, determined by expression of BMPs and exclusion of WNT activity (reviewed by Mallamaci and Stoykova, 2006).

Adjacent to the choroid plexus lies the cortical hem, an important signaling center, confined by WNT- and BMP expression. Proper signaling from the cortical hem is critical for patterning of the pallium into a medial (hippocampal) fate or dorsal (cortical) fate, for instance, loss of Wnt3a largely abolishes hippocampal (archicortical) development (Grove et al., 1998, Monuki et al., 2001, Shimogori et al., 2004). WNT signaling is also involved in the maintenance of M/L patterning by controlling cell cycle progression and therefore enlargement of the hippocampal progenitor pool (Muzio et al., 2005).

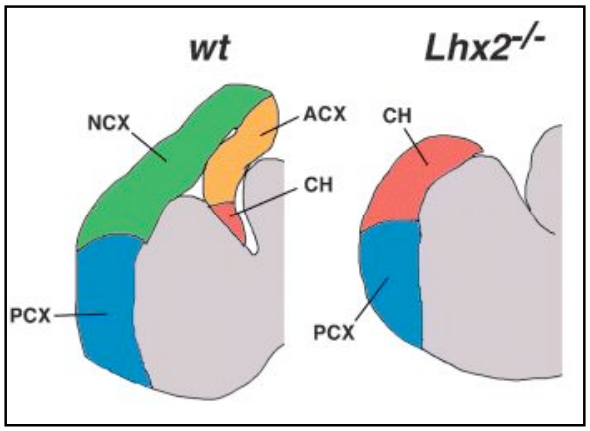

Figure 8: M/L subdivisions of the E15.5 cortex. The medial-most forebrain component is the roof plate or choroid plexus (CP). Adjacent lies the hippocampus-archicortex (ACX). Laterally, the neocortex (NCX) and paleocortex (PCX) reflects the major part of pallium. Loss of Lhx2 causes the absence of the archi- and neocortical territories. (adapted from Mallamaci et al., 2006)

Recently, another signaling center was identified and implicated to influence M/L patterning of the cortical primordium. The so-called anti-hem is a mirror image of the hem and its position corresponds to the PSB. There, members of the EGF and TCF families and WNT antagonists are expressed and associated with M/L patterning of the pallium, counteracting hem-derived signals. For example in Pax6KO embryos

numerous anti-hem markers are lost, inducing upregulation of hem marker genes and M/L patterning defects (Assimacopulous et al., 2003). In addition, a complex interplay of transcription factors like Lhx2, Foxg1 and Emx2 establishes distinct aspects of medial versus lateral identity of the early cortical neuroepithelium (Fig. 8, reviewed by Mallamaci and Stoykova, 2006).

1.2.5 Neurogenesis in the forebrain

The expression of proneural genes drives the commitment of stem cells in the neural tube towards a neuronal fate. The transcription factors Ngn1, Ngn2 and Mash1 promote neural fate in the murine PNS and CNS (reviewed by Guillemot et al., 2006). Mash1 defines neurogenic fate towards a basal ganglia fate, regulating the generation of mostly inhibitory/GABAergic interneurons (Casarosa et al., 1999). Conversely, Ngn2 is required for the generation of cortical neurons of an excitatory/glutamatergic phenotype (Schuurmans et al., 2004). Analysis of Mash1/Ngn2 double-deficient mice revealed that Ngn2 is the most important of the mentioned proneural genes. In fact, Ngn2 induces expression of Ngn1 and is necessary for negative regulation of Mash1 in the dorsal forebrain. Conversely, Mash1 and Ngn1 do not have the capacity to regulate the activity of Ngn2 (Fig. 9, Parras et al., 2002, reviewed by Guillemot et al., 2006).

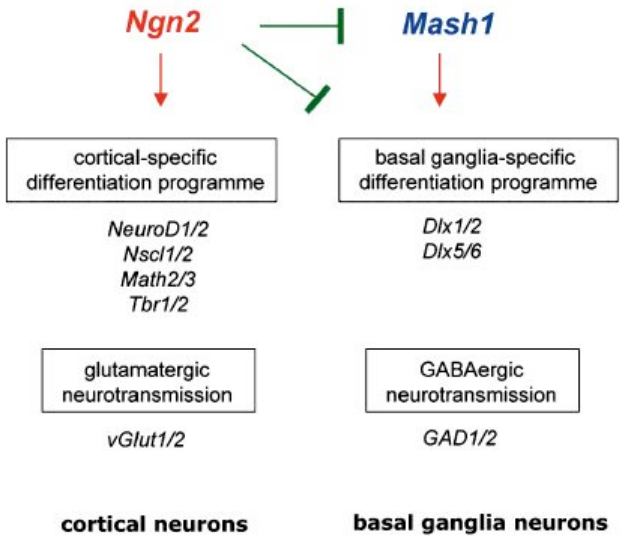

Figure 9: Proneural genes in neurogenesis. Opposing roles of the proneural genes Ngn2 and Mash1 for the neurogenesis in the forebrain. (adapted from Guillemot et al., 2006)

1.2.6 Differentiation of neuronal subtypes

The onset of pallial neuronal differentiation can be monitored by the upregulation of NeuroD1/2, Math2/3 and Nscl1 marker genes (reviewed by Guillemot et al., 2006). So far, the definite molecular events, which will trigger the transition from the generation of lower versus upper layer neuron fate, remain poorly understood. In Pax6-deficient cortices, a defective differentiation of upper layer neurons occurs, however, relatively unaffected deep cortical layers are apparent (Tarabykin et al., 2001). Conversely, the cortex of perinatal Ngn2 mutants is characterized by an altered generation of selectively deep layer neurons and largely normal upper cortical layers (Schuurmans et al., 2004, reviewed by Guillemot et al., 2006). These opposing phenotypes demonstrate a synergistic role of both factors during development of ordered cortical lamination. Recent work suggests further that after early requirement of Pax6 in the VZ, Tbr2 will be upregulated in the SVZ. Subsequently, terminal differentiation of SVZ-derived neurons requires downregulation of Tbr2 by instantly upregulating another transcription factor in those cells, Tbr1. Together with other accompanying studies it is now widely accepted that such a highly regulated sequence of transcription factor activity progressively enables the switch from the generation of deep layer neurons first and then supragranular layers afterwards. (Fig. 10, Englund et al., 2005, Hevner et al., 2006).

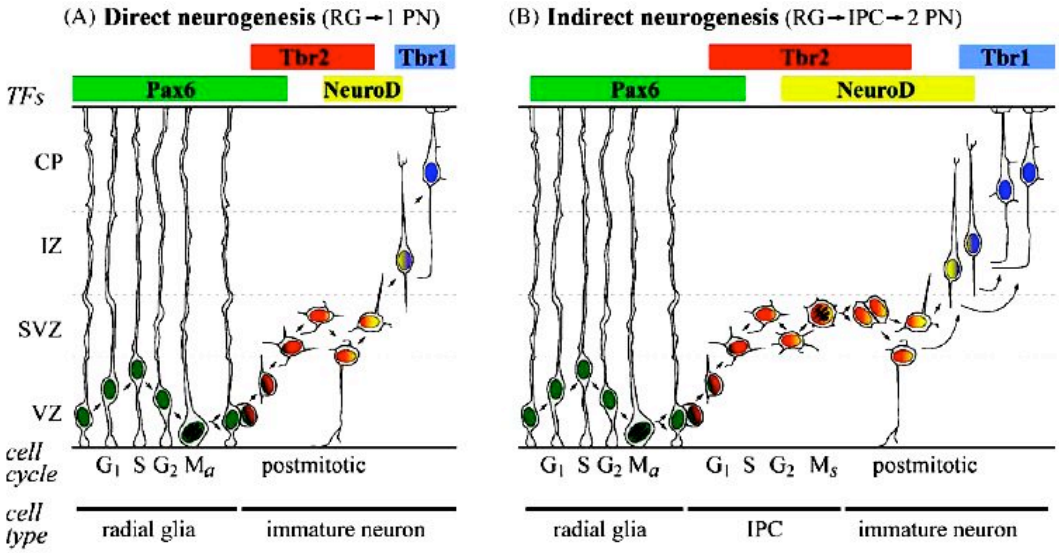

Figure 10: Transcription factor sequence during cortical neurogenesis. (A): Deep-layer neurons are directly generated from radial glia cells (RG). Upper layer neurons are generated indirectly. First RG produce intermediate progenitor cells (IPC), and then those IPC generate postmitotic neurons (PN). The nuclear migration and the sequences of transcription factors are indicated. G1, S, G2 and M indicate the phases of the cell cycle. (adapted from Hevner et al., 2006)

1.3 Sp8 and its role during murine embryogenesis

The murine transcription factor Sp8 was identified as ortholog of the *Drosophila* buttonhead (btd) gene (Wimmer et al. 1993, Bell et al., 2003, Treichel et al., 2003). In *Drosophila*, the loss of function mutant is characterized by defective patterning of the anterior head and antennal segments (Wimmer et al., 1993, Schock et al., 1999, reviewed by Nakamura et al., 2004).

Functional analysis of mutant flies revealed that this transcription factor participates in the early patterning of the fly embryo in head versus trunk. Similarly to the transcription factors empty spiracles (ems) and orthodentricle (otd), btd belongs to the so-called head gap genes (Wimmer et al., 1995, Younossi-Hartenstein et al., 1997). Buttonhead interacts physically with empty spiracles on the protein level and therefore enables ems activity to escape from the functional suppression of hox-cluster genes during pattern formation of the embryo (Schock et al., 2000).

Sp8 is a zinc-finger containing transcription factor, belonging to the Sp1 family (Specificity proteins). So far, nine members of this gene family (Sp1-Sp9) were identified. Their regulatory function is transcriptional suppression and activation of target genes through three tandem C2H2 zinc-finger motifs (Fig. 11). Sp1 family members are partially expressed ubiquitously (Sp1, Sp3) and were shown to be part of the basal gene transcription machinery. Other members (Sp4, Sp5, Sp8, Sp9) are characterized by a more restricted expression in the developing embryo (reviewed by Nakamura et al., 2004).

Sp8-deficient mice exert a severe and complex phenotype. Embryos show a reduced rostrocaudal body axis, caused by malformations of lumbar and sacral vertebrae and lacked fore- as well as hindlimbs. The neural tube is malformed in Sp8 mutants, leading to Spina Bifida. In addition, the brain is malformed and most of the embryos develop exencephaly (Fig. 11, Bell et al., 2003, Treichel et al., 2003, Griesel et al., 2006).

Functional characterization of the limb phenotype revealed that Sp8 has a crucial function during limb development and outgrowth by positively regulating Fgf8 expression in the apical ectodermal ridge (AER) (Bell et al., 2003, Treichel et al., 2003).

In the midbrain, it was recently demonstrated that Sp8 function at the isthmic organizer and midbrain-hindbrain region in early developmental stages is required for the patterning of the midbrain-hindbrain border along the A/P axis. Loss of Sp8 function results in a posterior shift of molecular markers, expressed at the midbrain-hindbrain boundary (MHB) (Griesel et al., 2006).

By conditional inactivation of Sp8 in the basal forebrain it was recently found out that Sp8 controls distinct aspects of differentiation and proper migration of olfactory bulb neuroblasts. This study demonstrates that Sp8 contributes to the specification of calretinin-expressing and GABAergic-non-dopaminergic interneurons in the ganglionic cell layer of the OB. Additionally; the OB architecture shows local defects (Waclaw et al., 2006).

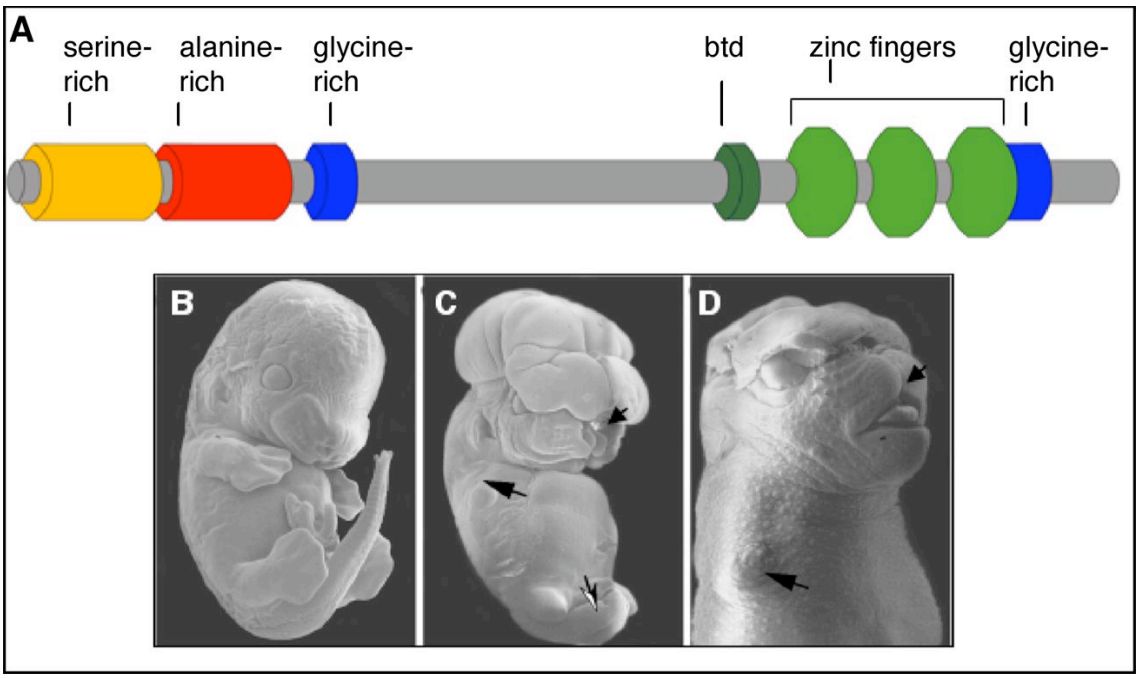

Figure 11: Structure of Sp8 and phenotype of Sp8-null mice. (A): Protein structure of Sp8. Sp8-null mutants show limb- (black arrow C, D) and tail truncations (grey arrow C), CNS-malformations (C, D), exencephaly (arrowhead C), upper cleft palate (arrowhead D). btd: buttonhead box. (adapted from Treichel, Thesis 2003)

1.4 Central objective of this study

A detailed analysis of the molecular function of Sp8 in the forebrain is lacking. Morphologically, the forebrain of Sp8-null mutant embryos appears severely reduced in size. Moreover, it is accepted that the ortholog of Sp8, the *Drosophila* buttonhead gene, is crucial for patterning of anterior head segments. Our preliminary analysis of Sp8-null knockout mutant mice revealed that the phenotype directly correlates with the gene expression domains of Sp8 during embryogenesis (e.g. expression in the forebrain and nose = exencephaly and loss of nasal structures, Fig.12). Furthermore, Sp8 is dynamically expressed in a stereotypic medial/high to lateral/low gradient in pallial progenitors, suggesting that Sp8 might function in a similar way to well known gradually expressed transcription factors, like Pax6 and Emx2. However, due to exencephaly, the analysis of the molecular phenotype in the forebrain was hampered. To overcome these difficulties, conditional Sp8 knockout mice, carrying a floxed Sp8 allele (Griesel, Thesis 2006), were generated. By using tissue specific Cre recombination, we wanted to study the role of Sp8 during development of the forebrain and its derivatives.

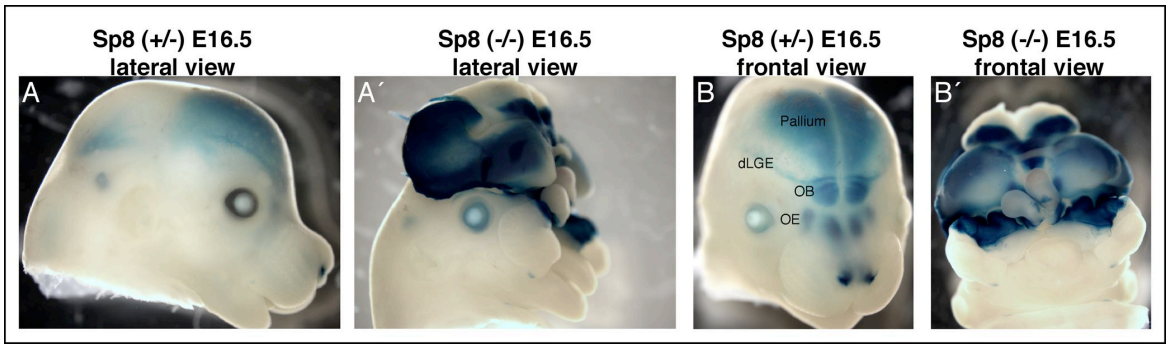

Figure 12: Expression of Sp8 and phenotype of Sp8-lacZ-null embryos. Expression (assayed by lacZ staining) of Sp8 in the midbrain, forebrain and OE (A, B) correlates with the phenotype in those regions of the embryos (A´, B´). dLGE: dorsal LGE, OB: Olfactory Bulb, OE: Olfactory Epithelium

2 RESULTS

2.1 *Expression of Sp8 during genesis of the forebrain and olfactory system*

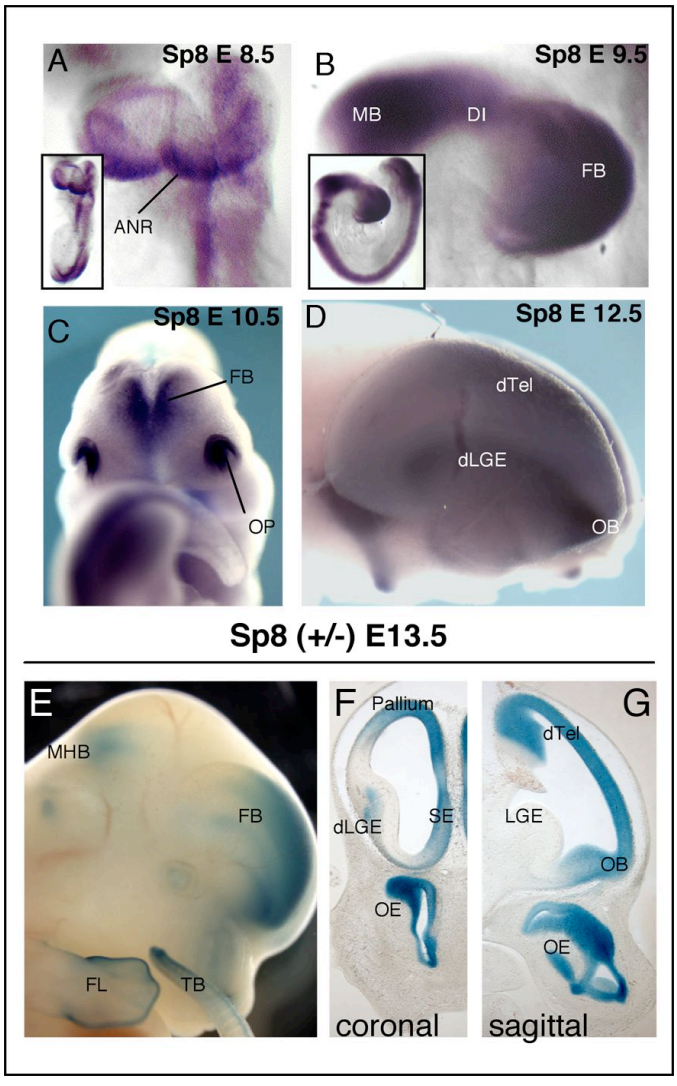

Figure 13: Dynamic expression of Sp8 during forebrain development. (A-D): WMISH for Sp8. lacZ-stained (E13.5 Sp8-lacZ-null) whole mount embryos (E) and sections (F, G). At E8.5, Sp8 is strongly expressed in the ANR and weaker in the FB neuroepithelium (A). At E9.5, the whole FB expresses high Sp8-levels (B). At E10.5, Sp8 is strongly active in the OP and in a medial/high to lateral/low gradient in the FB (C). At E12.5 and E13.5, Sp8 keeps its pallial expression gradient (E, F) and is evident in the dLGE, SE and OE (E, F, G). ANR: Anterior Neural Ridge, FB: Forebrain, DI, Diencephalon, MB: Midbrain, OP: Olfactory Placode, dTEL: dorsal Telencephalon, MHB: Midbrain-Hindbrain Boundary, FL: Forelimb, TB: Tail bud, SE: Septum.

During early development of the mouse embryo, Sp8 expression is evident in the primitive streak and anterior neural ectoderm (Treichel et al., 2003). At E8.5, Sp8 is strongly expressed in the anterior neural ridge (Fig. 13, A). Additionally, Sp8 is expressed at lower levels within the rostral neuroepithelium (Fig. 13, A). Starting from this stage, Sp8 expression in the putative pallium can be characterized as a stereotypic gradient with high expression at the midline and lower expression in lateral areas.

At E9.5, Sp8 transcripts can be detected throughout the whole presumptive forebrain neuroepithelium, sustaining the medial/high to lateral/low expression gradient (Fig. 13, C). Additional expression can be found in the olfactory placode,

the anlage of the invaginating olfactory neuroepithelium (Fig. 13, B). At stage E10.5, we analyzed that the strengths of the Sp8 expression gradient is downregulated in the ventricular zone of the forebrain vesicle, but strong expression persists in the olfactory placode (Fig. 13, C).

At E12.5-E13.5, transcription of Sp8 is strongly visible in the telencephalic midline, the septum and in the medial and dorsal pallium with a typical gradient. Laterally in the forebrain, the subventricular zone of the dorsal LGE starts to express Sp8 (lacZ staining: Fig. 13, F, G, mRNA staining: Fig. 26, F). This region is the source of olfactory neuroblasts progenitors (Waclaw et al., 2006). In agreement with this finding, a cell population in the RMS is labeled with Sp8 mRNA at E13.5 (Fig. 13, F). Further characterization revealed that Sp8 is expressed within the olfactory epithelium and in olfactory sensory neurons (OSNs) (Fig. 13, F, G, Fig. 43, A-B).

At midgestation, the expression level of Sp8 within the cortical VZ is downregulated, although the CP exhibits weak Sp8 signal (data not shown). Moreover, Sp8 expression levels remain stronger active in the SE, dLGE, RMS and olfactory epithelium (Fig. 14, A, E, data not shown). After birth, Sp8 mRNA synthesis is downregulated in the proliferative zone of the cortex and is only kept in some cortical plate cells (layer II, III and V and subplate/layer VI b, Fig. 14, A, C) and in a subpopulation of cells in the lateral olfactory cortex (data not shown).

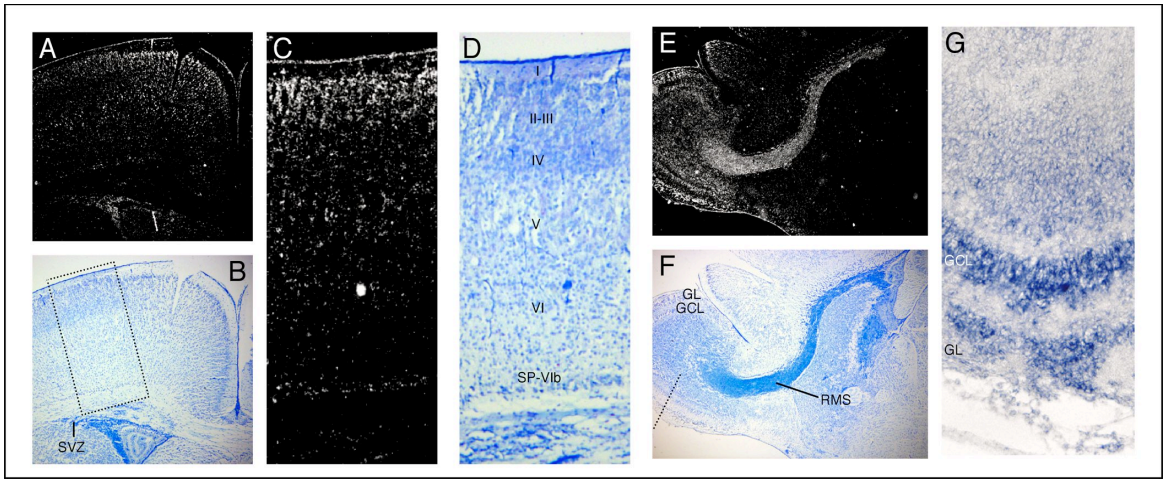

Figure 14: Postnatal expression of Sp8. ISH, using radioactive mRNA probes (A, C, E) and DIG-labeled probes (G) for Sp8 on coronal (A-D, G) or sagittal (E, F) sections. GIEMSA counter-stained sections (B, D, F). Sp8 is expressed in the SVZ of the lateral ventricle (A), RMS (E) and in the GL and the GCL of the OB (E, G). Further Sp8 is expressed in some neurons in cortical layers II/III, V and the SP/layer-VI b (A, C). Dashed line in (F) indicates the plane of the coronal section in (G.) Square in (B) indicates the cortical region shown in (C, D). SVZ: Subventricular Zone, SP: Subplate, RMS: Rostral Migratory Stream.

In parts of the basal telencephalon, Sp8 activity is apparent throughout adulthood (Waclaw et al., 2006). The septum expresses Sp8 mRNA at P5 and furthermore through adulthood (data not shown).

During late embryonic and early postnatal development, the dLGE transforms into the subventricular zone of the lateral ventricle and remains Sp8-positive (Fig. 14, A). Beside the hippocampus, this brain region is one source of neuronal stem cells and generates olfactory neuroblasts, renewing the olfactory bulb interneuron circuitry (reviewed by Campbell and Gotz, 2002). Therefore, Sp8+ cells can be found within the rostral migratory stream and in the ganglionic and glomerular cell layers of the olfactory bulb (Fig. 14, E, G), indicating that Sp8 might be involved in the generation of the OB (Waclaw et al., 2006). Olfactory sensory neurons express Sp8 postnatally, too (data not shown). This indicates that Sp8 is expressed in all components of the primary olfactory system in mice and therefore might be necessary for its proper genesis. This suggestion is strongly underlined by the absence of nasal structures in Sp8-null animals (Treichel et al., 2003). In addition, Waclaw and coworkers (2006) recently reported that Sp8 is crucial for the genesis of OB interneurons and OB morphology.

2.2 Characterization of the Foxg1-Cre knock-in mouse line

Our strategy for the conditional inactivation of Sp8 is based on the Foxg1-Cre driver line. This transgenic mouse line is the earliest active and most ubiquitously expressed Cre driver line for conditional gene-inactivation in the forebrain and adjacent head structures, described so far (Hebert et al., 2000). Cre activity was monitored by generating double transgenic mice, expressing the Cre transgene and a reporter transgene, R26R (Soriano, 1999) or hrGFP (Schindehutte et al., 2005). In those animals, the reporter gene (lacZ for R26R, or GFP for hrGFP) will be activated in cells that have completed Cre-mediated recombination.

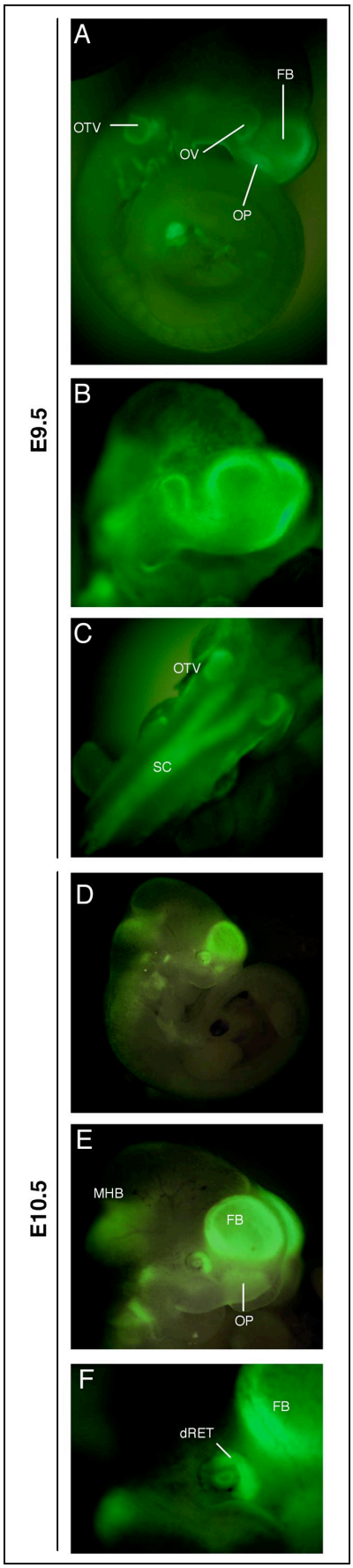

←Figure 15: Early expression of the Foxg1-Cre transgene. GFP staining of Foxg1-Cre-hrGFP double transgenic embryos (A-F). GFP staining/ Foxg1-Cre activity is visible at E9.5 in the FB, OTV, OP and SC at E9.5 (A-C). At E10.5 (D-F), the GFP signal is strong in the FB, OP and dRET. OTV: Otic Vesicle, OV: Optic Vesicle,

Foxg1-Cre-transgenic mice were generated in the lab of Susan McConnell (Hebert et al., 2000) by knocking-in the Cre gene into the 5´ open reading frame of the Foxg1 locus close to the transcription start site. Therefore, the targeted allele does not produce functional Foxg1 protein, but Cre protein instead. This leads to activation of the functional Cre activity in cells expressing Foxg1, on the expenses of Foxg1 mRNA itself. In this respect, breeding of the Cre allele in mice to homozygozity produces Foxg1 knockout animals. So far, an extensive examination of Cre-expressing, Foxg1 heterozygous, mice used in this study does not reveal any obvious phenotype (data not shown). This correlates with published findings of other groups, who also used and characterized this Cre line (Hebert et al., 2000, Gutin et al., 2006, Tole et al., 2006).

To get further information about the spatiotemporal distribution of Cre activity, we assayed the GFP signal of Foxg1-Cre/hrGFP double transgenic embryos. Foxg1-Cre activity starts around E8.5 (Hebert et al., 2000). Slightly later, Cre recombination is evident as a strong GFP signal in the forebrain neuroepithelium. At E9.5, the anterior head region strongly expresses the marker transgene. Additionally, Cre activity is evident in the developing optic and otic vesicles and scattered in the branchial arches (Fig. 15, A, B). With a varying penetrance, we observed GFP+ cells in the spinal

cord (Fig. 15, C). In accordance to endogenous Foxg1 expression, the GFP/lacZ signal covers the whole forebrain at E10.5 (Hebert et al., 2000, Fig. 18, A). The nasal placode starts to express Cre protein, as well as some cells in the MHB-region, too (Fig. 15, D, E). The Cre expression in the eye appears restricted to its dorsal part (Fig. 15, F).

Foxg1-promoter-driven Cre recombination occurs in both the dorsal and ventral part of the forebrain (Hebert et al., 2000), as highlighted by a strong GFP signal at E15.5 (Fig. 16, A, D). However, strong activity is additionally visible in the developing olfactory epithelium, OSNs and dorsal retina at this stage (Fig. 16, B, C).

Sp8 expression spatiotemporally overlaps with Foxg1-Cre activity (Fig. 18, A, B) during early phases of development. Furthermore, Foxg1-Cre activity covers the Sp8 expression domains in the forebrain and the olfactory placode (Hebert et al., 2000). Therefore, the Foxg1-Cre mouse line is a suitable experimental tool to study the role of Sp8 in both regions of the embryo simultaneously. By using this conditional inactivation strategy, we speculated to generate a phenotype that overcomes the limitations of exencephaly and additionally is as close as possible to the Sp8 knockout (Treichel et al., 2003), but restricted to the forebrain- and olfactory placode territories.

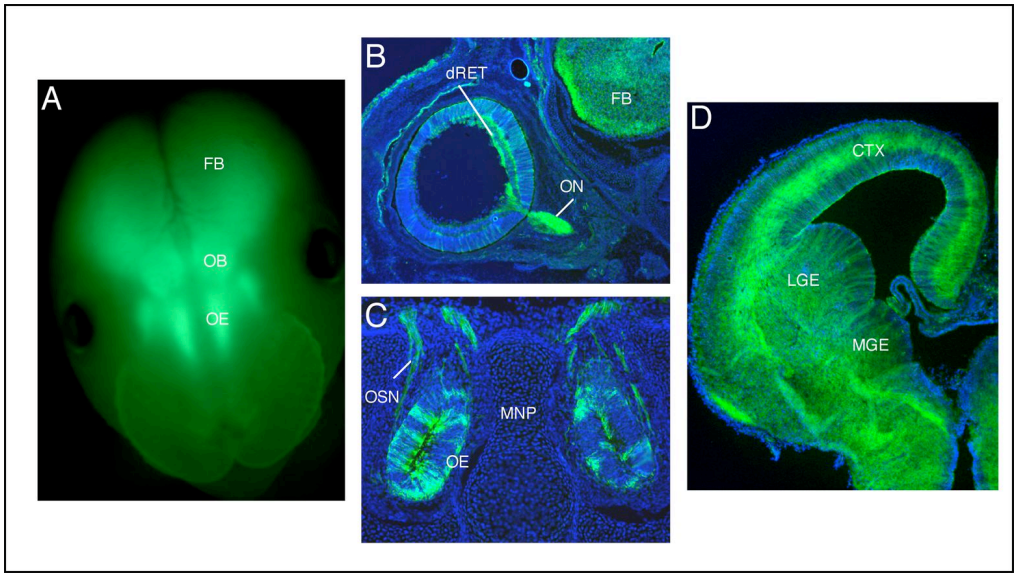

Figure 16: Late expression of the Foxg1-Cre transgene. GFP staining of Foxg1-Cre/hr-GFP double transgenic E15.5 embryos (A-D). Coronal sections, counterstained with DAPI (B-D). The Cre transgene is active in the FB, OB and OE. Further GFP signal is evident in the dRET, ON, OE and OSNs (B, D). The Foxg1-Cre transgene is strongly active in the dorsal and the ventral telencephalon (D). ON: Optic Nerve, OSN: Olfactory Sensory Neurons. MNP: Medial Nasal Process, MGE: Medial Ganglionic Eminence.

2.3 Generation and maintenance of the conditional Sp8 mutant mouse line

To establish the conditional Sp8 mutant mouse line, we developed a breeding paradigm, as indicated in Fig. 17. First, Sp8-floxed homozygous animals were crossed with heterozygous Foxg1-Cre-expressing mice. These matings generated an intermediate generation of mice. Only few of those animals were suitable for further matings. Namely those double transgenic mice only, carrying the Cre transgene and a floxed Sp8 allele. Those conditional double heterozygots were further crossed to mice, which were homozygous for the floxed Sp8 allele. The resulting offspring produced homozygous Sp8 conditional mutants, Sp8 heterozygous and control embryos, according to the Mendelian ratio (Fig. 17, data not shown).

Double transgenic mice (Sp8 floxed (+/-), Cre (+/-)) were further intercrossed to C57/BL6 wild type mice, to maintain them in a C57/BL6 genetic background. The conditional Sp8 mutants will further be termed cKO in the text and cKO^{fox} in the figures.

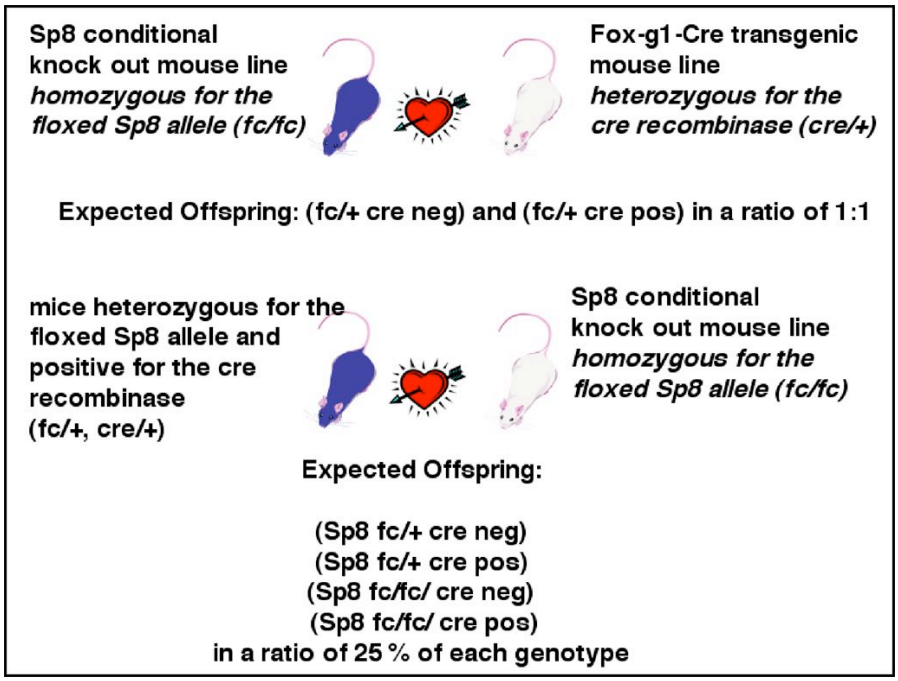

Figure 17: Mating strategy to generate conditional Sp8-mutants. The conditional Sp8-inactivation mouse line was generated, as described in the breeding paradigm.

2.4 Phenotype of Sp8 cKO mutants

In order to assay recombination efficiency of the Foxg1-Cre driver line, we performed whole mount *in situ* hybridization (WMISH) using the Sp8 probe. Sp8 mRNA was completely absent from the forebrain and olfactory placode of E10.5 cKO embryos (Fig. 18, B). Conversely, Sp8 staining remained visible in the spinal cord, limbs and MHB (data not shown). Furthermore, we analyzed the Sp8 expression level by using quantitative RT-PCR of isolated total RNA from E12.5 forebrain tissues. The normalized Sp8 mRNA content of cKO specimens was 0.89% (+/- 0.85%) and double heterozygots had 70.43% (+/- 7.98%), as compared to the control littermate expression values of Sp8 (100%, +/- 18.35%) (Fig. 18, C). Therefore in cKO, the expression level of Sp8 is at barely detectable levels. We conclude from this data that Foxg1-Cre-driven recombination of the floxed Sp8 locus efficiently abolishes Sp8 function during early forebrain development.

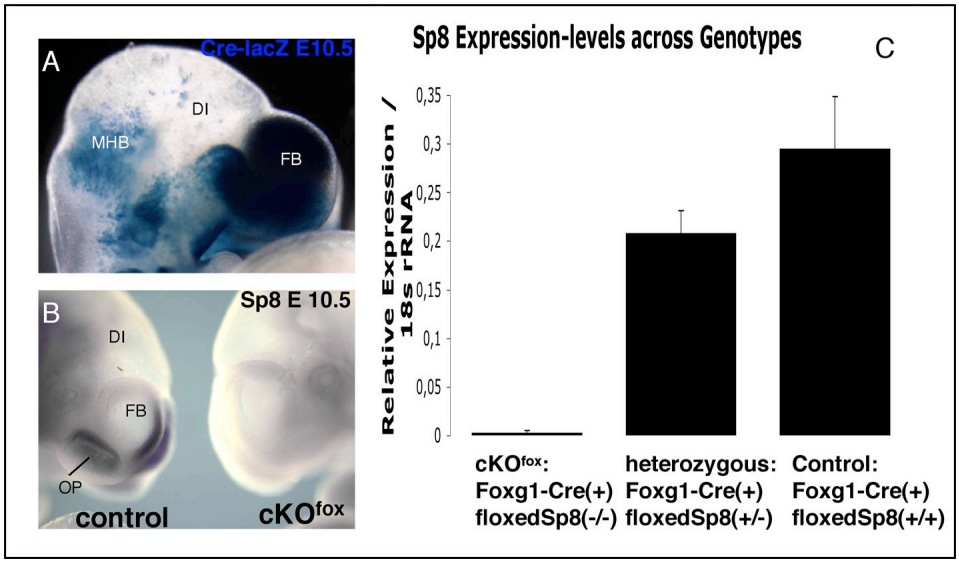

Figure 19: Foxg1-Cre-driven inactivation of Sp8. (A). Foxg1-Cre-activity, visualized by X-Gal staining of Foxg1-Cre/R26R embryos, is active throughout the telencephalon at E10.5 (B). Cre recombination ablates Sp8 expression in the FB and OP of cKO at E10.5 – visualized by ISH (C). RT-PCR quantification shows that Sp8 expression levels are below 1% of the wild type value (C).

2.4.1 Morphological phenotype of cKO

cKO mice die at birth. Therefore, we were interested in the morphological appearance of the forebrain at embryonic stages, first at midgestation stage E15.5. Mutant individuals were easily identifiable upon evident malformations of the rostral head region (Fig. 20, A, A´). All mutant embryos developed strong craniofacial abnormalities. The nose was much smaller as compared to wild type littermates. Upper cleft palate is evident, with a penetrance of 15% (n=25) of the mutant population (Fig. 20, F, F´).

The histological analysis of nissl-stained (E18.5) sections revealed that the forebrain, nose and its surrounding tissue appear severely hypoplastic in mutants, when compared to controls. The most dramatic defect rostrally was the enormous reduction of the olfactory epithelium and the medial nasal process (black and red arrows Fig. 20, D, E, D´, E´). Additionally, morphology and positioning of the whiskers were abnormal in cKO (data not shown).

Further analysis revealed that the A/P axis of the mutant forebrains appears significantly shorter (78.5% +/-3,8% of wild type, n=15) than in wild type littermates. Nissl staining on coronal

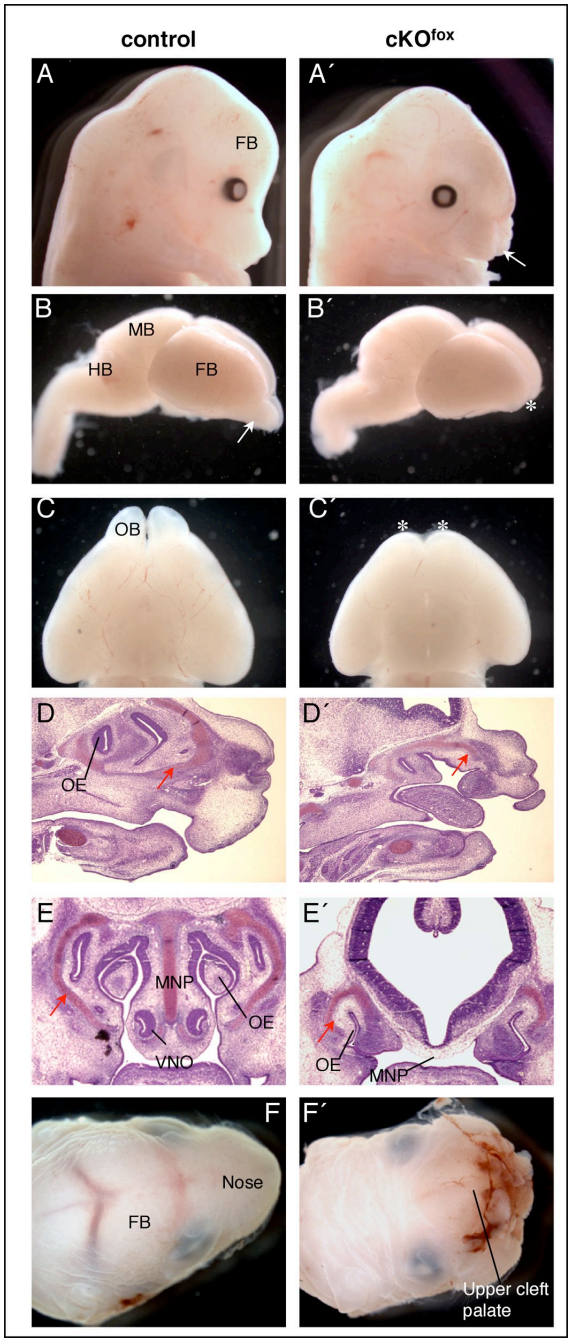

Figure 19: Phenotype of cKO at midgestation. E15.5 cKO heads (A, A´) and brains (B, B´) appear smaller than controls and lack the OB (arrow C, asterisk C´). Further, the nasal region, the cartilage (red arrow, D, D´) and the OE appears hypoplastic on nissl-stained sections (sagittal D, D´, coronal E, E´) and upper cleft palate is partially evident (arrow A´, F, F´). VNO: Vomeronasal Organ.

brain sections at rostralmost levels highlights that the olfactory bulb is completely missing in cKO (data not shown). The basal ganglia are reduced in size and medially the SE is missing. The preoptic area (POA) lies in close vicinity to the overlying mutant cortex (Fig. 20, A, A´). Furthermore, the corpus callosum is not formed in cKO. Callosal axons seem to grow out initially, but do not cross the midline, remaining within the ipsilateral hemisphere of the brain (Fig. 20, A, A´), forming probst bundles (PB). The anterior commissure (AC) will not enter the contralateral side of the brain in 50% of the examined mutants (n=30). Apart from the basal telencephalon, we could identify

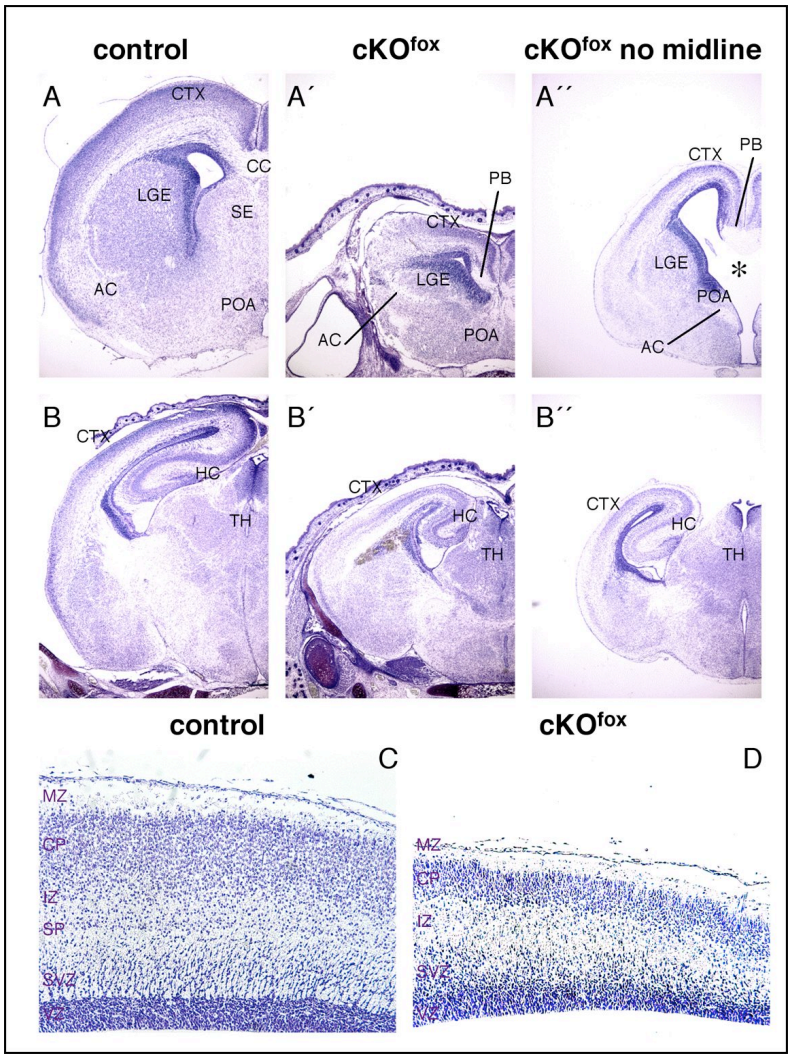

Figure 20: Histological phenotype at E18.5. On E18.5 nissl-stained coronal sections, mutant brains miss the SE and reveal a reduced size of the telencephalon (A´, B´). Callosal fibers do not cross the midline and form probst bundles unilaterally (A´, A´´). On (nissl-stained) sagittal sections, a strongly reduced cortical diameter is characteristic for cKO at E18.5 (C, C´). With 15% penetrance, cKO brains show an enhanced phenotype, highlighted by the complete absence of midline derivatives. These mutants were termed “cKO no midline” (A´´, B´´). cKO and “cKO no midline” only differ at rostral levels of the forebrain. In “cKO no midline” specimens, a delamination of the cortex from the basal telencephalon is apparent medially, as a visible hole (asterisk A´´). Caudally in the brain, the difference between low- and high-penetrant phenotypes is not significant (B´, B´´). CTX: Cortex, PB: Probst Bundles, HC: Hippocampus, TH: Thalamus.

that the cerebral cortex diameter is strongly reduced in cKO (Fig. 20, C, C´). More caudally in the forebrain, neuronal fibers form aberrant bundles between the internal capsule and the basis of the telencephalon (Fig. 20, B, B´).

With 15% penetrance (n= 25), cKO brains show a more severe phenotype, characterized by complete absence of midline derivatives, termed "cKO no midline". cKO and "cKO

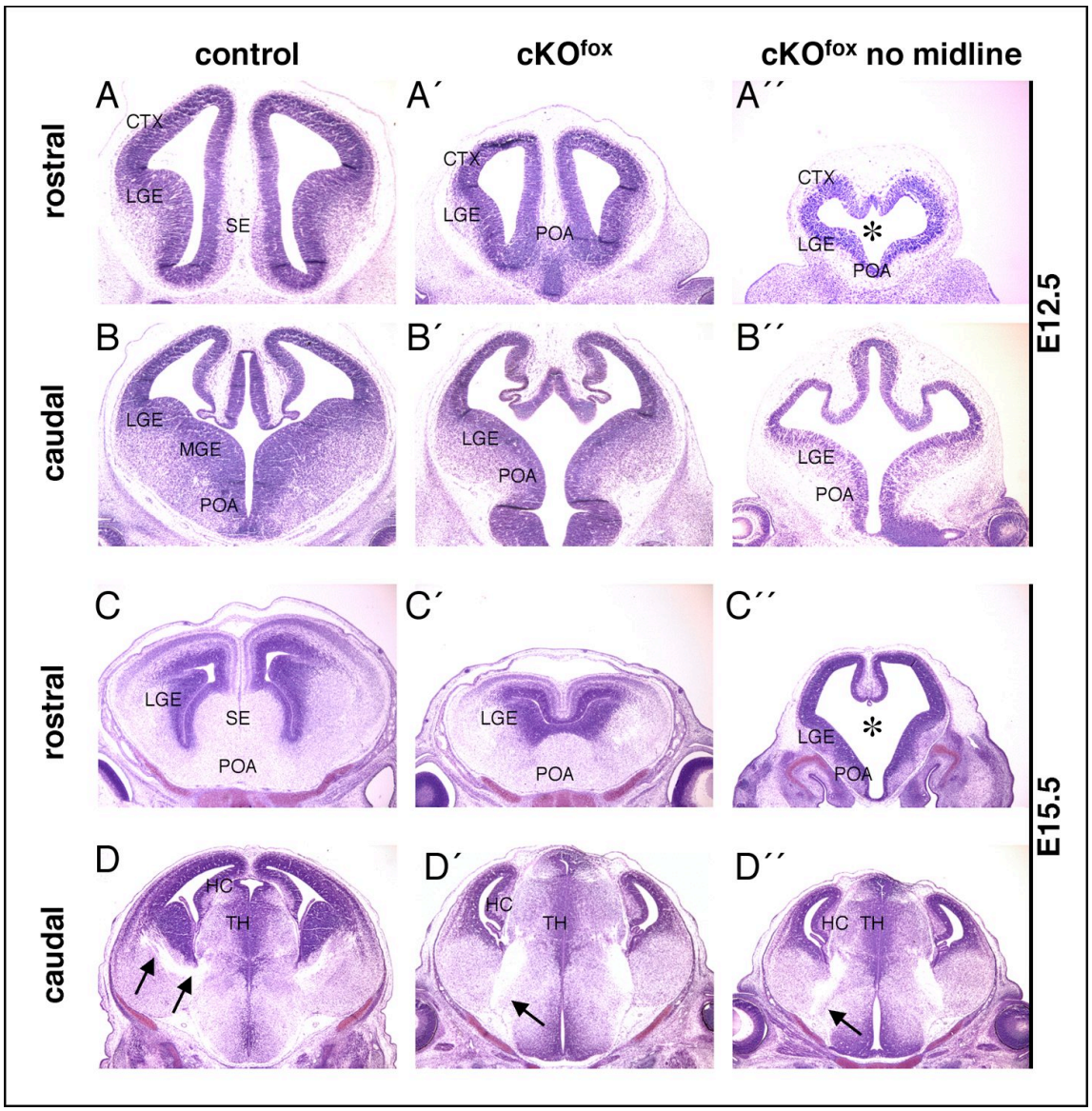

Figure 21: Histological phenotype at E12.5 and E15.5. Comparison of nissl-stained coronal sections of controls (A-D), cKO (A´-D´), and the high penetrant Sp8 phenotype – "cKO no midline" – (A´´-D´´) from E12.5 to E15.5. At E12.5, Sp8 mutant tissue sections reveal a significant size reduction of the telencephalon and the morphological absence of the SE at rostral levels (A´, A´´). Caudally, the basal ganglia appeared as a single eminence (B´, B´´), when compared to controls (B). At E15.5, cKO forebrains lacked the SE (C, C´). The "cKO no midline" phenotype exposed a much more severe reduction of the brain size, when compared to controls or the low penetrant cKO phenotype (compare C-C´´). Due to an almost complete disgenesis of the midline, the lateral ventricles appeared as a single aqueduct space (compare C, asterisk in C´´). At more caudal levels, low- and high penetrant Sp8 phenotypes appeared grossly indistinguishable from each other (D´, D´´). Although, when comparing them to wild type embryos, conditional mutant specimens showed aberrant fiber bundles between the internal and external capsules (arrows D, D´, D´´).

no midline" specimens differ only at rostral levels of the forebrain. This difference is evident by delamination of the cortex from the basal telencephalon as a visible hole in the medial telencephalon (asterisk Fig. 20, A´´), where normally SE and/or POA would appear and contact the pallium. This phenotype is characterized by the appearance of a single ventricle (Fig. 20, A, A´, A´´). Caudally in the brain, low- and high-penetrant phenotypes are indistinguishable (Fig. 20, B´, B´´).

In order to identify the developmental onset of the forebrain hypoplasia in mutants, we further investigated E15.5 and E12.5 histological sections. At E15.5, the above reported abnormalities and the forebrain hypoplasia were already strongly evident (Fig. 21, C-D´´). At E12.5, the basal ganglia of cKO specimens formed a single ganglionic eminence. A discernable constriction between the MGE and LGE is not obvious in mutants (Fig. 21, B, B´, B´´). More rostrally, the septal area of cKO brains appeared morphologically distinct from controls. We think that at comparable levels of the brain, the midline of the POA is visible in cKO (Fig. 21, A, A´´). Taken together, conditional Sp8 mutant forebrains develop a histologically visible phenotype, starting at E12.5 of embryonic development.

By labeling commissural axons of the CC and the AC with the lipophylic tracer DiO, we confirmed the histological data and could highlight that the CC and in some cases the AC does not cross the midline in Sp8 mutants (Fig. 22).

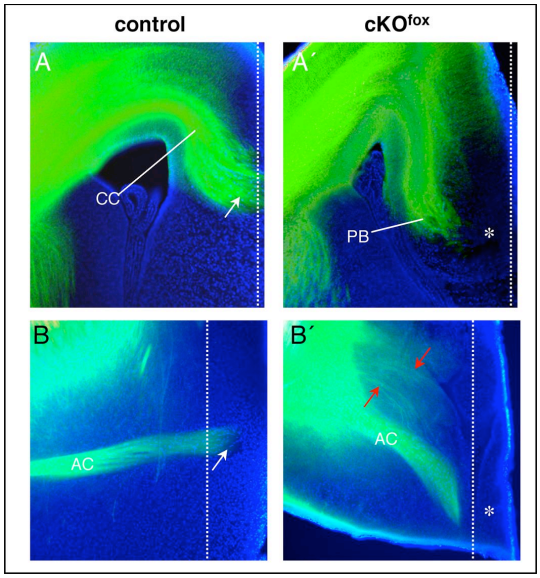

Figure 22: The CC and the AC do not cross the midline in cKO. Coronal sections of DiO injected cortices (E18.5). Callosal fibers in cKO form PB unilaterally (asterisk A´). The AC does not cross the midline and appears defasciculated (asterisk, arrows B´). Dashed lines indicate the cortical midline.

2.4.2 D/V patterning in cKO mutants

In order to understand what molecular mechanisms were affected by the loss of Sp8 in the forebrain, we first focused our analysis on those molecules that were shown to act on brain patterning. Fgf8 is expressed in the ANR and later on within the telencephalic midline and establishes the early patterning of the telencephalon (reviewed by Mallamaci and Stoykova, 2006). Shh is expressed in the basal telencephalic vesicle and affects ventral characteristics, independent from FGF signaling. Shh and Fgf8 mutants were shown to lack distinct ventral cell types, resulting in severe D/V patterning defects (Chiang et al., 1996, Storm et al., 2006). However, both factors are normally expressed in cKO (Fig. 23, A, A´, Fig. 24, A, A´). Pax6 and Emx2 are important factors, which pattern the dorsal forebrain along the A/P and the D/V axis (reviewed by O'Leary and Nakagawa, 2002, Sur and Rubenstein, 2005). The characteristic rostral/high to caudal/low expression gradient of Pax6 is initiated, but appears diminished in mutants (Fig. 23, E, E´). Emx2 expression levels, which are caudal/high and dorsal/low, appear conversely enhanced in cKO, as compared to wild type littermates (Fig. 23, F, F´).

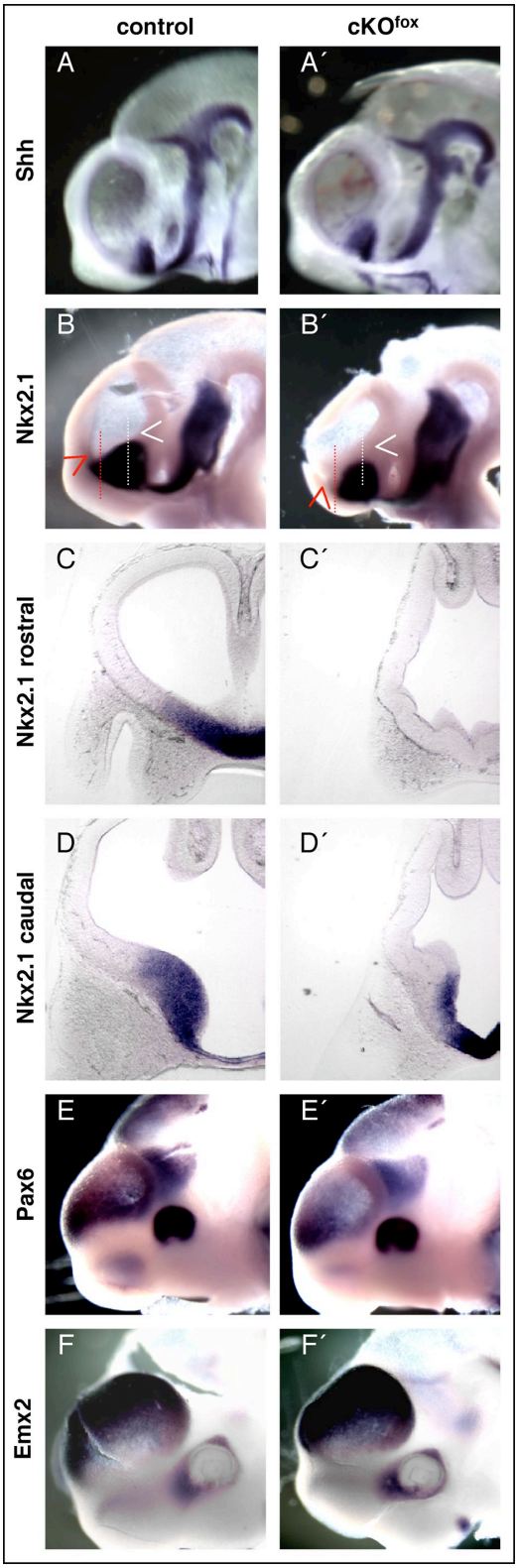

Figure 23: Early patterning of the telencephalon. WMISH, using E9.5 embryos. Shh activity (A, A´) at E9.5 is unchanged in cKO. The SE and large parts of the MGE anlage (red + white arrowhead B, B´, dashed lines indicate the plane of coronal sections in C, C´, D, D´) are free of Nkx2.1 activity. Pax6 activity is diminished in cKO (E, E´). Emx2 is slightly upregulated in mutants (F, F´).

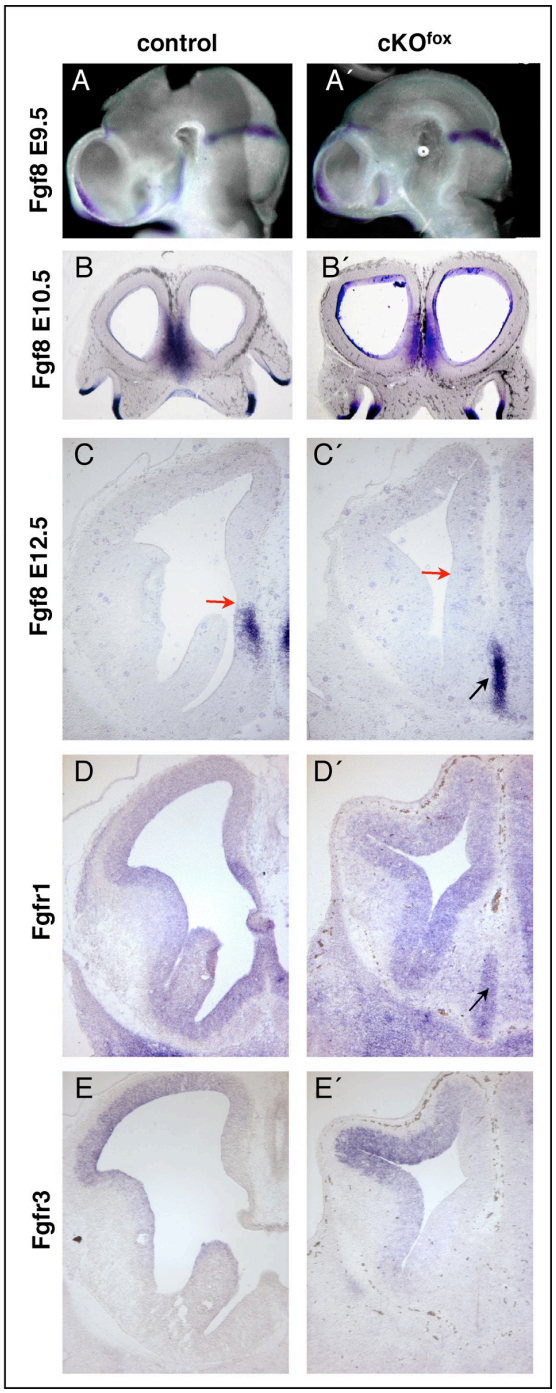

Figure 24: FGF signaling in the embryonic forebrain. WMISH of E9.5 A, A´), sectioned E10.5 embryos (B, B´) and ISH of E12.5 coronal sections (C-E´). Fgf8 expression (A, A´) at E9.5 is unchanged in cKO. At E10.5, Fgf8 is expressed in the telencephalic midline and the SE-anlage of mutant and control embryos (B, B´). At E12.5, Fgf8 mRNA is specifically lost in the SE (red arrow C, C´, D´) of mutants. The Fgf8 positive domain in cKO at E12.5 matches the midline of the POA (black arrow C´). The expression of Fgfr1 (D, D´) and Fgfr3 expression (E, E´) appears similar in both genotypes.

Remarkably, the activity of Nkx2.1, which induces MGE-fate in progenitors (Sussel et al., 1999), is strongly reduced in cKO (Fig. 27, B, B´). Rostrally, the septum-anlage is free of Nkx2.1 staining (Fig. 23, C, C´). Posteriorly, its expression domain consists of an Nkx2.1-positive patch at the putative telencephalic-diencephalic ventral border and POA, leaving the majority of the MGE-anlage dorsally free of Nkx2.1 activity (Fig. 23, D, D´). Slightly later at E10.5, Fgf8 is expressed in the septum-anlage and telencephalic midline in mutant and control embryos (Fig. 24, B, B´).

The initial expression of major patterning molecules at E9.5 is not affected in cKO. However, altered activity of Emx2, Pax6 and Nkx2.1 led us to analyze forebrain patterning in more detail at E12.5. At this stage, Fgf8 expression is visible in the SE of wild type embryos (red arrow Fig. 24, C). Surprisingly, this subpallial expression domain is specifically lost in mutants (red arrow Fig. 24, C´). More ventrally, an Fgf8 expression domain (matching to the midline of the POA) is still visible in mutants (black arrow Fig. 24, C´). This finding is in accordance to the fact that the POA does not belong to the forebrain and that the Foxg1-Cre transgene is not

expressed there (Hebert et al., 2000). Interestingly, the loss of the Fgf8 expression domain in mutants does not influence the expression of both, Fgfr1 and Fgfr3 (Fig. 24, D, D´, E, E´). Next we examined patterning of the gene expression interface at the border of the pallium-subpallium in the medial telencephalic wall, designated medial pallial-subpallial boundary (mPSB).

The expression of Emx2 overlaps with that of Sp8 in the medial and dorsal pallium, and is slightly modulated in cKO at E9.5. Furthermore, the pallial Emx2 domain shows an enhanced gradient, when compared to controls at E12.5 (arrowheads Fig.25, A, A´). At the mPSB, Emx2 activity expands ventrally in mutants (arrows Fig. 25, C, C´). The lateral/high to medial/low pallial expression gradient of Pax6 is diminished in mutants (arrowheads Fig. 25, B, B´). At the midline, the strongly Pax6+ domain expands ventrally into the septum (arrows Fig. 25, D, D´), in almost the same manner as the domain of the direct Pax6 target gene Ngn2 (Scardigli et al., 2003), occupying the presumptive SE (Fig. 25, E, E´). In accordance with the reported inhibition of Mash1 by Ngn2 (Parras et al., 2002), the Mash1+ domain in the dorsal SE is lost in cKO (Fig. 25, J, J´). Conversely, the unaffected expression boundaries of Pax6 (Fig. 25, B, B´), Ngn2 (Fig. 25, E, E´), Dlx1 (Fig. 25, G, G´), Mash1 (Fig. 25, J, J´) and Gsh2 (Fig. 25, H, H´) at the lateral pallial-subpallial boundary (PSB) demonstrate that the lateral pallium and the LGE might keep their molecular identity. On the other hand, the expression territories of Gsh2, Mash1 and Dlx1 in the dorsal septum are lost in Sp8 mutants (arrows Fig. 25, H, H´, J, J´, G, G). Together these results suggest that in the absence of Sp8, a dorsalization of gene expression territories at the mPSB occurs. The molecular dorsalization of the ventral midline is still evident at E15.5, as highlighted by an enlarged Ngn2- and a shrunken Dlx1 domain (Fig. 25, L, L´, M, M´).

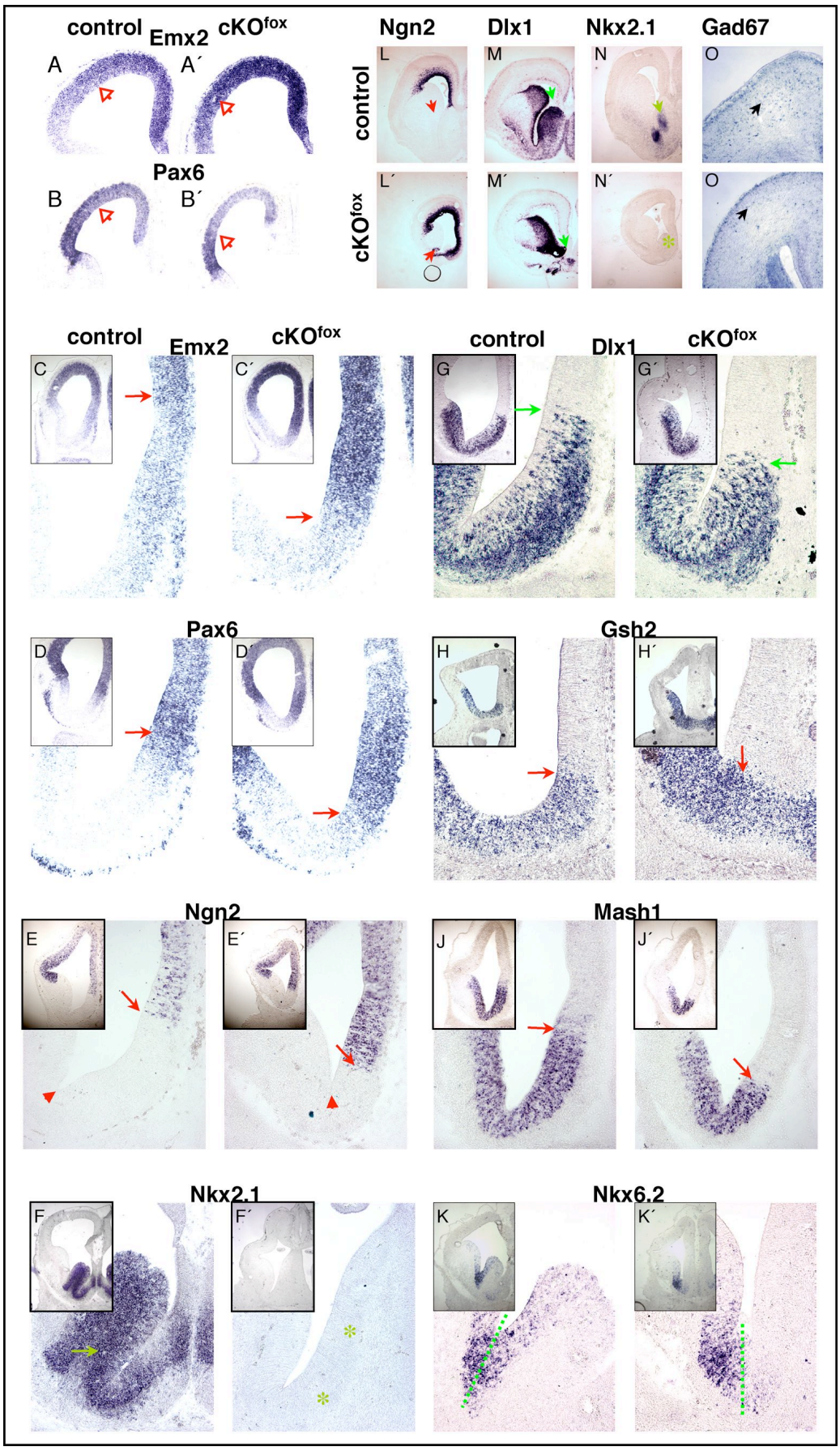

Figure 25: D/V-patterning at the mPSB.

↑ **Figure 25: D/V patterning at the mPSB.** ISH on E12.5 (coronal) forebrain sections. Images show the right brain hemisphere. (C-K): Blow-up images of the medial/ventral part of each boxed section. In cKO, the pallial markers Emx2 (A, A´, C, C), Pax6 (B, B´, D, D´), and Ngn2 (E, E´) expand into the ventral midline. Conversely, ventral markers Dlx1 (G, G´), Gsh2 (H, H´), and Mash1 (J, J´) are not expressed in the dorsal SE. Nkx2.1 activity is lost in the SE and rostral MGE of Sp8 mutants (F, F´). The Nkx6.2+ domain might reflect a rudimentary MGE territory in cKO and contacts the Emx2+, Pax6+ and Ngn2+ midline (K, K´). Note, the expansion of the Ngn2+ domain (arrows L, L´) and the reduction of the Dlx1+ domain (arrows M, M´) around the midline of the Sp8-deficient telencephalon at E15.5. Nkx2.1 (arrow N, N´) remains absent in the SE and rostral MGE of cKO at this stage. Depletion of Gad67+ interneurons in the Sp8 mutant cerebral cortex (arrow O, O´) at E18.5. For a better visualization of the shift in gene activity, the arrowheads in E, E´ point at the constriction between the SE-anlage and the LGE. ISH for Emx2/Pax6 (A, A´, B, B´, C, C´, D, D´) and Ngn2/Mash1 riboprobes (E, E´, J, J´) were performed on adjacent sections.

In contrast to the partially preserved expression at E9.5, Nkx2.1 activity is almost absent from the cKO telencephalon at E12.5, namely in the SE and MGE (Fig. 25, F, F´). However, at caudal levels (matching the putative caudal ganglionic eminence) a small Nkx2.1+ stripe remains visible in mutants (data not shown). The expression domain of Nkx6.2 is a specific marker for the junction between MGE and LGE (Xu et al., 2005, Fig. 25, K). In cKO, this domain is visible, however, its location is at much more medial levels and contacts the ventrally enlarged Emx2+, Pax6+ and Ngn2+ midline territory in cKO (Fig. 25, K´).

Given the dramatic reduction of the Nkx2.1 activity and therefore depletion of the MGE territory, we examined the differentiation of interneurons on E18.5 sections. As a consequence of the strongly diminished MGE progenitor pool (Sussel et al., 1999), cKO cortices contain a dramatically low amount of Gad67+ interneurons (Fig. 25, O, O´).

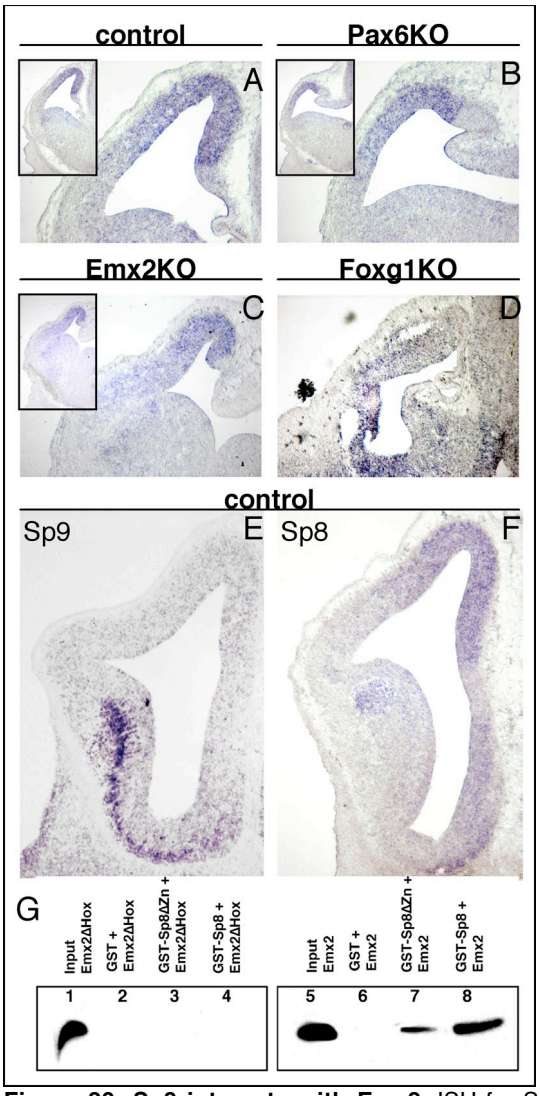

Figure 26: Sp8 interacts with Emx2. ISH for Sp8 (A-D, F) and Sp9 mRNA (E) on E12.5 coronal sections. Sp8 expression in the medial and dorsal pallium of Emx2KO and Pax6KO specimens appears indistinguishable from controls (A, B, C). Sp8 staining in Foxg1KO embryos remains active in many telencephalic cells (D). Sp8 and Sp9 are expressed in mostly non-overlapping domains (E, F). Sp9 is expressed at the PSB (E). GST-pulldown reveals that GST-Sp8 and GST-Sp8 lacking Zn-fingers interact with Emx2 (G, lane 7-8). Emx2 protein lacking homeobox does not interact with GST-Sp8 isoforms (G, lane 3-4). 10% protein input for binding assays is shown in lane 1 and 5. Emx2 isoforms does not bind GST alone (G, lane 2, 6).

The presented results indicate a molecular ventralization of marker genes at the mPSB, suggesting that Sp8-deficient rostral forebrains exhibit a mispatterned midline. The downregulation of the main MGE fate determinant Nkx2.1 and Fgf8 in the rostral forebrain results in loss of the SE. Furthermore, the PSB remains preserved and therefore the subpallium displays genetic LGE properties, possibly causing the histological appearance as a single ganglionic eminence in mutants.

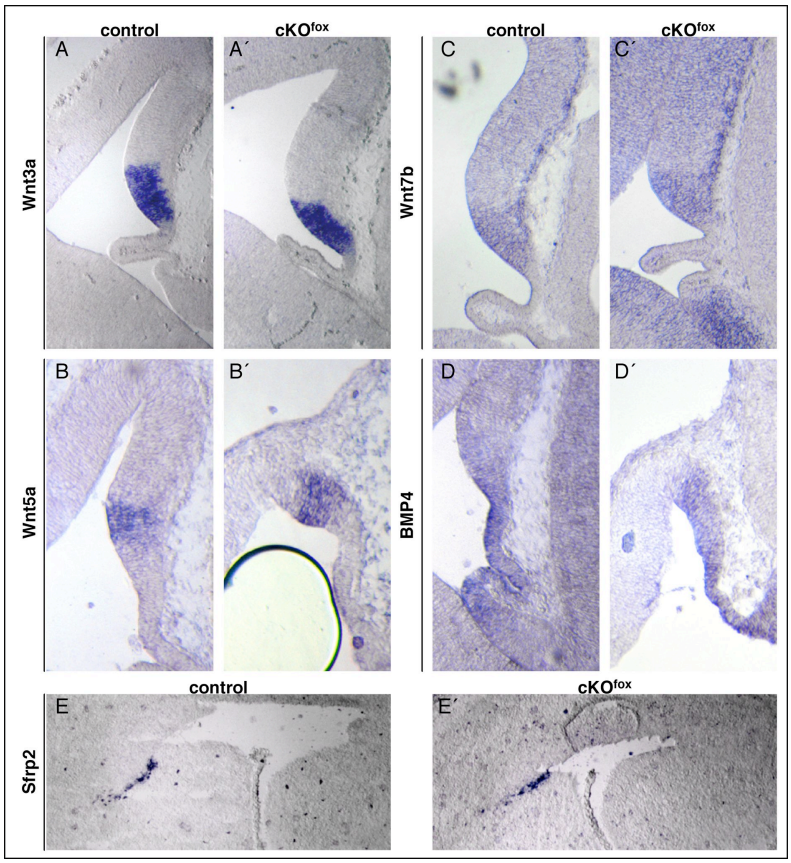

Figure 27: WNT/BMP signaling in the embryonic forebrain. ISH of E12.5 (A-D´) and E14.5 (E, E´) coronal sections. The expression of Wnt3a (A, A´), Wnt 5a (B, B´), Wnt7b (C, C´) in the cortical hem, BMP4 in the roof plate (D, D´) and the WNT antagonist Sfrp2 in the antihem (E, E´) is not affected in cKO.

WNT signaling plays a crucial role during the molecular patterning of the CNS, including the forebrain. Several WNT family members are expressed in the cortical hem, which antagonizes rostral signaling from FGFs. It is an accepted view that WNT signaling acts upstream of Emx2 and is able to induce its ectopic expression or causes enlargement of Emx2-expressing domains (Theil et al., 2002, Assimocopoulos et al., 2003, reviewed by Mallamaci and Stoykova, 2006). Therefore, we investigated the expression of Wnt3a, Wnt5a and Wnt7b in the cortical hem and the expression of the WNT antagonist Sfrp2 in the antihem. No changes of either expression domains were evident (Fig. 27) in cKO, suggesting that the affected Emx2 expression gradient is

probably not due to modulated WNT signaling. Additionally, this indicates a functional role of Sp8 in the forebrain that operates downstream or independent from WNT signaling.

To test, whether Sp8 might influence function of Emx2 through a direct interaction, like previously shown for the *Drosophila* orthologs (Schock et al., 2000), we performed GST-pulldown assay. SDS-PAGE analysis of GST-Sp8 and GST-Sp8 lacking Zn-fingers (GST-Sp8ΔZn) fusion proteins, incubated with either *in vitro* translated $^{[35]}$S-methionin labeled Emx2 or Emx2 isoform lacking the homeobox (Emx2ΔHox) reveals that both full-length proteins physically interact with each other *in vitro* (Fig. 26, G, lane 8). The truncated Emx2 isoform binds GST-Sp8 as well (Fig. 26, G, lane 7) However, Emx2 lacking the homeobox does not bind both Sp8-GST fusion proteins (Fig. 26, G, lane 3-4). In addition to conserved *in vitro* protein-protein interaction, the Sp8 expression gradient in cortical progenitors is not affected in Pax6KO or Emx2KO forebrains at E12.5 (Fig. 26, A-C). Taken together, our data indicates that in the forebrain, Sp8 directly interacts with Emx2 on the protein level and furthermore acts independent from Emx2 and Pax6.

2.4.3 A/P patterning in cKO mutants

Given the important role of Emx2 and Pax6 for cortical arealization (Fukuchi-Shimogori and Grove, 2003, Hamasaki et al., 2004, reviewed by O'Leary and Nakagawa, 2002, Sur and Rubenstein, 2005), the observed alteration of the Emx2 and Pax6 expression gradients in Sp8 cKO (Fig. 23, E, E′, F, F′, Fig. 28, A, A′, B, B′) prompted us to analyze intrinsic cortical regionalization at E18.5. The mature cortex is divided into three functionally distinct main areas. From anterior to posterior, these are the primary motor cortex, primary somatosensory cortex and primary visual cortex area, respectively. Recently, several genetic markers were identified and their expression used to characterize specific primary cortical areas (intrinsic cortical arealization, Nakagawa et al., 1999, Rubenstein et al., 1999, Zhou et al., 2001, reviewed by Mallamaci and Stoykova, 2006).

We assayed intrinsic molecular arealization by ISH on E18.5 sagittal sections. The expression of the EphA7 receptor labels the region of the motor/visual- and the EphrinA5 ligand the region of the somatosensory cortex, respectively (Nakagawa et al., 1999, Rubenstein et al., 1999). In the mutant cortex, the EphrinA5+ somatosensory domain extends rostrally (arrows Fig. 28, C, C′). Accordingly, the motor cortex area, normally expressing EphA7 at high levels, shrinks (Fig. 28, D, D′).

In addition, we examined the expression of ID2. The switch from high levels of ID2 transcripts in upper cortical layers to high ID2 expression in layer V neurons, normally highlights the border from motor cortex to somatosensory cortex (arrowhead Fig. 28, F) and more caudally the somatosensory/visual transition, respectively (Rubenstein et al., 1999) (black arrow Fig. 28, F). However in mutants, a homogenously high ID2 expression domain from caudal, up to the rostral cortex is typical (Fig. 28, F′). Furthermore, it is evident that expression of ID2 in upper layers of the putative motor cortex is lost in cKO (asterisk Fig. 28, F′). The enlarged ID2+ domain suggests a molecular caudalization of the pallium along the A/P axis in Sp8 mutants.

Finally, we assayed the expression of Coup-TF1, in the wild type strongly expressed in the visual-, but weak in medial/rostral areas (Zhou et al., 2001). Coup-TF1 expression in the cKO is strong in the caudal and medial CP; note that the transition to low Coup-TF1 levels is dramatically shifted towards the rostral cortex, when compared to controls (arrows Fig. 28, E, E´).

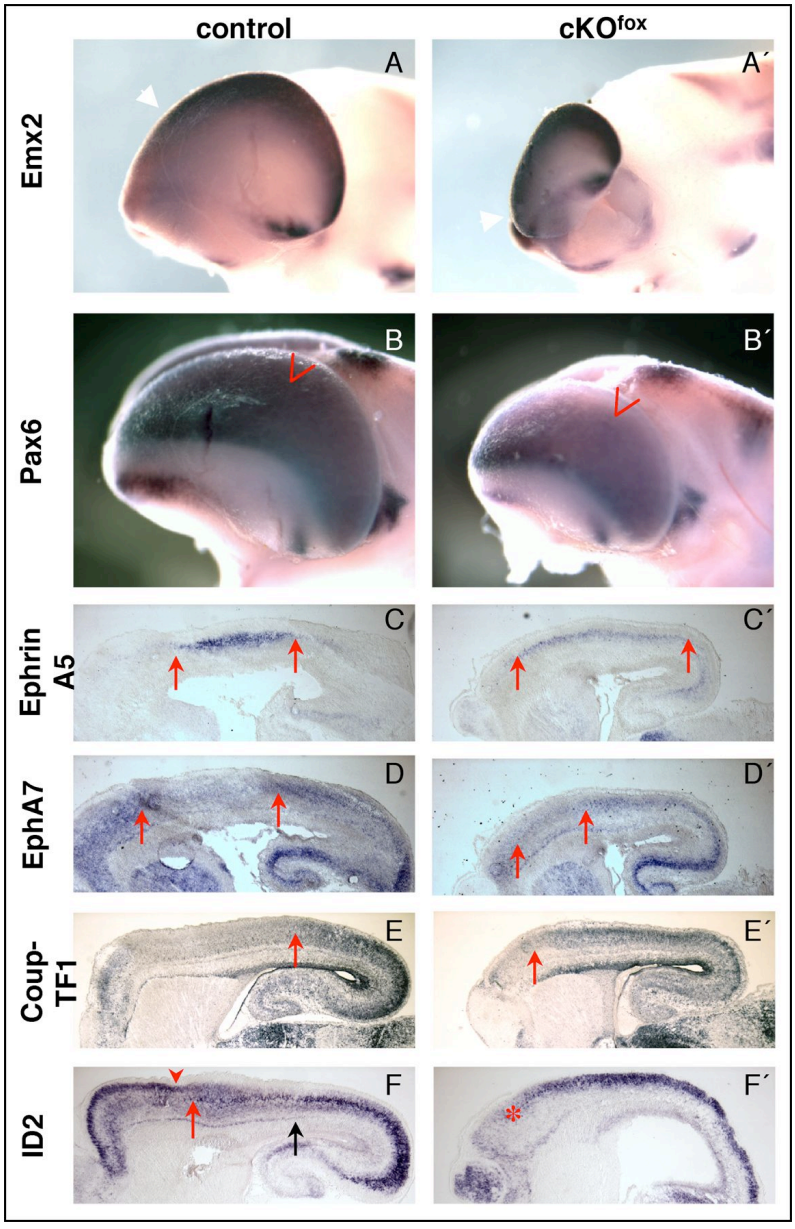

Figure 28: Caudalization of the molecular A/P of the Sp8 cKO telencephalon. WMISH on dissected E12.5 forebrains, using Pax6 and Emx2 mRNA probes (A, A´, B, B´). The Emx2 gradient is upregulated in cKO (arrows A, A´). Pax6 transcript levels are diminished (arrowheads B, B´) in Sp8 mutants. Analysis of the area specific marker genes EphrinA5 (C, C´), EphA7 (D, D´), Coup-TF1 (E, E´) and ID-2 (F, F´) on E18.5 sagittal sections, using ISH (rostral is to the left). The visual cortex area in cKO cortices appears extended towards the rostral brain, as demonstrated by EphA7, ID-2 and Coup-TF1 expression (strong rostral domain of EphA7 in D, D´, strong ID-2 domain in F, F´, strong domain of Coup-TF1 in E, E´). The somatosensory cortex area shifts rostrally in mutants (between arrows in C, C´, D, D´, between red arrowhead and black arrow in F, asterisk in F´) in Sp8 cKO. The motor cortex expression area appears condensed (rostral to left arrow in C, C´, D, D´) in Sp8 deficient specimens. ISH for EphrinA5/EphA7 (C, C´, D, D´) was performed on consecutive sections.

Taken together, these results indicate that in the absence of proper Sp8 function, the expression boundaries of caudal cortical areas extend rostrally. This finding suggests that Sp8 controls the A/P patterning of the forebrain, by respectively down- and upregulating the Pax6 and Emx2 expression gradients in cortical progenitors.

2.4.4 The caudalization of area-specific marker genes in cKO is correlated with functional domains

To test whether the caudalized molecular A/P axis of the cKO cortex keeps its functionality, we performed axon tracing by labeling E18.5 control and mutant brains simultaneously with the diffusible dyes DiI (red color) and DiO (green color). We retrogradely labeled thalamocortical axons by inserting a crystal of DiI into the presumptive visual/occipital cortex region. Subsequently, a crystal of DiO was placed into the presumptive somatosensory/parietal cortex (Bishop et al., 2000, Garel et al., 2003, Fig. 29, A, A´) as well. After 4 weeks diffusion time, we assayed the projection nuclei in the thalamus on coronal sections.
In controls, the red dye, inserted into the occipital cortex, specifically labeled neurons in the dorsal lateral geniculate nucleus (dLGN), a region in the dorsolateral thalamus. Conversely, green dye was only found in neuronal cell bodies of the ventroposterior complex (VP), medially of the dLGN (Fig. 29, B). However in cKO, such a clear separation of the two different dyes was not evident. Moreover it was obvious that a significant portion of retrograde green-labeled axons were found ectopically in the dLGN (Fig. 29, B´).

In addition, we inserted both dyes into the presumptive parietal cortex area (DiI slightly caudal to DiO, Fig. 29, C, C´). We expected that in controls, both dyes would retrogradely label neurons specifically in the VP – leaving the dLGN free of such retrograde labeling (Bishop et al., 2000, Garel et al., 2003). In accordance with this predicted thalamocortical connectivity, the red dye specifically labeled neurons in the lateral VP, while green staining was largely found in a more medial compartment of the VP in control samples (Fig. 29, D). In cKO brains, it was evident that a significant amount of dLGN neurons was labeled with the red dye. With respect to the described rostral extension of caudally enriched gene activity (Fig. 28), these DiI tracing

experiments strongly indicate a partial change of caudal cortical area identity in Sp8 mutants, due to the elevation of the Emx2 expression level.

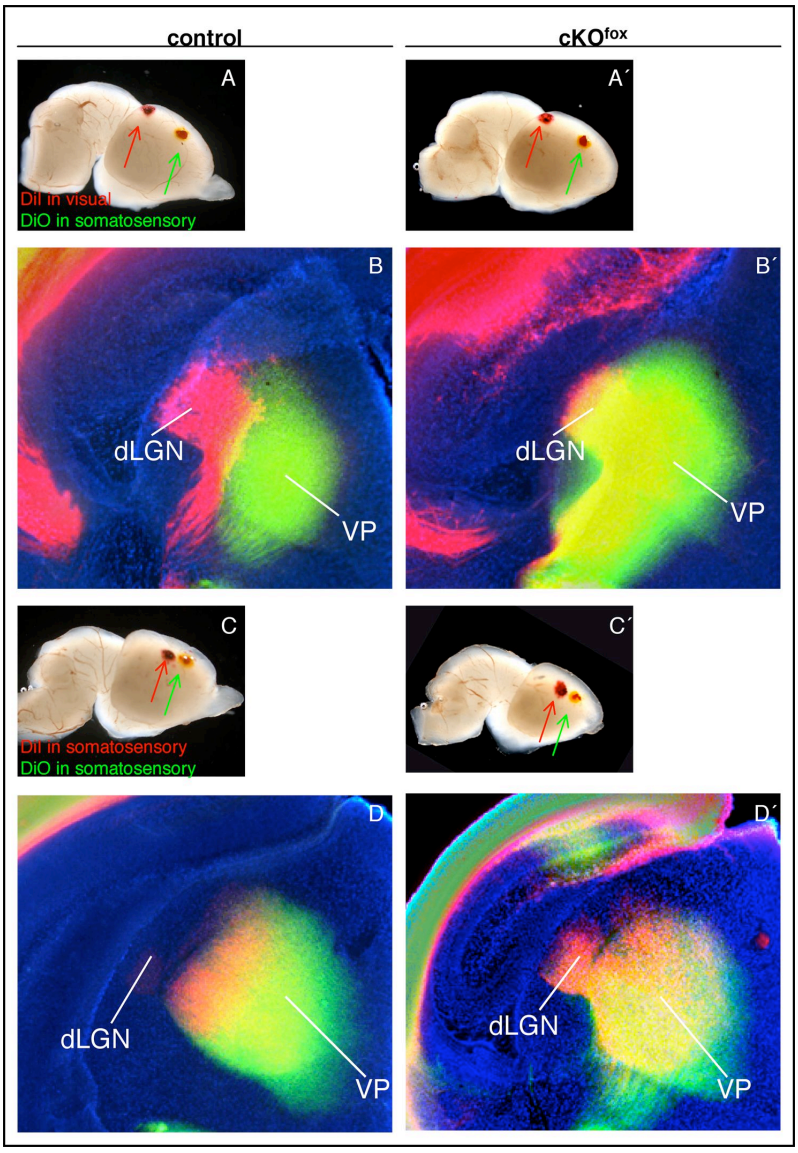

Figure 29: Functional enlargement of caudal cortical areas in cKO. DiI was injected in the visual cortex and DiO in the somatosensory cortex of E18.5 brains (arrows A, A´). Brains were additionally labeled with both dyes in the somatosensory cortex, respectively (arrows C, C´). (B, B´, D, D´). 100μm coronal sections after 4 weeks diffusion time, counterstained with DAPI. DiI retrogradely labeled neurons from the visual cortex to the dLGN in controls and cKO (red domain B, B´). However in cKO, some neurons (labeled with DiO) ectopically project into the dLGE as well (yellow domain in dLGE B´). In control embryos, only neurons in the VP are labeled (green domain B). DiI and DiO (injected into the somatosensory cortex), only traces the lateral and medial domain of the VP (red, yellow, green domain D) in controls. Conversely in cKO, DiI (red) ectopically labels neurons in the dLGE (red domain D´), indicating a partial change of caudal cortical area identity. dLGE: Dorsal Lateral Geniculate Nucleus, VP: Ventroposterior Nucleus.

2.4.5 cKO neuronal progenitors have normal cell cycle characteristics

The histological analyses revealed that Sp8 mutants develop a strong hypoplasia of the forebrain. This indicates that a variety of neurons is either not generated or died. The relative growth rates of tissues during embryonic development are on one hand controlled by a tight balance of cellular proliferation, and on the other hand by coordinated elimination of super numerous cells by apoptosis (reviewed by Chan et al., 2002). Recently, an increasing number of molecules, which are able to control and influence these processes, were identified (Depaepe et al., 2005, Putz et al., 2005).

In addition, Sp8 function was shown to control proliferation in the midbrain (Griesel et al., 2006). We therefore analyzed cell cycle parameters on E12.5 sections. To test S-phase parameters, we labeled E12.5 embryos with a BrdU-pulse. Immunohistochemical detection and counting of positive nuclei on sections (S-phase labeling index), however, did not show significant differences in the BrdU-uptake behavior, when Sp8 is not functional (Fig. 30, G, G´, H, H´, J).

Furthermore, detection and counting of forebrain cells, positive for the M-phase marker phospho HistoneH3 displays comparable values in mutant and control embryos (Fig. 30, D, D´, E, E´, F). Thus, in conditional forebrain mutants the tested S- and M-phase parameters are not affected at E12.5.

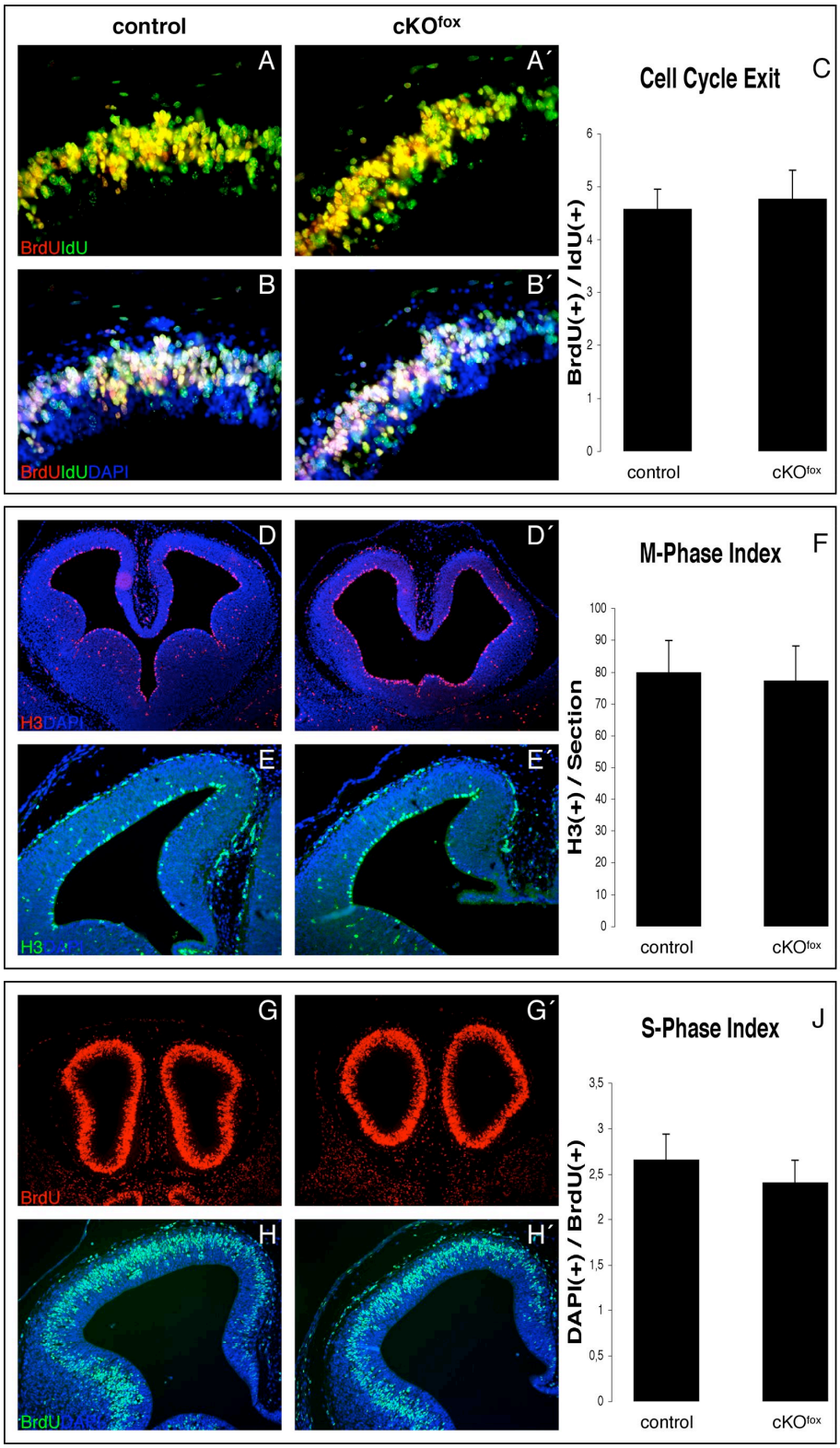

Figure 30: The cell cycle is not affected in cKO. Estimation of cell cycle parameters, using BrdU- (1 hour pulse labeling G-H´, quantification in J, n=5), Phospho Histone H3- (D-E´, quantification in F, n=4), and BrdU/IdU staining (sequential injection approach, Martynoga et al., Burns et al., 2005 in A-B´, quantification in C, n=3) on representative E12.5 coronal sections. None of the tested cell cycle parameters were significantly abnormal in Sp8 conditional mutants.

In addition, staining for the neuronal marker Tuj does not reveal a possibly occurring premature differentiation (Fig. 31, A, A´, B, B´, C, C´). Nevertheless, it remained possible that lengthening of the cell cycle may cause the reduced brain size in cKO. A similar phenotype was previously reported in Foxg1 knockout mice (Martynoga et al., 2005). Noteworthy, the expression of this forkhead transcription factor is not modulated in Sp8 mutants (Fig. 31, D, D´). To check the cell cycle exit of cortical neuronal progenitors in more detail, we took advantage of a sequential labeling and detection approach with BrdU and IdU at E12.5. This technique allowed us to calculate the fraction of cells, leaving the cell cycle within the labeling interval (Burns and Kuan, 2005, Martynoga et al., 2005). However, in Sp8 mutants and controls, no difference could be detected (Fig. 30, A, A´, B, B´, C). In summary, our results show that proliferation and cell cycle progression is not affected in cKO at E12.5.

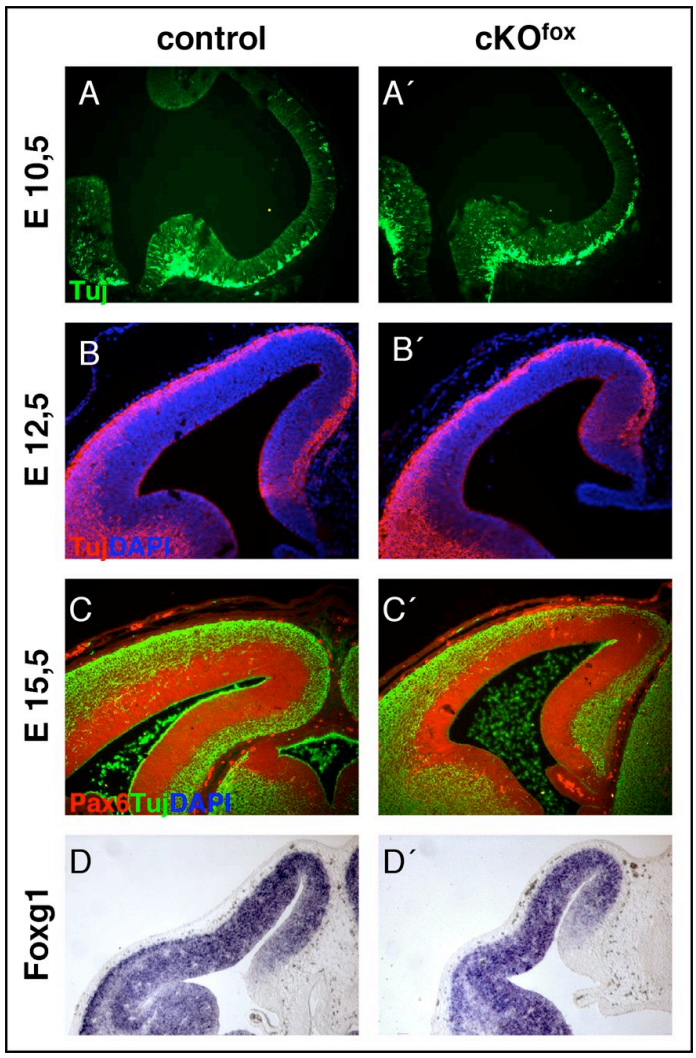

Figure 31: No premature differentiation in cKO. Immunohistochemistry for Tuj- (A, A´, B, B´) and Tuj/Pax6 (C, C´) antibodies on coronal sections. Tuj staining reveals no increase in the thickness of the CP of cKO at E10.5 (A, A´), E12.5 (B, B´), and E15.5 (C, C´). ISH for Foxg1 mRNA on E12.5 coronal sections appears normal in cKO (D, D´).

2.4.6 Sp8 controls cell death in the embryonic forebrain

Our findings so far indicate that the neuronal loss and the hypoplasia of the forebrain in Sp8 cKO are not due to changes of cell cycle characteristics. Therefore, we checked the abundance of programmed cell death on E12.5 forebrain sections by using TUNEL assay. This approach visualizes apoptotic cells by a specific detection of characteristic DNA fragmentation in pycnotic nuclei during the terminal phase of programmed cell death.

We found a dramatic increase in the content of TUNEL+ cells (Fig. 32, A, A´, B, B´) in Sp8 mutant samples. The distribution of TUNEL+ cells was random, without significant differences in density when comparing cortex to basal ganglia, and caudal to rostral forebrain, respectively (Fig. 32, A, A´, B, B´, data not shown). Apoptotic cells in cKO often formed clusters, containing three to six individual nuclei (arrow, inset Fig. 32, C). Statistically, these cell aggregates were considered as one cell. To affirm that mutant brains show increased programmed cell death, we additionally immunolabeled E15.5 sections with an antibody for activated Caspase3, a specific marker for apoptosis. Positive cells were super numerous in cKO (Fig. 32, F, F´), underlining that excessive apoptosis takes place.

A time course of TUNEL activity on E10.5, E15.5 and E18.5 tissue sections revealed that cKO sections contain six times more apoptotic cells at stage E10.5 and three times more from stages E12.5 to E18.5 (Fig. 32, E). We furthermore found TUNEL+ nuclei at E15.5 predominantly in the ventricular/subventricular zone (Fig. 32, D; 78,4% TUNEL+/Tuj- at E15.5, n=2) and less abundant in the intermediate zone (white arrows Fig. 32, D) or the cortical plate (blue arrow Fig. 32, D).

We conclude that conditional Sp8 inactivation leads to severe forebrain hypoplasia by inducing excessive and progressive apoptosis. Furthermore, it appears that enhanced cell death in cKO affects some postmitotic neurons, but mainly early neuronal progenitors.

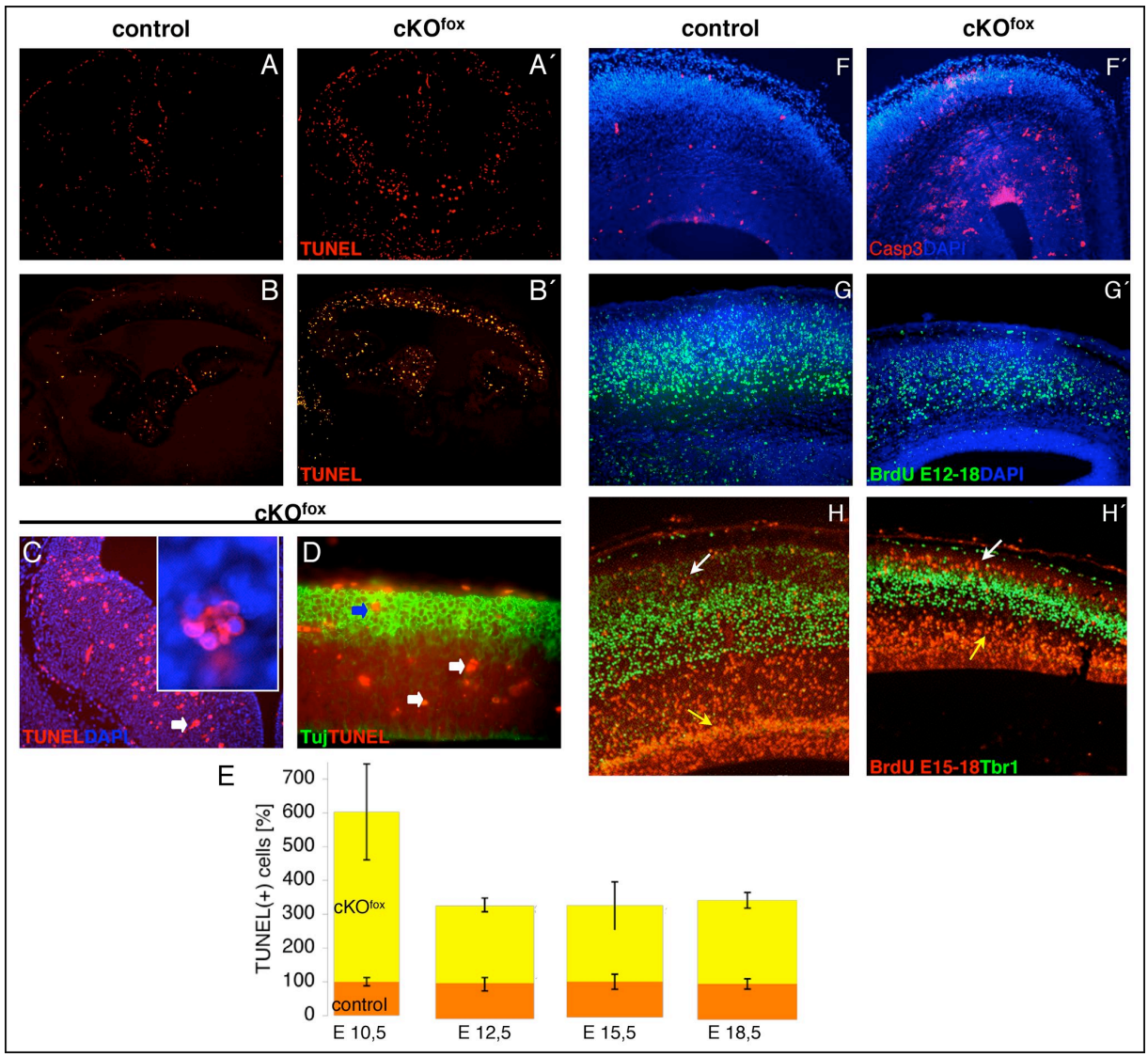

Figure 32: Loss of Sp8 induces excessive progenitor apoptosis. TUNEL staining on E12.5 (coronal, A, A`, C) and E15.5 forebrain sections (sagittal, B´, B´, D, rostral is to the left). The arrow in C demarcates a typical cluster of apoptotic cells, found in cKO. Those clusters were observed from E12.5 to E18.5. Clusters typically contained 5-7 apoptotic cells (blow-up in C). (D): Tuj/TUNEL double staining in cKO reveals TUNEL+ cells within the putative CP (blue arrow) and presumptive proliferative zones and the IZ (white arrows). Quantification of TUNEL+ nuclei on E10.5, E12.5, E15.5 and E18.5 forebrain sections (E, n=3-4 for each stage) shows an increased cell death without Sp8 function. Immunolabeling using a Caspase3 antibody reveals super numerous Caspase3+ cells in cKO sections (F´), as compared to controls (F). Fate mapping of early-born (G, G´) and late-born (H, H´) pallial neurons using BrdU injection at E12.5 or E15.5 on E18.5 sagittal sections. Putative early-born neurons migrate through the CP (G, G´). Their number is diminished in mutant cortices (G´) as compared to controls (G). In cKO, BrdU+ neurons populate ectopic positions in the upper CP, when compared to the relative position of Tbr1 immunoreactive cells (white arrow H´), possibly reflecting the thinned cortex. BrdU labeling at E15.5 appears reduced in the SVZ of mutants (yellow arrow H, H´).

2.4.7 Preplate development in cKO mutants

By considering severe apoptosis starting early during cortex development and its potential influence on subsequent corticogenesis, we investigated the formation of the preplate (PPL) in Sp8 cKO, the primary stage of cerebral cortex development. The PPL contains early-born (E10-11.5) postmitotic neurons of pallial origin. Later born neurons from the pallium and tangentially migrating subpallial interneurons will progressively split the PPL into the marginal zone (MZ), the subplate (SP) and the cortical plate (CP) proper (Hevner et al., 2001, Kolk et al., 2005, Dupont et al., 2006, Rakic et al., 2006). The separation of the transient subplate cells to a position below the arising CP was shown to be crucial for the formation of normal cortical projections. With respect to the handshake hypothesis, incoming thalamic axons use SP cells as a pioneering substrate during their invasion of cortical target areas (reviewed by Molnar et al., 2006).

By using ISH for Tbr1, we labeled early PPL and SP cell populations (Hevner et al., 2001, Kolk et al., 2005) at midgestation. In controls, Tbr1+ (Fig. 33, A) SP cells are well separated from CP cells and those inside proliferative compartments of the cortex. In cKO samples, there is, however, no evident separation of those SP- and CP cells (Fig. 33, A´).

Two possibilities might presumably explain this alteration of PPL development in cKO: Firstly, all SP cells die by apoptosis or secondly, the PPL will not split in Sp8 cKO. We therefore performed a suitable fate labeling approach: We injected BrdU at E11.0 (to label specifically SP-cells) and harvested tissue after a visible separation of SP and CP, e.g. visible in Fig. 33 A). Subsequently, detection of BrdU together with Tbr1 antibodies enabled us to follow the laminar position of double positive (putative) SP cells (Rakic et al., 2006).

In controls, double positive cells were indeed found in the SP (arrow Fig. 33, C). Conversely in cKO, double positive cells were positioned ectopically in superficial layers of the CP and MZ (arrow Fig. 33, C´). Virtually none of them occupied positions comparable to controls (Rakic et al., 2006). Hence, the cKO cortex develops no precise subplate, and we conclude that proper splitting of the PPL does not occur in Sp8 mutants.

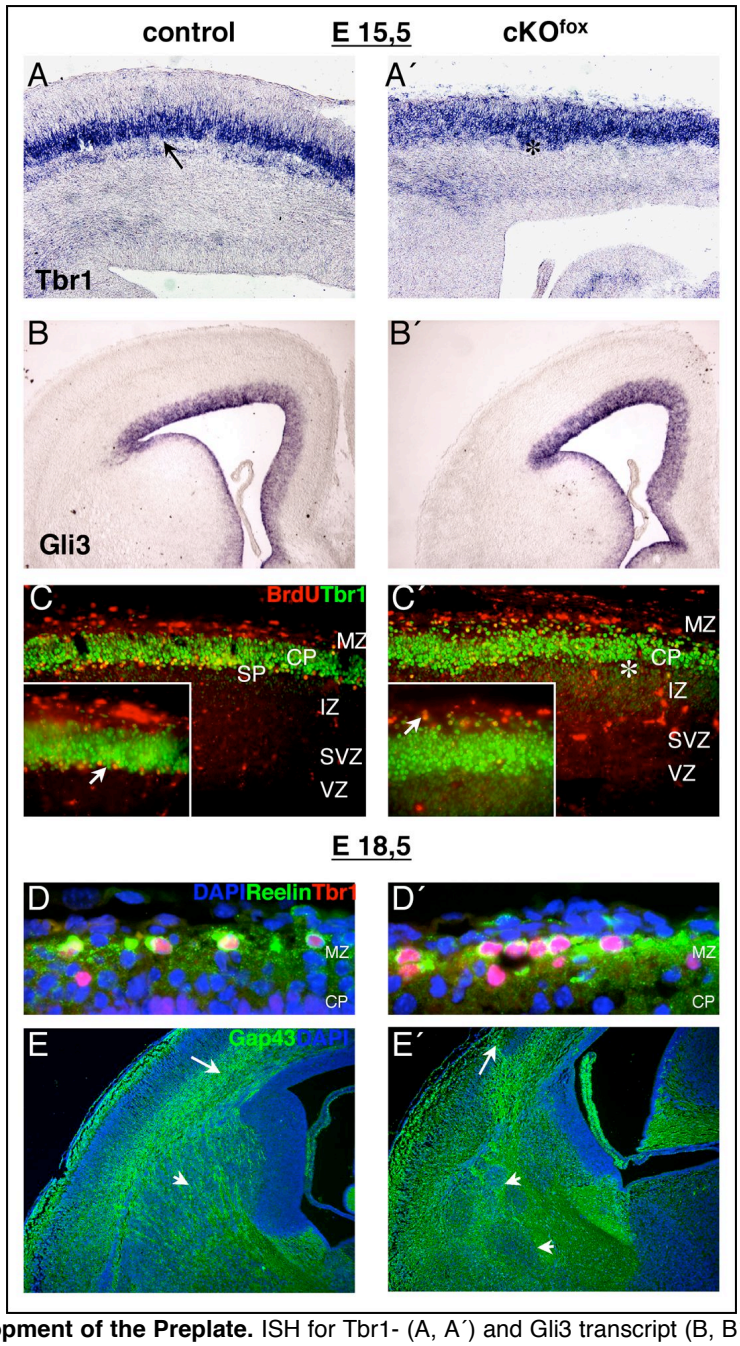

Figure 33: Development of the Preplate. ISH for Tbr1- (A, A´) and Gli3 transcript (B, B´) on E15.5 coronal sections (medial is to the right). Immunohistochemical co detection of Tbr1 and BrdU on E15.5 sagittal sections (rostral is to the left) (C, C´). Mutants lack clearly separated Tbr1+ – putative subplate – cells in the CP at E15.5 (asterisk, arrow A, A´). At this stage, BrdU+ (injected E11) cells, colabeled with Tbr1, populate the upper CP/MZ in cKO (arrow C´). In controls, those cells settle in the subplate (arrow C). (Insets C, C´): Representative blow-up images of the cortex regions shown in (C, C´). Arrows indicate the dislocation of BrdU+/Tbr1+ cells in mutants. Co detection of Reelin- and Tbr1 protein in the MZ on coronal sections at E18.5 (D, D´, medial is to the right) cKO comprise more Reelin+/Tbr1+ in the MZ (D´). The PPL does not split properly in cKO; additionally Gap43+ axons (on E18.5 coronal sections) form bundles around the internal capsule (arrowheads E, E´) and some axons project ectopically into the MZ (arrow E, E´), possibly reflecting a direct consequence of the defective subplate formation.

Recent data indicate that Gli3 is an important factor for the early PPL development (Theil, 2005). However, ISH reveals an identical expression pattern of Gli3 in mutant and control embryos (Fig. 33, B, B´). Additionally, Shh was shown to be crucial for the

early patterning of the forebrain by regulating the Gli3 repressor function. Both factors appear not affected in Sp8 mutants (Fig. 23, B, B´). Hence, the preplate defect does not result from Gli3-SHH signaling alterations.

To analyze, if the wiring of cortical axons is affected in Sp8 mutants, we performed staining for the neurofilament marker Gap43. Detection of Gap43 with an antibody visualizes fiber tracts in the E18.5 caudal cortex and the sub cortical connectivity. Gap43 staining in controls reveals an organized IZ, containing efferent and afferent fibers (arrow Fig. 33, E). Also, the internal capsule is traversed by many Gap43+ fibers (arrowhead Fig. 33, E). However in mutants, Gap43+ fibers form aberrant bundles within the internal capsule, with some neurons projecting ectopically into the MZ. Furthermore, the wiring of axons is disorganized in the IZ (arrows, arrowheads Fig. 33, E´) of Sp8 cKO. These axon trajectory abnormalities probably display a developmental consequence of the missing SP function and abnormal splitting of the PPL in Sp8 mutants (Dupont et al., 2006, Rakic et al., 2006).

2.4.8 Timing of neurogenesis and radial migration in Sp8 conditional mutants

The splitting of the preplate is an early and crucial process during embryonic corticogenesis. To determine in more detail how cortical development occurs in the absence of a regular subplate in cKO, we subsequently investigated important parameters of cortex development, like radial migration and specification of layers, in Sp8 conditional mutants.

Early-born cortical neurons will settle in deep cortical layers, conversely late-born neurons will populate the superficial CP, following a functional inside-out pattern (Noctor et al., 2004, reviewed by Mallamaci and Stoykova, 2006). By injecting BrdU at E12.5 (i) or E15.5 (ii) and sampling of the injected specimens at E18.5, we created samples, which had BrdU exclusively incorporated in early- (i) or late-born (ii) neurons. Analysis of E12.5-injected samples revealed that BrdU+ cells populated the deep CP and some migrated still in intermediate positions of the CP (Fig. 32, G). Mutant brains thereby showed a dramatic reduction (34.7%, ± 7,8% of wild type, n=3) of BrdU+ nuclei, but they were positioned comparable to control samples (Fig. 32, G´). Cells, labeled with BrdU at E15.5, populate mainly deep compartments (still migrating within the intermediate zone, towards their final position) (Fig. 32, H). One fraction of labeled cells was found (yellow arrow Fig. 32, H) in the cortical subventricular zone (SVZ) in mutant and control embryos. In the mutant cortex, the content of BrdU+ cells in the proliferative compartment is diminished (85.4% ± 3.8% of control, n=3; yellow arrow Fig. 32, H´) and much more labeled cells are seen within upper most positions of the CP (arrow Fig. 32, H). This distribution possibly reflects that, due to the reduced distance between the proliferative zones and the MZ in Sp8 mutants, neurons need less time to migrate to the apical surface. Furthermore, this analysis indicates that depletion of the early progenitor pool by apoptosis results in a diminished generation of cortical neurons in cKO.

To investigate, whether the generation of infra/supragranular layers is preserved in mutants, we labeled late-born/upper cortical neurons with Cux2 (Nieto et al., 2004, Zimmer et al., 2004), using ISH on E18.5 combined with immunolabeling for Tbr1, tracing early-born/lower layer neurons (Kolk et al., 2005) (i). The subsequent

combination of captured images revealed that in mutants and controls, Cux2+ cells were found in uppermost layers, and migrating radially within the CP, while most of the Tbr1+ cells were conversely found in deep cortex positions (Fig. 34, A, A´, B, B´, C, C´).

In addition, we analyzed specimens with a BrdU fate-labeling interval from E15.5 to E18.5 by double labeling with Tbr1- and BrdU antibodies (ii). We could never observe colocalization (Fig. 32, H, H´, Fig. 34, C, and C´) of the markers Cux2 and Tbr1 (i), or Tbr1 with BrdU (ii, applied E15.5). This indicates that – despite of the preplate splitting defect – the basic laminar organization of the cortex is not distorted in conditional Sp8 mutants. Moreover, the switch from early to late neuronal fate occurs correctly in cKO.

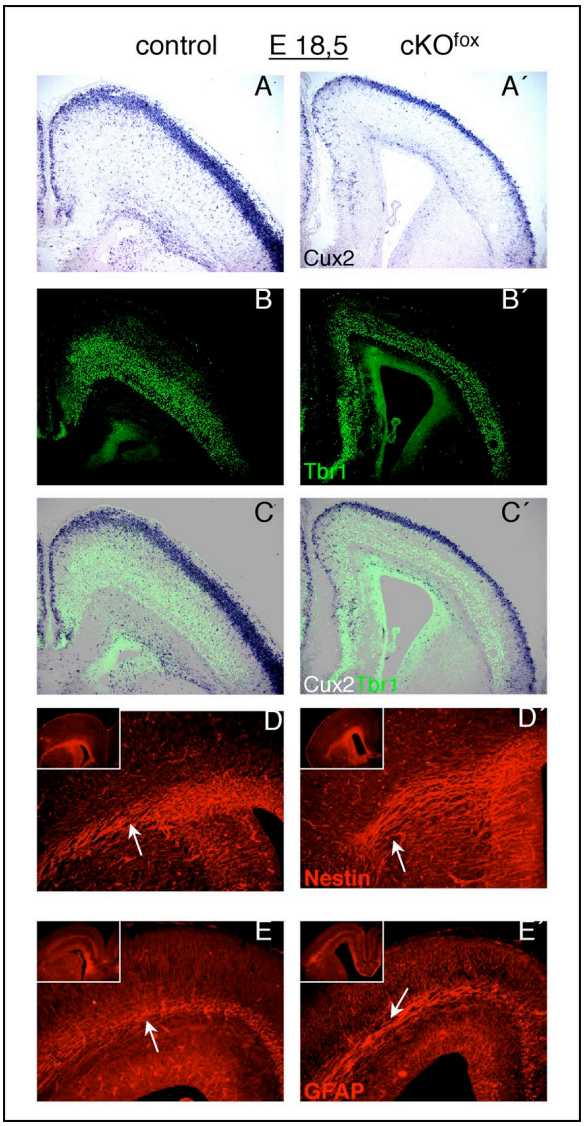

Figure 34: Timing of cortical neurogenesis and radial glia morphology. Coronal (E18.5) sections were double labeled with the Cux2 riboprobe and the Tbr1 antibody (A-C´). Cux2+ and Tbr1+ cell populations are separated from each other in controls and mutants (C, C´). Therefore, the generation of infra/supragranular layers seems preserved in Sp8 mutants. Coronal (E18.5) sections immunolabeled for glia markers GFAP and Nestin (D-E´). In cKO, the wiring and the morphology of radial glia cells appear affected (arrows D-E´).

Although cKO embryos die at birth (so that we are not able to get access to the postnatal maturation of the cortical layer formation), we wanted to assay components of the radial migration machinery. Radial migration in the cortex is directly linked to the function of radial glia cells. It was shown that migrating cortex neurons use glial processes as a substrate on their way upward, into the correct laminar position of the CP (reviewed by Campbell and Gotz, 2002). In this respect, we used GFAP and Nestin

antibodies as markers for radial glia cells.

Immunohistochemistry for these markers on E18.5 brain sections showed us that in cKO radial glia cells appear affected, because the morphology and wiring of these cells and their processes was disorganized and defasciculated (arrows in Fig. 34, D´, E´).

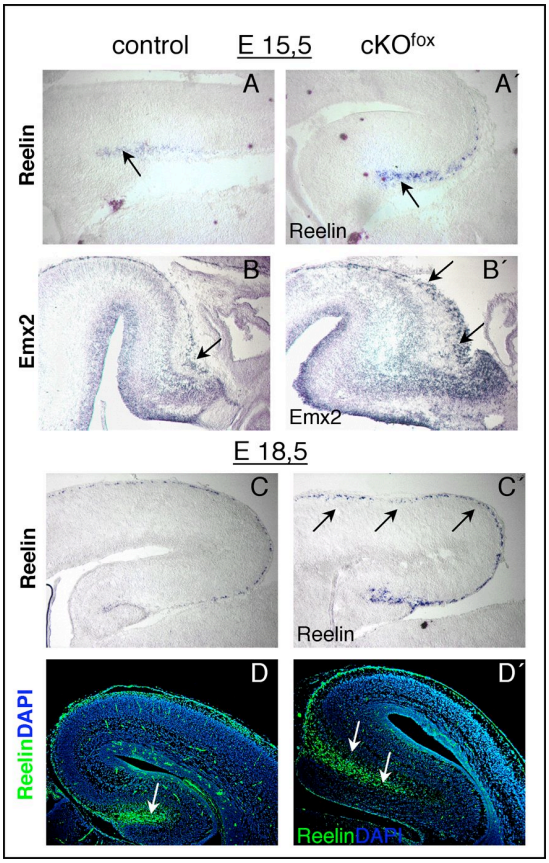

Figure 35: Excessive Reelin+ cells in the cKO cortex. ISH for Reelin shows an increase in the content of Reelin+ cells at E15.5 (A, A´) and E18.5 (C, C´) in the MZ of cKO. Immunohistochemical detection of Reelin on E18.5 coronal sections highlights an enlarged cingulum in mutants (arrows (D, D´) and super numerous Reelin+ cells in the cortex (142%, n=3). The upregulation of Emx2 in the hippocampal region at E15.5 (on coronal sections, arrows B, B´) might sustain the overproduction of Reelin+ cells.

Another important mechanism for the correct positioning of neurons in the cortex is the Dab1-mediated Reelin signaling pathway (reviewed by Tissir and Goffinet, 2003). *In situ* detection of Reelin mRNA at E15.5 and E18.5 uncovered that the number of Reelin+ cells in the MZ is increased in Sp8 mutants (Fig. 35, A, A´, C, C´). These findings were confirmed by the detection of Reelin protein by using a specific antibody and quantifying Reelin+ cells on E18.5 sections (142.2%, ± 6.4% of controls, n=3). It also appeared that the subgranular layer of the subiculum/CA1 area, where pallial CR cells are born (Shinozaki et al., 2002), is enlarged in Sp8 mutants (arrows in Fig. 35, D, D´). Recent analysis of Emx2- and Emx1-deficient mice revealed that Emx2 is sufficient and crucial for the generation and survival of pallial CR cells (Shinozaki, 2002). In our cKO mice, Emx2 expression levels remain progressively upregulated in the hippocampal region and medial pallium in E15.5 mutants (Fig. 35, B, B´). Therefore, in the absence of Sp8 function, the overproduction of CR cells is probably related to the upregulation of Emx2.

2.4.9 The Specification of individual cortical layer neurons is abnormal in cKO mutants

The specification of distinct cortical neuron subtypes during embryonic development leads to functional heterogeneity of cortical layers and functional neuronal circuits (reviewed by Guillemot et al., 2006, Mallamaci and Stoykova, 2006, Molnar et al., 2006). Our *in situ* data already highlighted that in Sp8 mutants, the MZ is hyper cellular and contains more CR cells. Additionally, the content of subpallial interneurons marked by Gad67 is strikingly reduced, suggesting further involvement of Sp8 in cortical cell type specification. To test potentially affected cell population in the Sp8 mutant CP, we assayed appropriate molecular markers at E18.5.

First, we tested for Tbr2-immmunoreactivity, a specific marker of SVZ progenitors of late-born glutamatergic projection neurons (Englund et al., 2005). The Tbr2+ cell content in the SVZ is largely reduced in cKO brains from E15.5 (data not shown) to E18.5 (49.4%, ± 4.3% of controls, n=3; square Fig. 36, E, E′), suggesting a reduced production of upper cortical laminae. In addition, this demonstrates that the early pool of cortical progenitors, which was reduced through apoptosis, is accompanied by the depression of SVZ progenitors. As a direct consequence, the expression of the upper layer neuron marker Lhx2 (Nakagawa et al., 1999) is strongly diminished (Fig. 36, C, C′) in mutants.

Cux proteins were recently implicated to have a functional role during cell type specification of SVZ progenitors and therefore for the upper cortical layers (Nieto et al., 2004, Zimmer et al., 2004). In addition to the evidently reduced content of Cux2+ neurons in the CP of mutants (Fig. 36, B′), we did not detect Cux1 mRNA in the Sp8-deficient CP at E15.5 (data not shown) and E18.5 (Fig. 36, A′). This indicates that the upper cortical layers of cKO are devoid of Cux1+ neurons.

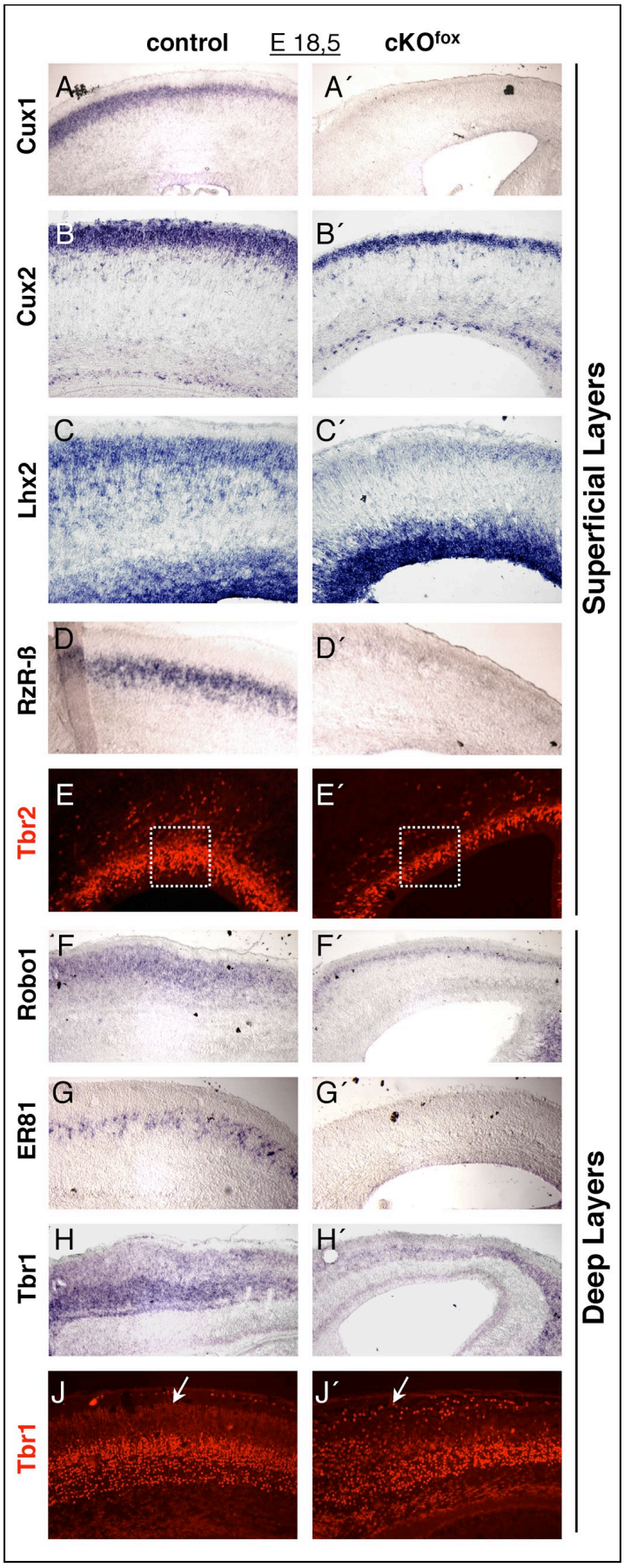

Figure 36: The specification of individual cortical layers is abnormal in cKO. ISH of layer-specific marker genes on E18.5 coronal (A, A´, C, C´, D, D´, G, G´ medial is to the right) and sagittal (B, B´, F, F´, H, H´, rostral is to the left) forebrain sections. Detection of Tbr1/2 protein on E18.5 coronal sections (E, E´, J, J´. medial is to the right). A reduced expression of Cux2 (B, B´), Lhx2 (C, C´), Robo1 (F, F´) and Tbr1 (H, H´) is visible in mutant cortices. In Sp8 cKO, subpopulations of Cux1+ (A, A´), RzR-ß+ (D, D´), and ER81+ (G, G´) cortical neurons are not molecularly specified. Tbr2 immunoreactive progenitors are diminished in the proliferative compartment of the Sp8 mutant cortex (square E, E´). Correlating to an affected PPL splitting, immunohistochemistry reveals that some Tbr1+ cells ectopically populate the upper CP and MZ in Sp8 mutants (arrow J, J´).

The orphan nuclear receptor RzR-ß was utilized to follow the genesis of layer IV (Rubenstein et al., 1999). At stage E18.5, RzR-ß+ neurons are completely missing in the CP of mutants (compare Fig. 36, D, D´). These findings are consistent with the previous observation of the reduced content of Cux1/2+ and Lhx2+ neurons, and strongly suggest that the pool of SVZ progenitors is diminished in cKO, due to the progressive death of neuronal progenitors.

ER81 was then implemented to trace a subpopulation of layer V neurons (Rubenstein et al., 1999), but we could not detect ER81 mRNA within the CP of E15.5 (data not shown) and E18.5 cKO cortex (Fig. 36, G´). Conversely, these neurons remained clearly visible in the CP of controls (Fig. 36, G). However, the examination of another marker of layer V neurons (Robo1) revealed that the content of Robo1 mRNA appears diminished in cKO. This demonstrates that in Sp8 mutants, Robo1+ layer V neurons (Rubenstein et al., 1999) are molecularly specified, but generated in a reduced quantity, when compared to controls (Fig. 36, F, F´).

Tbr1 is essential for the formation of layer VI (Hevner et al., 2001) and the subplate (Kolk et al., 2005) in mice. The detection of Tbr1 mRNA by ISH reveals layer VI neurons in the deep CP in mutants and controls (Fig. 36, H, H´). However in cKO, the staining only shows a less thick band of Tbr1 mRNA, when compared to controls, indicating that a diminished quantity of Tbr1+ (layer VI) neurons is evident in Sp8 mutants. By performing Tbr1 antibody staining we identified ectopic Tbr1+ cells in the superficial CP and MZ of cKO (Fig. 36, J, arrow J´). This finding reflects the affected positioning of neurons, due to the preplate splitting defect in mutants (Rakic et al., 2006).

Taken together, it appears that although the layering of the mutant cortex is not affected by the loss of Sp8, neuron subpopulations of Layer V (ER-81+), Layer IV (RzR-ß+) and Layer II/III (Cux1+) are not molecularly specified. Furthermore, the extension of all cortical laminae is hampered, due to the depletion of neuronal precursors by apoptosis.

2.4.10 Sp8-deficiency affects the generation of olfactory bulb neuroblasts within the dLGE

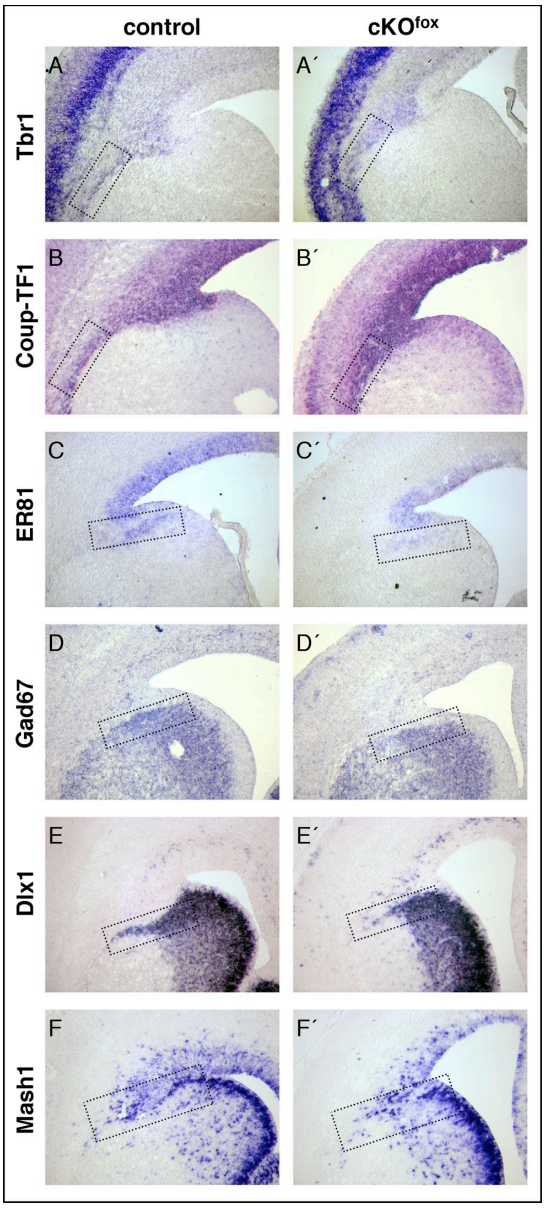

Figure 37: Enlarged RMS and reduced dLGE marker gene domains in cKO. ISH on E15.5 coronal sections reveals that the Tbr1+ and Coup-TF1+ cells in the RMS appear defasciculated in cKO (squares A-B´). Further the expression domain of ER81, Gad67, Dlx1 and Mash1 in the dLGE appears diminished in mutants and therefore suggests a depressed generation of OB neuroblasts (squares C-H´).

Morphological analysis already indicates that Sp8 mutants lack the olfactory bulbs (OB). This structure consists of neuroblasts and neurons, which are born in the embryonic dLGE and postnatally in the SVZ of the lateral ventricles. They reach the OB by migrating through the rostral migratory stream (RMS). Several genes, which are expressed in these domains, (like Tbr1, Dlx1), where shown to represent marker genes for specific subpopulations of olfactory bulb projection neurons or interneurons (reviewed by Lopez-Mascaraque and Castro, 2002). To address the molecular mechanisms underlying the disgenesis of the OB in cKO, we examined associated marker genes by using ISH on E15.5 sections.

In Sp8 conditional mutants, the expression of ER81, Gad67, Dlx1 and Mash1 in the dLGE appears downregulated when compared to control samples (squares Fig. 37, C-F´). Conversely, it seems that Coup-TF1 expression is upregulated in the forebrain and RMS of mutants (Fig. 37, B, B´). Note that the diameter of the area, which is occupied by Coup-TF1+ cells in the RMS, appears extended in cKO compared to controls (square Fig. 37, B,

B´). Therefore, we assayed the expression of another marker for OB projection neurons, Tbr1. Accordingly; the Tbr1 expression domain in the RMS seems as well expanded in mutants (square Fig. 37, A, A´). Analysis of cell density on nissl-stained sections in this area by counting did not reveal differences in mutant and control sections (data not shown), indicating that the mutant RMS appears defasciculated, hence occupies a broader area than in controls. This data is in accordance with the Nestin staining (Fig. 34, D, D´), highlighting that the area of the radial glia fascicle appears much wider at the PSB of Sp8 conditional mutants. Furthermore, our analysis indicates that several subpopulations of OB projection neurons are present, but several domains of interneuron marker genes in the dLGE are reduced in Sp8 mutant forebrains at E15.5.

2.4.11 Affected migration of neuroblasts within the RMS of cKO

The marker gene expression at E15.5 revealed that the generation of olfactory neuroblasts seems affected, but not completely depleted in cKO. Although a normal OB is missing in cKO we analyzed, whether migrating OB neuroblasts might be relocated to an ectopic position. This issue urged us to investigate cell migration in the ventral telencephalon. By using appropriate marker genes we analyzed the relative position of cells in the mutant subpallium, correlating with prominent compartments of the olfactory bulb-anlage in controls.

At midgestation, the expression domains of Pax6 and Ngn2 mark cells of the inner most ventricular layers of the OB in control samples (Fig. 38, A, C), later forming the glomerular- and periglomerular layers. ER81+ cells are found in a laminar position, superior to Pax6+ and Ngn2+ ones (Fig. 38, E), designed to contribute to the granule-, mitral cell- and the glomerular layer. The outermost layers of the OB-anlage at E15.5 are populated by projection neurons, positive for Tbr1 and ID2 (Fig. 38, G, J), highlighting neuron populations of the mitral- and the glomerular layer. Our analysis of mutant samples identified cellular aggregates in the ventrolateral forebrain. Those patches contained cells, which were positive for the assayed markers (Pax6, Ngn2, ER81, Tbr1 and ID2, squares Fig. 38, B´, D´, F´, H´, K´). We therefore conclude that these accumulating cells might correspond to an olfactory bulb-like structure, previously reported in Sey mice (Jimemez et al., 2000).

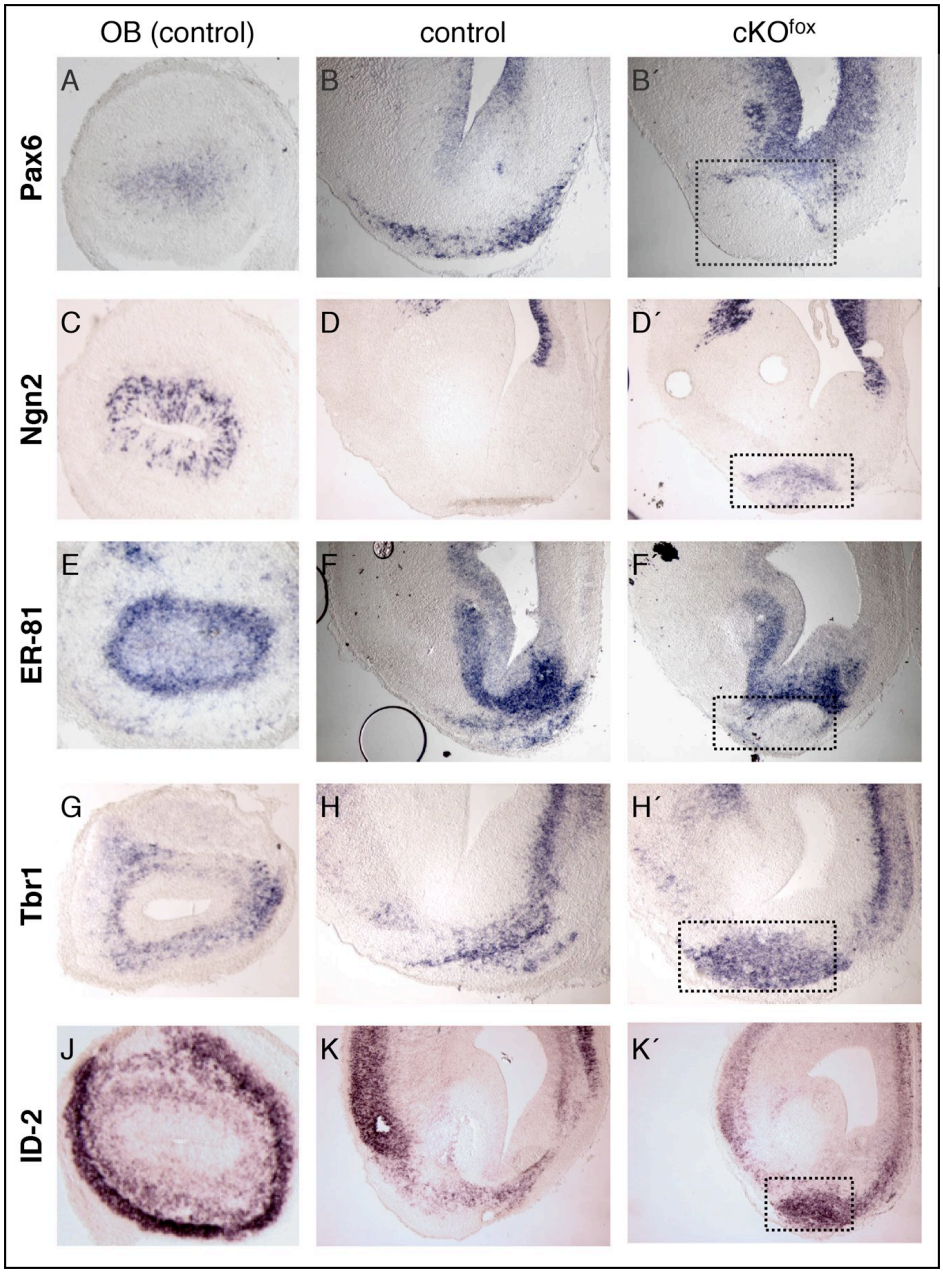

Figure 38: Abnormal aggregation of cells in the ventral telencephalon of cKO. ISH, using marker genes for OB neuron populations on E15.5 coronal sections. In controls Pax6, Ngn2, ER81, Tbr1 and ID2 mark different populations of neurons in the E15.5 OB (A, C, E, G, J). In cKO, those cell populations are found accumulated in the ventromedial telencephalon (B´, D´, F´, H´, K´). Those aggregates do not show an obvious lamination. (B, D, F, H, K): Sections of control samples at comparable levels as shown for the cell aggregates in cKO. In controls, those aggregates are not evident, suggesting that these cells represent an olfactory bulb like structure (OBLS, squares B´, D´, F´, H´, K´).

To further assess whether these aggregates reflect a reminiscent OBLS, we performed birthdate labeling by injecting BrdU at E12.5 and at E15.5. In stage E18.5 control samples (of E12.5-injected specimens), ventrally migrating BrdU+ cells were mostly found in the mantle of the OB (asterisk Fig. 39, A). Conversely, BrdU+ cells, injected at E15.5, were specifically located in the VZ of the E18.5 OB of control samples (arrow

Fig. 39, B). In cKO, the E12.5- and E15.5-injected cells were found accumulated in the ventral telencephalon (squares and arrows Fig. 39, A´, B´). These cell aggregates in the ventral telencephalon presumably represent an OBLS in cKO.

Although we could determine an OBLS in the ventral forebrain of Sp8 mutants, this structure is devoid of a laminar organization. For instance in the E15.5 OB of controls, Ngn2+ cells and ID2+ cells are dispersed in a pepper and salt-like pattern (Fig. 38, C, J). In contrast, these cells appear mixed in Sp8 mutants (Fig. 38, D´, K´). Accordingly, two other tested populations of OB cells (Lhx2+ and ID2+) accumulate in an abnormal OBLS in the ventral forebrain of mutants at E18.5 (Fig. 39, D´, E´). This region corresponds to the area, where BrdU-injected cells accumulate (compare squares in Fig. 39, A´, B´ to D´, E´). On E18.5 sections, we could identify that Reelin+ cells in the mutant OBLS accumulate in an unusual w-like shape (Fig. 39, C´). In controls, Reelin+ cells exclusively populate the forming periglomerular- and mitral cell layer of the OB (Fig. 39, C). Therefore, the aberrant distribution of Reelin+ cells (Laub et al., 2006) in cKO might affect the lamination of the OBLS in cKO.

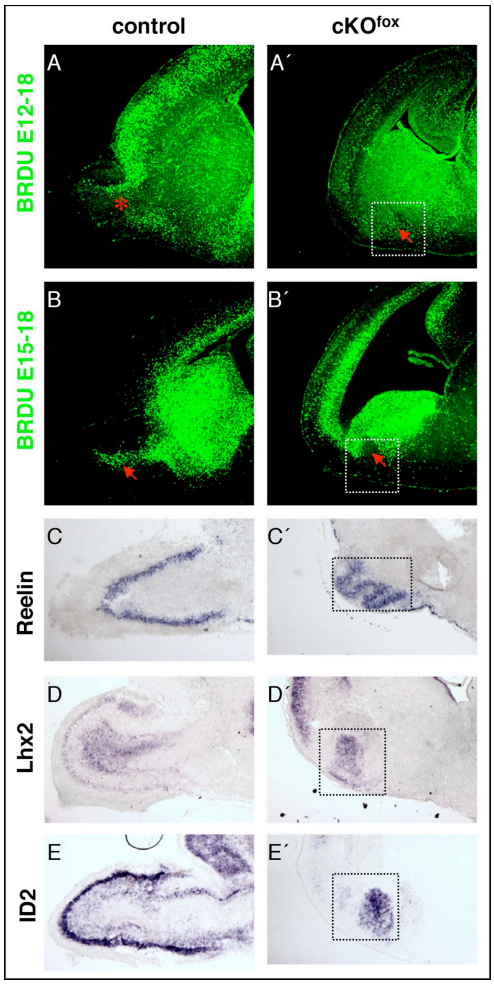

Figure 39: Cell aggregates in cKO are likely an OBLS. BrdU-injected cells in sagittal section of controls populate the VZ (when injected at E15.5, arrow B) or the mantle (when injected at E12.5, asterisk A) of the E18.5 OB. In cKO, both ventrally migrating cell populations aggregate in the ventral FB (arrow in square A´, B´). (C-E´): ISH on sagittal sections, showing the OB/rostroventral FB. In controls Reelin (C), Lhx2 (D) and ID2 (E) mark cells in the OB. However in cKO, those cells seem to accumulate in the ventral FB (square C´, D´, E´). This region coincides with the position of the BrdU labeled cells in mutants and presumably reflects an OBLS.

2.4.12 Progressive degeneration of the olfactory epithelium in Sp8 mutants

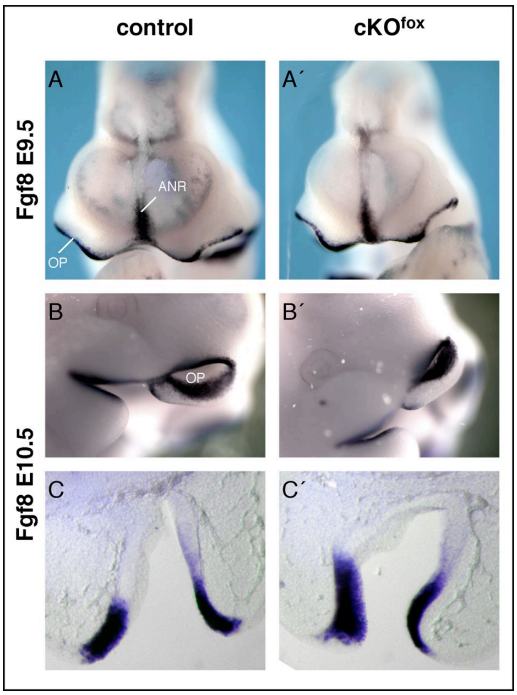

Figure 40: Early Fgf8 activity in the OE. WMISH of E9.5 (A, A´) and E10.5 (B-C´) embryos, using the Fgf8 *in situ* probe. Fgf8 is expressed in the rim of the OP at E9.5 (A, A´) and E10.5 (B, B´, coronal sections of the OP: C, C´) in mutant and control specimens.

The proper development and positioning of the olfactory bulb anlage was shown to be under the influence of signals, released by incoming pioneering axons from olfactory sensory neurons (OSNs) (Laub et al., 2006, reviewed by Lopez-Mascaraque and Castro, 2002). We therefore analyzed the development of the olfactory epithelium in Sp8 mutants.

The olfactory epithelium (OE) develops from an evagination of the olfactory placode and expresses Fgf8 (Fig. 40), Sox2, Mash1, Ngn1, Foxg1 (Kawauchi et al., 2005, data not shown) and Sp8 (Figure 18) at E9-E10.5. In the absence of Sp8, these markers are not affected at E10.5 (Fig. 40, A-C´, data not shown). During early OE development, the olfactory placode of mutants does not differ morphologically from controls (data not shown). Thus, the early fate of the olfactory epithelium is probably correctly established.

Therefore, we examined the subsequent event of olfactory epithelium genesis, the early neurogenesis at E12.5 (reviewed by Lopez-Mascaraque and Castro, 2002). Hes5 and Mash1 are marker genes for populations of early OSN progenitor cells (Cau et al., 1997, Cau et al., 2000). The expression of Hes5 and Mash1 is completely lost in the mutant OE at E12.5 (Fig. 41, A-B´), indicating a loss of neuronal precursors. To test, whether this may have an effect on the production of OSNs, we assayed the expression of two related neuronal markers Emx2 and Pax6 (Dellovade et al., 1998, Mallamaci et al., 1998, Collinson et al., 2003). The analysis showed that the loss of progenitors is corroborated by a strong downregulation of Emx2 and Pax6 mRNA in the OE of cKO. Only very few cells remain positive for Emx2 in the dorsal OE (Fig. 41, C, C´),

demonstrating that the epithelium of conditional Sp8 mutants contains a severely diminished amount of postmitotic olfactory sensory neurons.

Our data may suggest that the hampered neurogenesis in the OE of cKO could also be related to altered cell survival properties, as previously demonstrated in the forebrain (Fig. 32). TUNEL staining on E12.5 coronal sections revealed an 4.5-fold increase in the content of TUNEL+ cells in Sp8-deficient samples, compared to control samples (Fig.42, A, A´, B). The majority of TUNEL+ cells was located in the ventral half of the OE, close to the upper cleft mesenchyme and the medial nasal process. This area was recently shown to contain neuronal stem cells of the olfactory epithelium (Kawauchi et al., 2005), representing ancestors of neuronal precursors in the OE. Reduced expression of neuronal markers in the OE might therefore be the consequence of the death of neuronal stem cells. To test this, we analyzed the BrdU uptake in mutants and controls at E12.5. The S-phase labeling index revealed that proliferation is strongly reduced in the entire OE of cKO (Fig. 42, C, C´, D, 46.5%, +/-2.9% of controls, n=3). Therefore, the induction of excessive apoptosis together with impaired proliferation of remaining cells provokes the dysgenesis of the Sp8-deficient olfactory epithelium.

It was shown that molecular signaling from the surrounding mesenchyme affects proliferation of precursors and OE development indirectly (Shou et al., 1999). However, we did not find an affected expression of the signaling molecules

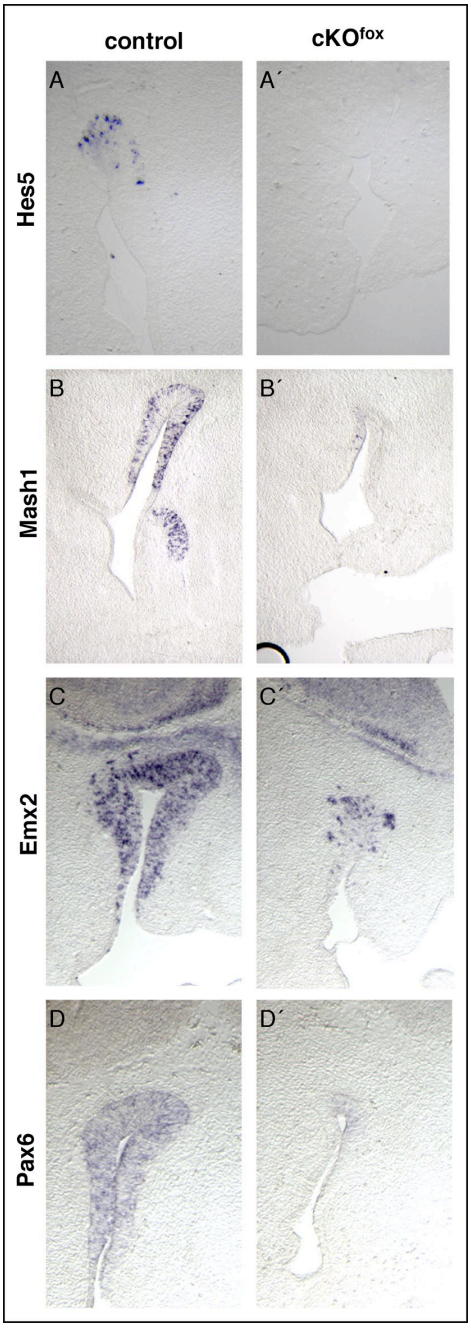

Figure 41: Affected neurogenesis in the OE of cKO. ISH on E12.5 coronal sections of the OE (A-D´). Hes5 and Mash1 are crucial factors for the neurogenesis in the OE (A, B), their expression is lost in cKO (A´, B´). Pax6 and Emx2 mark populations of early OE neuron progenitors (C, D). However, only some Emx2+ cells are detectable in Sp8 mutants (C´), Pax6+ cells are not evident (D´). This indicates a severely depressed neurogenesis in the OE of cKO.

BMP4 and Wnt5a in the lateral or medial nasal processes (Fig. 42, H-J´). Fgf8 is another signaling molecule, which is associated with the genesis of the OE (Kavauchi et al., 2005). Although expressed in the ventral OE at E10.5 (Fig. 40), Fgf8 expression could not be detected in the OE of conditional Sp8 mutants at E12.5 (Fig. 42, E, E´). However, FGF receptors (Fgfr1 and Fgfr3), mediating FGF signaling in the OE (Hebert et al., 2003), remain expressed in mutant and control embryos (Fig. 42, F-G´). The defect of the OE of Sp8 mutants might be associated with the loss of Fgf8 activity at E12.5 (Kawauchi et al., 2005).

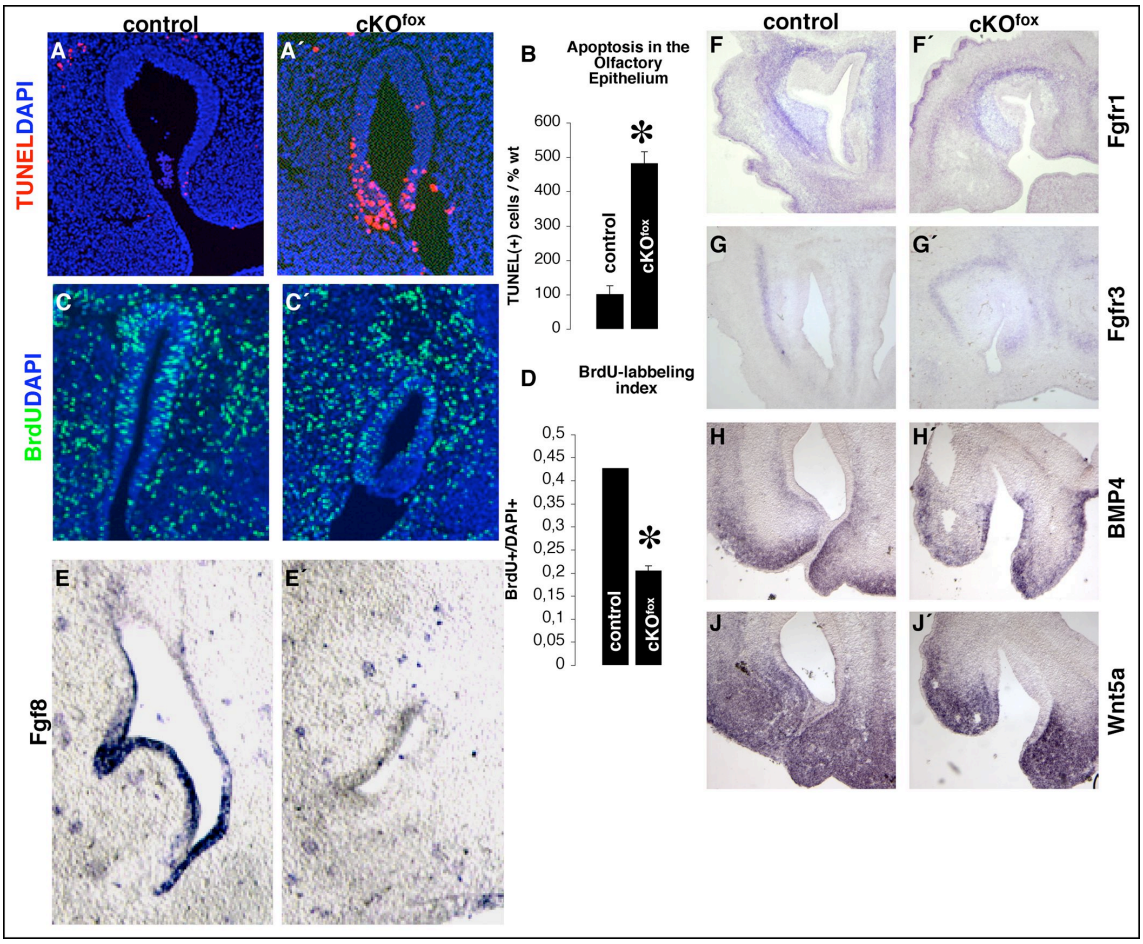

Figure 42: Loss of Fgf8 correlates with the onset of apoptosis and depressed proliferation in the OE of cKO. ISH on E12.5 coronal sections reveals that in cKO, the expression of Fgfr1 (F, F´), Fgfr3 (G, G´), BMP4 (H, H´) and Wnt5a (J, J´) is not affected. However, the expression of Fgf8 in the E12.5 OE is not detectable in cKO, when compared to controls (coronal sections, E, E´). In the ventral OE (overlapping with the Fgf8+ domain), enhanced apoptosis is evident in Sp8 mutants (A, A´, quantification in B, n=3). Conversely the BrdU uptake is severely diminished in the OE of cKO (B, B´, quantification in D, n=3). These defects might correlate to the loss of Fgf8 activity in the OE.

2.4.13 Sp8-deficient olfactory sensory neurons do not connect to the brain

The gene expression data revealed that the Sp8 mutant OE generates some postmitotic OSNs, as concluded from remaining Emx2+ cells. So far we do not know, whether these neurons are able to fulfill their proper function. In this respect, we analyzed the innervation of olfactory sensory axons into the rostral forebrain, which triggers the correct initiation, placement and subsequent layering of the OB-anlage (Gong and Shipley, 1995, LaMantia et al., 2000, Wang et al., 2001, Laub et al., 2006).

In addition, Sp8 is expressed in olfactory sensory neurons during the critical period (E12.5-E15.5) of their innervation into the forebrain (Fig. 43, A, B). To track OSN and their axons in Sp8 cKO embryos, we generated triple transgenic cKO mice, expressing the hrGFP reporter transgene and not the R26R ß-Galactosidase reporter transgene. The advantage of the hrGFP mouse line is that recombined cells express membrane-tagged GFP (Schindehutte et al., 2005). The Foxg1-Cre is strongly expressed in virtually all OE cells (Hebert et al., 2000, Fig. 18, A, Fig. 43, C). Therefore, it is possible to reveal targets of GFP+ OSN axons in cKO and control embryos.

At stage E12.5, GFP staining showed a robust track of OSN axons between the olfactory epithelium and rostromedial forebrain of control embryos. Many GFP+ fibers seem to have already established a connection to their targets in the ventral forebrain (Fig. 43, C, D). In Sp8 mutants at E12.5, not a single GFP+ axon leaves the olfactory epithelium (Fig. 43, C´, D´). To further reveal whether axonal outgrowth might be only delayed in Sp8 cKO, we continued the analysis of triple transgenic mice at E15.5. In control embryos, the olfactory tract is well established, and OSN processes now enwrap the forming olfactory bulb tightly (Fig. 43, F, G). However in all examined Sp8 mutant specimens, no GFP+ axon was detected outside the olfactory epithelium (Fig. 43, F´, G´). Additionally, a discernable olfactory bulb is not evident in the rostral forebrain (Fig. 43, F´, G´). Our data indicate that the remaining postmitotic neurons in the olfactory epithelium fail to extend axons towards the forebrain.

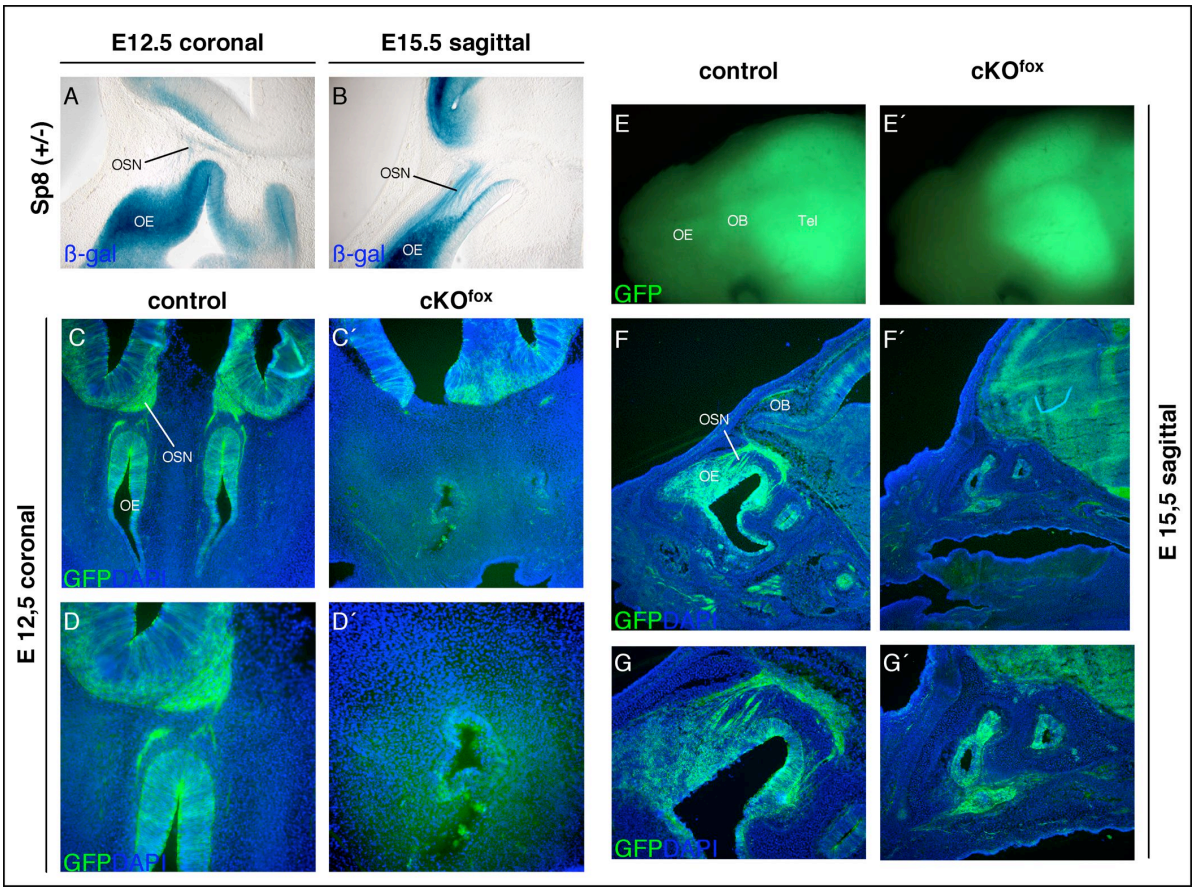

Figure 43: OSNs do not extend axons and therefore fail to connect to the forebrain in cKO. (A, B): lacZ staining of Sp8 null-lacZ (+/-) embryos reveals that the OE and the OSNs express Sp8 at E12.5 (coronal section A) and at E15.5 (sagittal section B). The GFP signal on DAPI counterstained sections of cKO-hrGFP triple transgenic Sp8 mutants highlights that at E12.5 (coronal C´, D´) and at E15.5 (sagittal F´, G´) no axons of OSNs leave the OE. In controls, the GFP signal strongly labels the OSNs at E12.5 (coronal C, D) connecting the OB at E15.5 (sagittal F, G). Only in control (whole mount) brains, the GFP signal is visible in the FB, OB and OE. In mutants, this staining is only apparent in the FB. These findings indicate that the remaining OSNs in cKO fail to extend axons to the FB.

3 DISCUSSION

3.1 Conditional inactivation of Sp8 in the early developing forebrain

We used a conditional inactivation approach to study the role of Sp8, the ortholog of the *Drosophila* transcription factor buttonhead, during murine forebrain development. The analysis of Foxg1-Cre-driven Sp8 mutants revealed several abnormalities during multiple steps of forebrain development. We report that the absence of Sp8 provokes a dysplasia of the rostromedial forebrain (septum region), perturbs A/P patterning and results in apoptosis of neuronal progenitors. A marker gene analysis further reveals that although the layering of the mutant cerebral cortex seems normal, the specification of neuronal subpopulations is perturbed.

3.1.1 Sp8 has an essential role for the formation of the telencephalic midline

One of the major defects of conditional Sp8 mutant embryos was the dysgenesis of the septum. On the molecular level, this phenotype might result from the ventral expansion of Emx2, Pax6 and Ngn2 expression territories at the cortical midline. As a consequence, the expression of several ventral markers – such as Fgf8, Mash1, Dlx1, and most importantly, Nkx2.1 – is regionally downregulated or completely abolished. Interestingly, SHH and WNT expression seems to be preserved in Sp8 mutants, suggesting that the observed perturbation is independent from these signaling pathways. Our data highlights that the mPSB, similar to the established role of the gene expression interface at the lateral pallial-subpallial boundary (PSB), might represent an important region for D/V patterning of the medial telencephalon. Our findings suggest that Sp8 might have a critical role for the maintenance and not for the initiation of proper

molecular characteristics at the mPSB, since early marker gene expression of particularly Fgf8 is not affected.

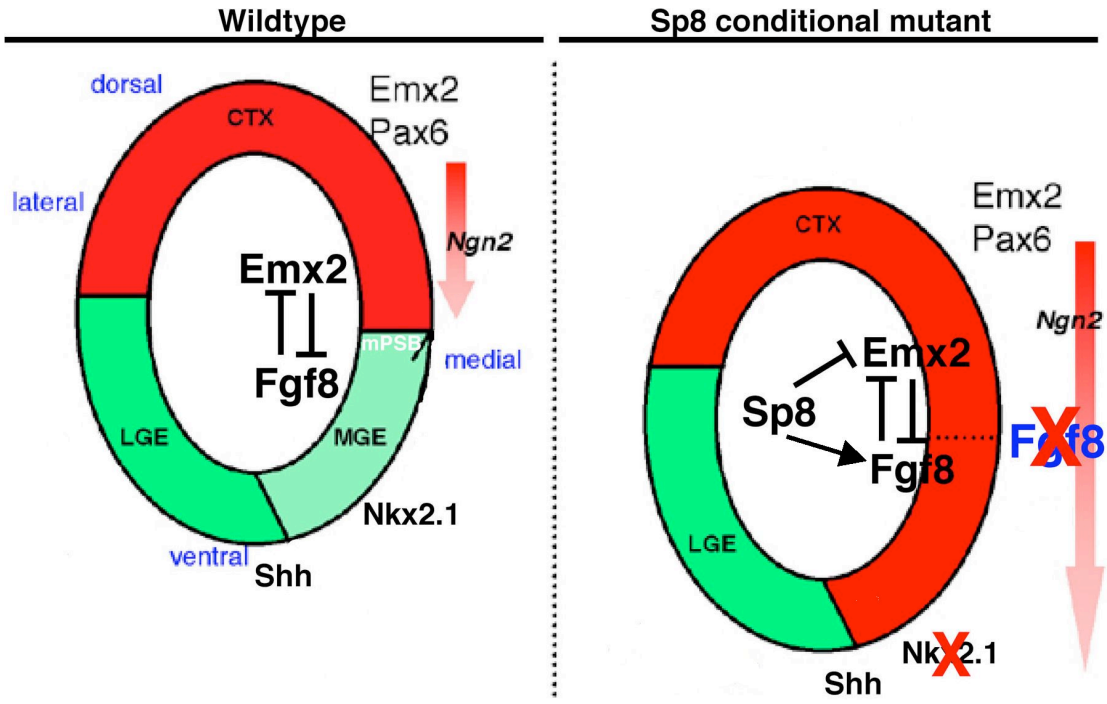

Figure 44: D/V patterning at the mPSB. Scheme recapitulating the expression of marker genes at the medial and lateral PSB. In conditional Sp8 mutants, a dorsalization of gene activity around the midline occurs, as highlighted by ventral expansion of the domain marked in red. Dorsal: red domain, Pax6, Emx2, Ngn2. Ventral: green and light-green domain, Gsh2, Dlx1, Mash1. Reciprocally, the expression area of ventral markers is lost in the dorsal septum (light green domain). Accordingly, Fgf8 and Nkx2.1 expression domains are not maintained in the mutant cortical midline. We favour a model, in which Sp8 regulates the AP regionalization of the cortex by directly suppressing Emx2, while the role of Sp8 in the maintenance of Nkx2.1 activity in SE and MGE could consist in the control of Fgf8.

Interestingly, both Sp8 and Fgf8 are expressed in the septum-anlage at early developmental stages (Hamasaki et al., 2004, this study). Recent findings demonstrate that FGF signaling acts downstream of Shh to promote the differentiation of ventral telencephalic cell types and affects their survival (Gutin et al., 2006). Our study demonstrates that, while preserved in the midline and septum-anlage until E10.5, expression of Fgf8 in the septum and Nkx2.1 in the septum and MGE is completely abolished at E12.5. In support of these findings, recent reports provide strong evidence that FGF signaling may regulate Nkx2.1 expression and that loss of Nkx2.1 expression interferes with proper axial patterning of the telencephalon (Gutin et al., 2006, Tole et al., 2006). Sp8 expression overlaps with Nkx2.1 in the septum only, and conversely does not in the MGE. That is why Sp8-deficiency might influence Nkx2.1 activity in the MGE indirectly through modulation of a yet unidentified SHH-independent pathway or through affecting Fgf8 expression.

Although it appears reasonable that septal precursors might be selectively eliminated by apoptosis, we have no supporting evidence for a detectable regionalized increase of cell death in this region of Sp8-deficient forebrains. Therefore, our findings strongly suggest that in Sp8 conditional mutants, loss of Fgf8 may be responsible for the midline defect.

Sp8 and Fgf8 share overlapping expression domains in the telencephalic wall. Although Sp8 appears downregulated in the medial telencephalon of Fgf8-hypomorphic and conditional mutants (Storm et al., 2006) it is, however, not clear whether Fgf8 activity might therefore directly influence the expression of Sp8. Strikingly in other tissues, it was shown that Sp8 positively regulates Fgf8 activity in the mouse AER (Bell et al., 2003, Treichel et al., 2003) and in the zebrafish pectoral fin (Kawakami et al., 2004), areas where both factors share overlapping expression territories. Whether this regulation is direct or indirect remains to be addressed. Other results, suggesting an interaction between Sp8 and Fgf8, were demonstrated for loss of Sp8 function in the MHB. There, Sp8-deficiency provokes an expansion of the Fgf8 expression domain (Griesel et al., 2006). Due to these multiple examples of affected Fgf8 expression characteristics in different Sp8-deficient compartments of the mouse embryo, we assume that the defective molecular activity in the medial wall of Sp8 cKO is probably also a consequence of an interaction between these two factors. In summary recent work and this study strongly indicates that a context-dependant and probably bi-directional interplay between Sp8 and Fgf8 is important for proper gene expression at the AER/pectoral fin, MHB and mPSB signaling centres. FGF signaling was lately shown to be crucial for the development of the SE (Tole et al., 2006). Our results support the notion that late Fgf8 activity is also necessary for the maintenance of ventral cellular identity of septal precursor cells. Accordingly, in the absence of late Fgf8 activity in Sp8 cKO, the septal territory abnormally expresses dorsal markers and therefore might obtain pallial molecular properties (Fig. 44).

In contrast to the medial telencephalic wall (mPSB), the patterning at the lateral pallial-subpallial boundary (PSB) is not disturbed in mutants, although Sp8 is expressed in the dLGE, which is a part of the PSB. On the one hand, D/V patterning at the PSB might derive from early-established axial patterning (reviewed by Stoykova and Mallamaci, 2006), which appeared normal in Sp8 mutants. On the other hand, Sp9, a closely related Sp1 family member (Kawakami et al., 2004) is expressed in the ventral telencephalon

(Fig., 26, E). Remarkably, the expression of Sp9 remains preserved at the PSB of conditional Sp8 mutants (data not shown), suggesting that functional redundancy between Sp8 and Sp9 might exist.

3.1.2 Sp8 affects the cortical arealization along the A/P axis

The genetic arealization of the early cortical primordium requires the regionalized expression of ligands belonging to the FGF, WNT/BMP and EGF signaling pathways, which are released by the ANR, cortical hem, roof plate and antihem, respectively (reviewed by Mallamaci and Stoykova, 2006). Those ligands control the expression of region-specific transcription factor gradients in a dose-dependant manner, thus transmitting distinct positional information to the cortical primordium. So far only few regionally enriched transcription factors have been shown to critically influence cortical arealization. For instance, in mice where either Pax6 or Emx2 is not functional, corresponding rostral and caudal cortical regions – where these genes are expressed at high levels – appear malformed and cortical areas are displaced in opposite directions (Bishop et al., 2000, Bishop et al., 2002, Fig. 6).

The functional connectivity of cortical areas seems to rely just in part on molecular specification (protomap model). Moreover, the area identity is ultimatively terminated and maintained by innervation of thalamic axons into distinct cortical areas (protocortex model) (reviewed by O'Leary and Nakagawa, 2002, Sur and Rubenstein, 2005). According to the recent view about the genesis of functionally distinct primary areas of the cerebral cortex, it is conceivable that a convergence of both, the protomap model and the protocortex hypothesis might establish the anterior-posterior axis formation. This would mean that early genetic determination establishes the frame of primary cortical areas. On this basis, locally distinct cell cycle parameters ensure growth control among cortical regions. Finally, incoming thalamic axons would ultimatively establish the functional character of different primary cortex areas on the genetically prepatterned but still plastic proto map (reviewed by Mallamaci and Stoykova, 2006).
Our findings suggest that conditional inactivation of Sp8 causes a prominent caudalization of molecular characteristics of the cortical neuroepithelium, as highlighted

by ectopic rostral expansion of the expression domains of regionally enriched marker genes ID-2, Coup-TF1, EphrinA5 and EphA7. Importantly, Sp8 cKO cortices display an enhanced Emx2 and a reciprocally downregulated Pax6 expression gradient in neuronal progenitors. This is consistent with a genetic interplay between Pax6 and Emx2, which is involved in the establishment of their normal expression gradients (Muzio et al., 2002b). In contrast to the direct relationship between Emx2 and Pax6 expression levels, we were able to show that the loss of Emx2 and Pax6 does not affect the medial-high to lateral-low expression gradient of Sp8 in pallial progenitors, suggesting a role of Sp8 upstream of Emx2 and Pax6 (Fig. 45).

In addition to the role of the transcription factors Emx2 and Pax6, Fgf8 signaling from the ANR seems to have a crucial role for the patterning of the cerebral cortex along the A/P axis (reviewed by Mallamaci and Stoykova, 2006). Moreover, it has been suggested that Emx2 might control cortical arealization indirectly, through the regulation of Fgf8 signaling (Fukuchi-Shimogori and Grove, 2003). Recent data, however, challenged such a view by demonstrating that Emx2 may operate directly and independent from Fgf8 to specify cortical progenitors as well as primary cortical areas (Hamasaki et al., 2004). Because the early Fgf8 signaling from the ANR does not seem to be affected in the Sp8 cKO forebrain, our findings strongly suggest that the interaction between Sp8 and Emx2 is controlling the arealization of the cerebral cortex (Figure 45). The alteration of Pax6 transcript levels might therefore probably be a consequence of the enhanced activity of Emx2 (Muzio et al., 2002b).

Interestingly, our strong evidence about a genetic interplay between Sp8 and Emx2 correlates with experiments, previously performed in *Drosophila* embryos. In the fly, combined activity of empty spiracles, the Emx2 homolog, and buttonhead generates and specifies head segments and A/P pattern formation through a physical interaction of the N-terminal parts of both proteins (Schock et al., 2000). In this context we were able to demonstrate that Sp8 and Emx2 proteins interact *in vitro*, indicating a conserved and tight nature of this regulatory network in *Drosophila* and in mice as well. Therefore, it seems conceivable that during murine forebrain development, regulation of Emx2 function by the buttonhead ortholog Sp8 relies on such mechanisms.

The results of the DiI labeling experiments are consistent with changes of the molecular profile in Sp8-deficient cortices and clearly demonstrate a partial change of caudal

cortical area identity in Sp8 cKO. In contrast to this severe defect in Sp8 mutants, the primary cortical area profile of hypomorphic Fgf8 mutant- and Pax6 knockout embryos does not change the functional connectivity to the host thalamic nuclei, although molecular markers are shifted (Garel et al., 2003, reviewed by Stoykova and Mallamaci, 2006). Taken together these findings support a model, in which Emx2 controls Pax6 expression levels and importantly functions independently from Fgf8 to act on A/P patterning of primary cortical areas, as suggested previously (Hamasaki et al., 2004, Figure 45). Additionally, our data provides evidence that both, molecular patterning and thalamic connectivity are distinct crucial aspects of cortical pattern development. By interacting with Emx2 and repressing its activity, Sp8 is crucial for patterning of the murine forebrain along the A/P axis.

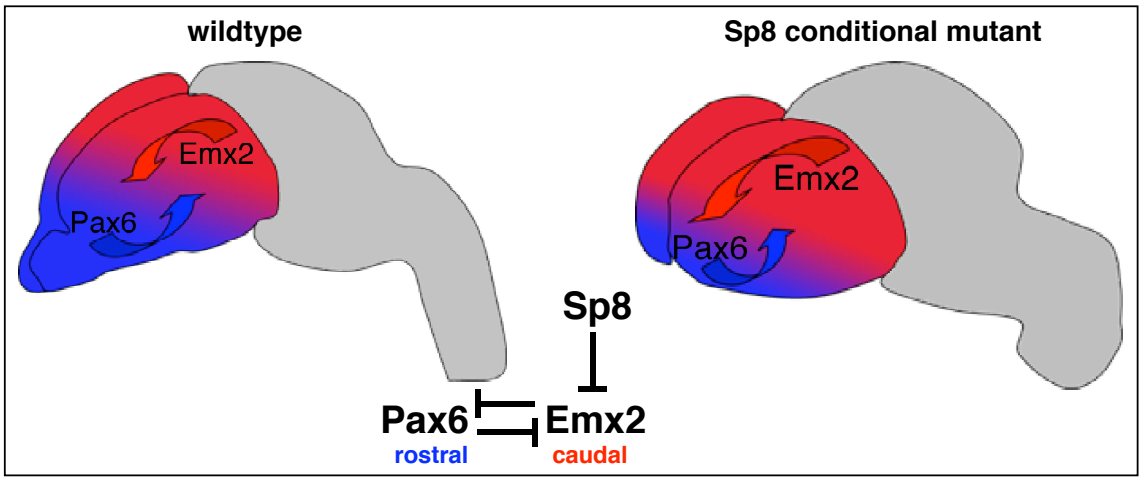

Figure 45: The role of Sp8 for the cortical A/P patterning. Schematic drawing, showing how Sp8 might influence the molecular A/P patterning of the cerebral cortex. In Sp8 cKO mutants, Emx2 activity is upregulated (bigger red cortical domain in cKO). Conversely, the activity of Pax6 is diminished (smaller blue cortical domain in cKO). Both factors, Emx2 and Pax6, mutually influence their graded expression characteristics along the A/P axis in cortical progenitors (red and blue arrows). Emx2 alone is capable of directly specifying cortical area fate in a dose-dependant manner. We favor the hypothesis that, similar like in *Drosophila*, Sp8 and Emx2 interact physically and are critical for the patterning of the forebrain along the A/P axis. Sp8 might act to repress Emx2 activity.

3.1.3 Sp8 plays a critical role in the neurogenesis of the cerebral cortex

Our analysis revealed that the forebrain of conditional Sp8 mutants appears severely reduced in size. However, investigation of key parameters (like S-Phase, M-Phase and cell cycle exit) of the cell cycle did not show differences in control and mutant embryos. Therefore, our data provide evidence that the forebrain hypoplasia provoked in Sp8 cKO mice is primarily due to cell death. In fact, additional experiments could show that the induced cell death in Sp8 cKO embryos is affecting both early and late neuronal progenitor pools. Conversely, we have no evidence that apoptosis is selectively induced in a distinct precursor population (e.g. septal precursors or subplate cells). Our data indicates that upon wide spread depletion of neuronal progenitors throughout main stages of neurogenesis, a diminished production of postmitotic neurons occurs in cKO. As a consequence, the Sp8 mutant forebrain only develops a strikingly reduced size. The induction of apoptosis was previously reported in the absence of Sp8 in the basal telencephalon (Waclaw et al., 2006) as well as in the limbs (Bell et al., 2003, Treichel et al., 2003). In these reports, apoptosis provoked a remarkable size reduction of affected Sp8-deficient tissues. Therefore, our findings are in line with the previous, demonstrating that Sp8 might have an important role in cell survival during embryonic development and neurogenesis.

Loss of Sp8 function in the forebrain abolishes proper preplate splitting. The splitting of the preplate into subplate and marginal zone is an early and critical process of corticogenesis. Recently, defective migration of cortical plate neurons and targeting defects of invading thalamic axons were linked to impaired preplate splitting. These studies followed different strategies like subplate ablation approaches as well as the analysis of loss of function mice for Emx1/2, Reelin or p35/Cdk5 (Shinozaki et al., 2002, Dupont et al., 2006, Rakic et al., 2006). The Gap43 expression data, together with the DiI-tracing experiments highlight several axon trajectory abnormalities in cKO, indicating that the establishment of a subplate and proper preplate splitting is also a critical step of correct axonal targeting in Sp8 conditional mutants. Molecularly, it was demonstrated that the formation of preplate and subplate relies on the activity of Emx1/2 (Shinozaki et al., 2002), Tbr1 (Hevner et al., 2001) and Pax6 (Stoykova et al., 2003). In addition, the function of various members of the WNT- and Reelin signaling

pathways are involved in this process (Theil, 2005, reviewed by Tissir and Goffinet, 2003). Our analysis demonstrates that expression of Emx2, Pax6 and Tbr1 is affected and that Reelin+ cells are super numerous in the cKO cortex. So far it is not definitely clear, whether reduced expression of Pax6, Tbr1 and/or altered expression levels of Emx2 and Reelin have a direct role for the preplate defect provoked in Sp8 cKO, because the role of these molecules was only shown in knockout animals. Upcoming it remains to be tested in detail, whether PPL development responds to changes of Emx1/2, Pax6 and Tbr1 activity in a dose-dependant manner. Particularly, the putative role of an excessive Reelin content in cKO cortices requires further investigations. Although the detailed mechanisms, which generate the specification of subplate cell identity and preplate splitting remain poorly understood so far, the affected markers are consistent with altered development of the PPL in cKO and underlines a specific role of Sp8 in this critical process.

Surprisingly, the basic lamination of the cortex is not compromised in cKO. This issue was demonstrated by birth date experiments and could highlight that in conditional Sp8 mutants, positioning of postmitotic neurons in the cortical plate keeps the inside-first, outside-last organization. However, some of the markers delineating specific neuronal subtypes, such as ER81, RzR-ß and Cux1 are perturbed, indicating that Sp8 may be required to promote the specification of some subpopulations of those cortical layer neurons. Interestingly, the conditional ablation of Sp8 in the basal telencephalon similarly causes the misspecification of a subset of interneurons that are descendents of the dLGE (Waclaw et al., 2006). Given the established role of Emx2 in maintenance and specification of Reelin+ cells in the MZ (Shinozaki et al., 2002), we assume that the enhanced Emx2 level in Sp8 mutant forebrains might contribute to the overproduction of CR cells. Furthermore, sustained expression of Emx2 comes together with Pax6 downregulation and results in a depressed differentiation of upper layer neurons, a subset of cortical neurons, which is also affected in Sp8 cKO (Tarabykin et al., 2001, Muzio et al., 2002b, Schuurmans et al., 2004). However, due to perinatal lethality of Sp8 conditional mutants, we were not able to investigate maturation of the cerebral cortex. Therefore, generating surviving Sp8 knockout mice will be necessary to investigate the impact of Sp8 on postnatal maturation of the mouse cortex.

3.1.4 Sp8 is essential for the development of the olfactory bulb

Our findings clearly demonstrate that Sp8 has a critical role for the genesis of the olfactory system in mice. Recently, it was shown that conditional inactivation of Sp8 using the Dlx5-Cre driver line, disrupts normal architecture of the OB and the specification of a subpopulation of OB interneurons. In these mutants, calretinin-expressing and GABAergic-non-dopaminergic interneurons of the ganglionic cell layer in the olfactory bulb are not specified. This defect was correlated with loss of Sp8 activity in the dLGE, where the progenitors of missing interneuron subpopulations are generated (Waclaw, 2006). Additionally, depletion of interneuron subpopulations was associated with induced apoptosis of neuroblasts in the dLGE (Waclaw et al., 2006).
Our data is in line with these findings, however, our Sp8 conditional mutant mice show a much more severely affected OB. Conditional inactivation of Sp8 using the Foxg1-Cre driver line induces apoptosis not only in the dLGE, but in the rest of the forebrain as well. In addition, we were able to detect downregulation of several marker genes in the dLGE, associated with a diminished generation of olfactory neuroblasts. Waclaw and coworkers used the Dlx5-Cre mouse line in their study, mediating recombination only in the ventral forebrain starting at E10.5 (Ruest et al., 2003). Due to the almost ubiquitous expression of the Foxg1-Cre in the forebrain and its initiation as early as E9 (Hebert et al., 2000), it is convincing that the spatiotemporal limitation of a Dlx5-Cre-mediated inactivation of Sp8 only generates a partial phenotype.
Furthermore, our analysis identified an OBLS in the ventral forebrain of Sp8 cKO, a structure also described in Pax6 mutant (Sey) mice (Jimenes et al., 2000). In contrast to the OBLS in Sey mice, no lamination of this structure was obvious in Sp8 mutants (Jimenez et al., 2000). In agreement with recent data, abnormal placement of Reelin+ cells in the OBLS of cKO might explain the lack of proper lamination (Laub et al., 2006). Furthermore, it is widely accepted that the genesis of the OB is influenced by molecular guidance mechanisms. Especially, activity of chemo repulsive Slit- and Netrin signaling, two important factors released by septal cells, is important for correct migration of neuroblasts through the RMS and the correct development of olfactory bulb layering (reviewed by Lopez-Mascaraque and Castro, 2002). On the basis of these data, it seems likely that Sp8 cKO embryos show an affected OB layering, because the septum, serving as source for chemo repulsion, is lost.

3.1.5 Sp8 maintains the genesis of the olfactory epithelium

An additional striking phenotype of cKO embryos is the severely affected development of the olfactory epithelium of the nose. Molecular analysis could highlight that the expression domain of Fgf8 in the nasal placode represents a morphogenetic center, enabling proper maintenance of the developing olfactory system in mice. Conditional, Foxg1-Cre-mediated, Fgf8 mutant mice develop excessive apoptosis in the ventral OE (rim of the OE), and additionally reduced proliferation of cells in the dorsal OE was apparent (Kawauchi, 2005). This phenotype is reminiscent of the defects we observed in the olfactory epithelium of Sp8 cKO. Given the overlapping expression and possible interactions between Sp8 and Fgf8 observed in different tissues (AER, MHB, SE), the OE phenotype in cKO might result from a molecular interplay between Sp8 and Fgf8. Abnormal development of the nasal cavity in Sp8 mutants, as highlighted by misexpression of molecular markers and histological/morphological perturbations, might therefore result from ablated Fgf8 activity in the olfactory epithelium.

We additionally demonstrated that cKO embryos do not develop an axonal connection from the olfactory epithelium to the olfactory bulb. This finding corresponds to recent studies, linking proper OB genesis, layering and positioning to correct neuronal connection between olfactory bulb and olfactory epithelium (Gong, 1995, LaMantia, 2000, Jimemez et al., 2000, Wang, 2001). Although it is accepted that invasion of axons from the OE positively influences proliferation rate and neurogenesis in the forebrain target area, therefore corresponding to the onset of olfactory bulb genesis and formation, this theory is still discussed controversially and needs further experimental investigation (reviewed by Lopez-Mascaraque and Castro 2002). Such evidence was provided very recently by a report, demonstrating that partial innervation of olfactory sensory neurons into the olfactory bulb of KLF7 (Krüppel-like Factor7) knockout mice directly correlates to local restoration of olfactory bulb layering and morphology at these innervated spots (Laub et al., 2006) If we consider that the remaining OSNs in cKO do not invade the forebrain target area at all, it is conceivable that this defect might have an effect on the OBLS. This deficit of neuronal connectivity, together with impaired positioning of Reelin+ cells and loss of repulsive signaling from the septum, inhibits normal positioning and layer formation of the olfactory bulb in Foxg1-Cre-mediated Sp8 mutants. Interestingly, inactivation of genes, belonging to the Dlx family (Eisenstat

et al., 1999, Long et al., 2003), Arx (Yoshihara et al., 2005) or the conditional Sp8 knockout in the ventral forebrain (Waclaw et al., 2006) does not result in a complete absence or disgenesis of the olfactory bulb, but only in the reduction of the OB in its size and local defects of OB architecture. All these mutant mouse models show a completely normal development of the olfactory epithelium, including innervation of the olfactory bulb by incoming olfactory sensory neurons. In this context, our study of the conditional Sp8 phenotype in the olfactory epithelium provides new evidence for an important role for invading olfactory sensory neurons, representing a neuronal substrate for proper development of the olfactory bulb anlage.

3.2 Research Perspectives and outlook

This study describes new insights into the function of the transcription factor Sp8, during development of the murine forebrain. By using a conditional loss of function approach we were able to provide evidence that Sp8 is crucial for several distinct processes of early forebrain development, like pattern formation, preplate development, corticogenesis, olfactory system development and cell survival. However, the new findings also opened up directions for concomitant elucidation.

A main conclusion so far is that Sp8 interferes with normal expression of Fgf8 and remarkably Emx2 during forebrain development. In addition we were able to show that protein-protein interaction between Sp8 and Emx2 is conserved in mice. On this basis, an interesting outlook would be to test the cellular function of protein-protein interactions between Sp8 and Emx2. Therefore, it will be extremely interesting to assay for additional biochemical interactions of those genes *in vitro*. In particular, whether heterodimers of Sp8 and Emx2 might be able to bind specific DNA sequences or whether binding of Sp8 to Emx2 might have an impact on the recently characterized feed-back auto regulation of the Emx2 expression (Muzio et al., 2005b). Despite this, it is possible that Sp8, as a transcription factor, might have a functional role on the level of DNA interaction with regulatory sequences of the Emx2 locus and therefore direct transcriptional control. Upon analysis of promoter regions of Sp8, Emx2 and Fgf8 with activation assays, one might be able to find new interactions among these important genes. Following similar approaches it appears worth to elucidate, whether ER81, RzR-ß and Cux1, downregulated in Sp8 mutant cortices, might represent direct target genes of Sp8.

Additionally, another important question to answer would be, if the function of Sp8 might mutually interdepend directly on Fgf8 function, because evidence exists that interaction of Sp8 and Fgf8 might be bi-directional (Storm et al., 2006). Therefore, a detailed examination of Sp8 activity in Fgf8 mutant embryos should be considered. Moreover, the generation of compound mutants of Sp8 and Fgf8 appears as an attractive model system for future analyses of embryonic pattern formation.

Recently, another closely related Sp1 family member, Sp9, was identified. Although no *in vivo* Sp9 loss of function mouse model is available so far, *in vitro* loss of- and gain of function studies were recently performed (Kawakami et al., 2004). These authors,

together with our observations, could provide evidence for functional redundancy between Sp8 and Sp9 during embryogenesis. Since both genes are not only co expressed in parts of the forebrain, but in the MHB and the AER of the limbs as well, analysis of Sp8-Sp9 double knockout mice may serve as a potent tool for understanding molecular interactions of these signaling centers.

Perinatal lethality of conditional Sp8 mutants hampers a comprehensive analysis of Sp8 function, especially with regards to the elucidation of postnatal cortical maturation. Inactivation of Sp8 by additional Cre lines, generating surviving Sp8 mutants, remains a good possibility to overcome this limitation. Experiments are on the way to generate Emx1-Cre-mediated (Gorski et al., 2002) Sp8 mutants, enabling Cre recombination and Sp8 inactivation specifically in the dorsal forebrain neuroepithelium. Furthermore, using an *in vitro* slice culture approach with dissected E18.5 cKO tissues might represent a useful back up for the analysis of postnatal maturation processes under the condition of the affected embryonic corticogenesis of Foxg1-Cre-mediated Sp8 mutants. Finally, it is conceivable to assay how the forebrain might develop under the influence of Sp8 overexpression. To achieve this, one might develop appropriate *in vitro* and/or *in vivo* models for the spatiotemporal misexpression of the Sp8 gene.

4 SUMMARY

Sp8, the ortholog of the *Drosophila* zinc finger transcription factor btd, is essential for murine development. However, molecular analysis of the strong malformation of the forebrain was so far hampered due to exencephaly. To overcome this limitation, floxed Sp8 mice were generated and in this study a conditional Sp8 mutant mouse model analyzed.

Conditional inactivation of Sp8 driven by the Foxg1-Cre driver line provoked severe defects during forebrain development. Histologically, cKO forebrains lack the OBs, the SE, and a MGE proper and further show a severe hypoplasia. A marker gene analysis revealed that – although early patterning is established – the gene expression interface at the cortical midline (mPSB) is disturbed. Possibly, this accounts for a ventral extension of dorsal marker genes. Additionally, Sp8 maintains the activity of Fgf8 and Nkx2.1 in the midline. This activity preserves cellular identity of precursors of the SE and rostral MGE and thereby sustains D/V patterning in the rostromedial forebrain. Furthermore, Sp8 cKO exhibit an altered expression gradient of Pax6 (diminished) and Emx2 (enhanced) in cortical progenitors, causing a caudalization of genetic markers and disturbing thalamocortical connectivity of caudal cortical areas. Like in *Drosophila*, Sp8 binds Emx2 *in vitro* and contributes to patterning of the mammalian cortex along the A/P axis by repressing Emx2 activity.

During early corticogenesis, Sp8 activity is required for preplate splitting, but is not mandatory for switching from the generation of infragranular- versus supragranular layers. Noteworthy, the affected PPL development abolishes SP formation and tightly correlates with defective wiring of thalamic axons, invading the cortex. Moreover, examination of layer specific marker genes highlighted that Sp8 is crucial for the molecular specification of Cux1+, ER81+ and RzR-ß+ neurons. Furthermore, we found that Sp8-deficiency does not affect the cell cycle in the forebrain, but induces apoptosis. Cell death equally affects pallium, subpallium and both, early and late cortical progenitors.

In addition, Sp8 is important for olfactory system development. Instead of an OB proper, a non-laminated OBLS aggregates in the mutant subpallium. Paired with diminished expression of dLGE marker genes and apoptosis, the mutant OBLS contains less neuroblasts than controls. The lack of lamination might convergently originate from affected cell migration, impaired secretion of Reelin and the loss of the SE, as source of axon guidance cues. The mutant OE fails to establish axonal contact to the forebrain, but moreover reveals a probably Fgf8-dependant degeneration. Highlighted defects in the OE are diminished proliferation and neurogenesis as well as excessive apoptosis.

The study demonstrates that Sp8 is an indispensable transcription factor for proper development of the mammalian forebrain and olfactory system.

5 MATERIAL AND METHODS

5.1 Consumables

5.1.1 Chemicals

Analysis-graded chemicals were obtained from the following companies: J. T. Baker (Deventer, Netherlands), Biomol (Ilvesheim, Germany), BRL (Karlsruhe, Germany), Difco (Detroit, USA), Fluka (Buchs, Switzerland), Merck (Darmstadt, Germany), Roth (Karlsruhe, Germany), Serva (Heidelberg, Germany), and Sigma (Munich, Germany).

5.1.2 Plastic-material and Glassware

Consumable plastic material was obtained from Eppendorf (Germany), Falcon (Germany), Greiner (Germany), Nunc (Germany) and Sarstedt (Germany). Glassware was delivered by Schott (Germany) and autoclaved before use.

5.1.3 Commercial Enzymes and Buffers

Enzymes and reaction buffers were obtained from Promega (Mannheim, Germany), NEB (Schwalmbach, Germany), Gene Craft (Münster, Germany), Roche (Mannheim, Germany), Boehringer (Mannheim, Germany) and MBI Fermentas (St. Leaon Roth, Germany).

5.1.4 PCR Primer

Oligonucleotides were ordered from IBA (Göttingen, Germany). The concentration of primers was 0.1 nmol/μ and the quality was “molecular biology-graded”.

5.1.5 Solutions, buffers and media

Table 1: Solutions, buffers, media

Name	Protocol
0.5 M EDTA pH 8	93g Ethylendiamin Tetra acetate in 500 ml H2O, pH with 10M NaOH
1 M KCL	7.45g Kalium chloride in 200ml H2O
1 M Tris-CL variable pH	60.57g Tris in 500ml H2O, pH with $HCl_{conc.}$
10 X TBE	108g Tris 55g Boric acid 40ml 0.5M EDTA in 1000ml H2O
10% SDS	50g Sodium Dodecyl sulfate in 500ml H2O
10% Triton X	100ml Triton X in 1000ml H2O
10% Tween 20	100ml Tween 20 in 1000ml H2O
3 M Sodium acetate	40,8g Sodium acetate in 100ml H2O
30% Sucrose/PBS	30g Sucrose in 100ml PBS
4 M LiCl	16.96g Lithium chloride in 100ml H2O
4% PFA	20g Paraformaldehyde in 500ml H2O
Dipping solution	50% NTB-2 liquid film (Kodak) 50% H2O
Embryo powder	Homogenize E13.5 embryos in 4 Volume Acetone and spin at 10.000 rpm, three times. Air-dry the pellet
FCS	Sheep serum, inactivated by incubation at 70°C for 30 min.
Gelatin-Albumin mixture	2.2g Gelatine 135g Albumine 90g Saccharose in 450ml PBS
Giemsa stock-solution	0.85% Giemsa 50% Glycerol 50% Methanol
Glycine buffer	250ml PBS-DEPC 2mg/ml Glycine
H2O	Double distinguished water (Milli RX75, Millipore)

H2O-DEPC	1000ml H20 1ml DEPC
HEMG 1	0.5M NaCl 0.1% NP-40 1X Protease Inhibitors (EDTA-free, Roche)
HEMG 2	0.5M NaCl 0.01% NP-40 1X Protease Inhibitors (EDTA-free, Roche)
HEMG 3	0.1M NaCl 0.01% NP-40 1X Protease Inhibitors (EDTA-free, Roche)
Hybridization buffer (hot ISH)	1X Hybridization salt 0.1M DTT 10% Dextrane sulfate 0.5mg/ml yeast tRNA
Hybridization salt (10X) (hot ISH)	0.2% PVP 0.2% Ficoll 100mM Tris pH8.0 50mM EDTA 100mM Natrium phosphate buffer pH6.8 3M NaCl
KTBT	100ml Tris pH7.5 60ml 5M NaCl 20ml 1M Kcl 20ml Triton-X 100 H2O to 2000ml
LB (Luria-Bertani) media	10g Bacto Trypton 5g Yeast extract 10g NaCl 7.5ml 1N NaOH in 1000ml H2O
LB agar	15g Agar 50μg/ml Ampicillin or Kanamycin in 1000ml LB
Lysis Buffer	100mM Tris pH 8.0 5mM EDTA 0.2% SDS 200mM NaCl 100 μg/ml Proteinase K
Lysis buffer (GST-pulldown)	HEMG 1 50 mg/ml Lysozyme
Mowiol	9.6g Mowiol 24ml Glycerol 24ml H2O 48ml 0.2M Tris pH8.5

NTE	100mM Tris pH7.5 500mM NaCl 50mM EDTA
NTMT	100ml Tris pH9.5 20ml 5M NaCl 50ml 1M $MgCl_2$ 1ml Triton-X 100 H2O to 1000ml 2mM Levamisole
PBS (1X)	Dilute 1:20 in H2O
PBS (20X)	160g NaCl 4g KCL 23g Na_2HPO_4 4g KH_2PO_4 in 1000ml H2O
PBS-DEPC	1000ml PBS 1ml DEPC
PBT	1X PBS 0.1% Tween20
Prehybridization buffer (cold ISH)	50ml Formamide 25ml 20XSSC pH4.5 1gr Boehringer blocking reagent 1ml 0.5M EDTA 0.1ml Tween20 1ml 10%CHAPS 0.1ml 100mg/ml Heparin/H2O 1 ml 100mg/ml yeast tRNA H2O to 100 ml (for hybridization add mRNA-probe 1:50)
Prehybridization buffer (WMISH)	50% Formamide 5X SSC pH4.5 50μg/ml yeast tRNA 1% SDS 50μg/ml Heparin (for hybridization add 1μg/ml mRNA-probe)
Proteinase K buffer	12.5ml Tris pH 8.0 2.5ml 0.5M EDTA H2O-DEPC to 250ml 10mg/ml Proteinase K
Running buffer 1X (SDS-PAGE)	25 mM Tris-HCl 200 mM Glycine 0.1% SDS
Sample buffer 5X (SDS-PAGE)	10% SDS 10 mM ß-Mercapto Ethanol 20% Glycerol 0.2 M Tris-Hcl, pH 6.8 0.05% Bromophenolblue

Sol I	50% Formamide 5X SSC pH4.5 1% SDS
Sol II	0.5M NaCl 10mM Tris pH7.5 0.1% Tween20
Sol III	50% Formamide 2X SSC pH4.5
SSC (20X)	3M NaCl 0.3M Sodium citrate in H2O
TBST (10X)	8g NaCl 0.2g KCl 25ml 1M Tris pH7.5 10ml Tween20 H2O to 100ml
TBST (1X)	Dilute 1:10 in H2O
TE	10mm Tris pH8.0 1mM EDTA in H2O
X-Gal staining solution	1g X-Gal in 20ml Dimethyl formamide

5.2 Microscopy

5.2.1 Light microscopy

Light microscopic images were taken with a Binocular (Stemi SV11, Zeiss; SZX12, Olympus) or stereo microscope (Axiophot, Zeiss; BX60, Olympus) by using an attached digital camera. Images were processed with Analysis/Cell (Olympus) software.

5.2.2 Fluorescent microscopy

For fluorescence microscopy images, the fluorescence filter cube of the (BX60) stereo microscope (Olympus) was used. Merged images were produced using the Analysis/Cell (Olympus) software.

5.2.3 Confocal microscopy

Confocal microscopy images were captured using a confocal laser microscope (LSM 410invert, Leica). The images were processed with the attached microscope software package (Leica).

5.3 Animals and housing

Housing, caretaking and all performed animal procedures were approved and controlled by the regulations of the Regierungsbezirk Braunschweig. Wild type (C57/BL6) mice were obtained from Charles Rivers. They were used to obtain wild type embryos and for backcrossing of mouse lines to a C57/BL6 genetic background. Foxg1-Cre-expressing mice were a generous gift from S.K. McConnell and J. Hebert (Hebert et al., 2000). The Emx2KO, Pax6KO and Sp8KO (lacZ-null knock-in) mouse lines were created in the department (Pellegrini et al., 1996, St-Onge et al., 1997, Treichel et al., 2003) and

obtained from the lab stock. Foxg1KO mice were obtained by intercrossing of Foxg1-Cre heterozygous mice.

5.3.1 Mating strategies

The mating paradigm, developed for the conditional inactivation strategy is indicated in Fig. 17.

5.3.2 Genotyping of transgenic and knockout mice

To identify the genotype of housed mouse colonies or embryonic specimens, small tissue samples were dissected. In case of postnatal mice, a short piece of the tail was dissected. Embryonic membranes were used as tissue samples from embryos. The collected samples were lysed in Lysis buffer on a shaker at 56°C, overnight. Remaining hairs and cell debris was sedimented by centrifugation. The supernatant was transferred to a fresh tube and precipitated by shaking for several minutes in Isopropanol. After sedimentation, the DNA pellet was washed in 70% Ethanol. After removing excessive ethanol, the samples were air dried and resuspended in 100μl TE. Genotyping of the DNA samples was performed by PCR using appropriate specific primers (reaction mix is indicated below) and a PCR thermo cycler (MJ Research). Primers, used in this study, are summarized in table 2. Following the PCR reaction, analytical electrophoresis was done, using 0.7-1.5% agarose gels. The resulting DNA bands were captured with a digital camera (Biometra), equipped with a UV-light source. The corresponding genotypes were documented for further identification. The Foxg1KO, Sp8KO and Pax6KO individuals were identified upon the strong eye and brain phenotype.

The PCR reaction mix (per reaction) was prepared as a master mix and as described below:

H2O:	35.95μl
5X PCR buffer, GoTaq (Promega):	10μl
20 mM dNTP nucleotide-mix (GeneCraft):	0.75μl
Genomic DNA:	1μl
0.1 nM Primer (IBA)	0.1μl
5 U/μl Go-Taq-polymerase (Promega):	2μl
Total volume/reaction:	50μl

Table 2: PCR primers

Genotyping	Name and Sequence
Cre recombinase	CreF: ATG-CTT-CTG-TCC-GTT-TGC-CG
	CreR: CCT-GTT-TTG-CAC-GTT-CAC-CG
Emx2KO	Ex1: GAA-CGA-CAC-AAG-TCC-CGA-GAG-TTT-C
	Ex2: CTC-ATA-TTG-CCC-TAA-CAA-AGC-TGA-GC
	Ex3: CAC-GAG-ACT-AGT-GAG-ACG-TGC-TAC
GFP	GFPF: GAG-GAC-ATC-AGC-GAC-TTC-TTC-ATC
	GFPR: TCG-TTC-ATG-TAC-ACC-ACC-TCG-AAG
LacZ	LacZF: TTG-GCG-TAA-GTG-AAG-CGA-C
	LacZR: AGC-GGC-TGA-TGT-TGA-ACT-G
Pax6KO	Px1: GCA-TAT-GGG-GGC-AAG-ACT-ATG-TG
	Px2: CCA-GAG-AAA-GAC-CTG-AGA-CAC-TTA-C,
	Px3: CTG-TTG-GGA-AGG-GCG-ATC-GGT-G
Sp8-floxed	1: CCA-ATG-GGA-GGA-AAA-CAC-ACC-CCC-TCT-TAC-TCC-TC
	2: CCA-GCT-TCC-TGG-ACT-CTT-TCA-GTA-TAG-TTT-TGA-AG
	3: GCG-TGC-AAT-CCA-TCT-TGT-TCA-ATG-GCC-GAT-C

5.4 Histology

5.4.1 Sample collection and processing

Embryonic tissue was derived by appropriate matings of individual mice. Pregnancy of mated females was identified upon the appearance of a vaginal plug. The day of the vaginal plug was defined as day 0.5 after fertilization (E0.5). After the embryos had reached the desired embryonic stage, pregnant mice were killed by cervical dislocation and embryos were removed by cesarean section. Embryos were dissected from the uteri and washed in ice-cold PBS. Additionally, a running number was given and a tissue sample was taken from each individual specimen and processed for extraction of genomic DNA and genotyping. Fixation of the tissues was performed by incubation in 4% PFA for several hours to ON at 4°C and washing in PBS. Until use, the embryos were kept in the cold.

For whole mount *in situ* hybridization, fixed embryos were processed through an ascending methanol series and stored (up to several months) at –20°C in 100% Methanol.

Tissues of mice (older than P5) were fixed by perfusion fixation. Those animals were anaesthetized by an intraperitoneal injection of Avertin (30μl/g body weight). After opening of the thorax, the right atrium of the heart was cut and the left ventricle

punctated with a butterfly canula (25 G, Sarstedt). The attached peristaltic pump (MP II, Harvard) delivered PBS into the blood circular system. Excessive blood and buffer evacuated through the incision in the right atrium of the heart. After approximately 1 minute, the circulating blood was completely exchanged with PBS. Now, the anaesthetized animals were perfused using 4% PFA for several minutes. Following the perfusion fixation, brains were dissected from the skull and postfixed in PFA overnight. Excessive fixative was then removed by washing in PBS. Tissues were further processed for paraffin sectioning or cryo sectioning.

5.4.2 Cryo sectioning

To process harvested tissues and embryos for the cryo sectioning, samples were fixed for 4h to overnight in 4% PFA. After washing excessively in PBS, specimens were incubated in 30% Sucrose/PBS, until they declined to the bottom of the well, to achieve cryo protection. Afterwards, the specimens were transferred and positioned into wells filled with TissueTec (Jung) embedding medium and frozen on dry ice. Until sectioning with a cryostat (CM 3050 S, Leica), cryo blocks were kept at –20°C.
For the sectioning, cryo blocks were glued to the block holder of the cryostat using a drop of TissueTec and freezing. Sections were 8μm to 40μm thick. After cutting, sections were collected on gelatinized Superfrost plus (Menzel) slides and allowed to dry on a 28°C heating plate for 30 min. Afterwards, the slides were kept at –20°C until further use.

5.4.3 Paraffin sectioning

For the embedding in paraffin, specimens were dehydrated in an ascending ethanol series and overnight incubation in Isopropanol. Following, they were incubated in 25% Toluol/Isopropanol, 50% Toluol/Isopropanol, 75% Toluol/Isopropanol and 100% Toluol for 1 hour each step (clearing up of the tissue). Then, tissues were incubated in liquid paraplast at 60°C for three days (changing the wax every day). Afterwards, the specimens were embedded in appropriate paraplast-filled wells and chilled on ice. Until sectioning with a microtome (Leica), the solid blocks were kept at 4°C

Paraffin sections were cut in a thickness from 5μm to 10μm and transferred to a heated water bath (43°C). After sections had spread, they were collected on glass slides (Menzel), transferred to slide boxes and dried overnight at 37°C. The dried sections were stored at 4°C.

5.4.4 Vibratome sectioning

For vibratome sectioning, embryos were embedded in a mixture of Gelatin/Albumin, containing 70μl/ml 25% Glutaraldehyde. The solid blocks were glued onto the slide holder of the vibratome (VT 100 E, Leica) using superglue (Uhu). The cutting chamber was then filled with H2O and sections were cut in 40-100μm thickness. Subsequently, the sections were collected onto glass slides using a brush (Faber Castell). After drying for 10 min. at RT, the slides were mounted with Mowiol or DAPI-containing mounting medium (Vector) and kept in the dark.

5.4.5 Cresyl violet nissl staining (Histological nuclear staining)

Paraffin sections were dewaxed in Histoclear and rehydrated in a descending Ethanol/H2O series. After incubating the sections for 15 min. in 50% K_2SO3 and rinsing in H2O, the samples were stained for 15 min. in 1,5% Cresyl violet (Sigma) in 10 mM Sodium acetate/10mM Acetic acid (Acetate buffer). Afterwards, the sections were incubated in Acetate buffer, three times for one minute and finally dipped in H2O. Excessive Cresyl violet was removed by incubation in 70% Ethanol for 3 min. Sections were then dehydrated in 100% Ethanol and cleared in Histoclear for 5 min. each step. Stained sections were mounted with a glass cover slip (Marienfeld) using Eukitt (Kindler) mounting medium.

5.5 In situ hybridization

In situ hybridization (ISH) was used for the visualization of mRNA transcripts in tissues. For mRNA staining of whole embryos, ranging from stage E8.5 to E12.5, whole mount *in situ* hybridization (WMISH) was performed. For ISH on tissue sections (stage E12.5 to P10), staining was performed on cryo sections using DIG-labeled mRNA probes or on paraffin sections using $[\alpha]^{35}$S-UTP-labeled riboprobes. The solutions for ISH were prepared using DEPC-treated RNAse-free water or PBS. Further, the working conditions and the tools were kept and used under minimal exposure to potential RNAse contamination.

5.5.1 mRNA antisense probes

Riboprobes for *in situ* hybridization were obtained from the lab stock or provided from outside laboratories. The probes consisted of cDNA-fragments, encoding for a specific region of the gene of interest. The probes, used in this study, are listed in table 3. Plasmids containing the cDNA were harvested from transformed *E. coli* and purified as described below. The plasmids were linearized by using the appropriate restriction enzymes and purified, enabling the transcription of the anti sense transcript.

5.5.1.1 Synthesis of Digoxygenin-UTP-labeled mRNA probes

Linearized template DNA was transcribed *in vitro* to generate the anti sense mRNA probes by using Digoxygenin-labeled (DIG) UTPs. The *in vitro* transcription was performed as described below for 2 hours at 37°C:

DEPC-treated H2O:	14μl
10Xtranscription buffer (Roche):	2μl
DIG-Nucleotide mix (Boehringer):	2μl
Linearized template DNA:	1μg
Placental RNAse inhibitor (Promega):	0.5μl
SP6, T7 or T3 RNA polymerase (Roche):	1μl
Total volume:	20μl

Afterwards, in order to check the efficiency of anti-sense mRNA synthesis, an aliquot was run on a 1% Agarose gel. The reaction mix was further incubated with 2μl/reaction

DNAse I for 15 min. at 37°C (to degrade excessive template DNA). The reaction was then diluted with 100μl TE, 10μl 4M LiCl and RNA was precipitated by adding 300μl Ethanol, followed by incubation at –20°C for 2 hours. After spinning the tubes for 20 min. at 13.000 rpm at 4°C, the pellet was washed in 70% Ethanol and briefly air-dried. The RNA pellet was then resuspended in 100μl DEPC-treated H2O and kept at –20°C.

5.5.1.2 Synthesis of [α]^{35}S-UTP-labeled mRNA probes

For synthesis of the radioactive-labeled mRNA probes, the linearized template DNAs (Table. 3) were transcribed *in vitro*, according to the following scheme:

DEPC-treated H2O:	10μl
10Xtranscription buffer (Roche):	2μl
DTT (Boehringer):	100μM
[α]^{35}S-UTP (Amersham):	80μCi
Linearized template DNA:	1μg
Placental RNAse inhibitor (Promega):	10U
SP6, T7 or T3 RNA polymerase (Roche):	10U
Total volume:	20

The reaction mix was incubated for 60 min. at 37°C. Afterwards, 1μl yeast tRNA (10mg/ml) and 2μl DNAse I (Promega) were added and incubated for 15 min. at 37°C. The DNA was then purified using G50 columns (Amersham) and the final volume was adjusted to 50% Formamide/50mM DTT. The radioactivity of 1μl of the transcribed probe was measured in a Scintillation counter (Beckmann) and should have at least 2x10^7 cpm.

Table 3: mRNA anti-sense probes for ISH

Gene	Linearization	Polymerase	Supplier
BMP4	BamHI	T3	C. Tickle
Coup-TF1	EcoRI	T3	A. Cooney
Cux1	HindIII	T7	J. Liu
Cux2	XbaI	T3	J. Liu
Dlx1	XbaI	T3	M. Price
Emx2 (long)	EcoRI	T7	A. Mallamaci
EphA7	BamHI	T3	D. Wilkinson
EphrinA5	HindIII	T3	J. Frisén
ER81	ApaI	SP6	V. Tarabykin
Fgf8	XhoI	T7	G. Martin
Fgfr1	NotI	T7	S. Tole
Fgfr3	XbaI	T3	S. Tole
Foxg1	Sfi	T7	Lab stock
Gad67	XhoI	T3	Lab stock
Gli3	HindIII	T7	A. Joyner
Gsh2	NotI	T7	A. Mallamaci
Hes5	HindIII	T3	R. Kageyama
ID2	SalI	T3	Lab stock
Lhx2	NotI	T7	G. Bernier
Mash1	XbaI	SP6	F. Guillemot
Ngn2	BamHI	T7	F. Guillemot
Nkx2.1	XbaI	T3	M. Price
Nkx6.2	Nco	T7	J. Ericson
Pax6	EcoRI	T3	C. Walther
Reelin	SpeI	T7	Lab stock
RzR-ß	EcoRI	T3	C. Kaznovski
Sfrp2	EcoRI	SP6	J. Nathans
Shh	HindIII	T3	A. McMahon
Sp8	HindIII	T7	D. Treichel
Sp8 (long)	SacI	T7	A. Zembrzycki
SP9	XhoI	T3	G. Griesel
Tbr1	HindIII	T3	J. Rubenstein
Wnt3a	EcoRI	SP6	A. McMahon
Wnt5a	EcoRI	Sp6	A. McMahon
Wnt7b	HindIII	T7	A. McMahon

5.5.2 Whole mount ISH

WMISH was performed with modifications, according to Wilkinson and Nieto (1993).

5.5.2.1 Pretreatment

Embryos were kept in Methanol at –20°C. For WMISH, tissues were processed through a descending Methanol/PBT series. After washing twice in PBT for 5 min., the head vesicles of the embryos were punctated with a small canula (27G, Neolus). Afterwards, they were bleached for 60 min. in 6% Hydrogen peroxide/PBT at RT. The bleaching solution was removed by washing the embryos three times in PBT (5 min.). Afterwards, the specimens were digested in 10μg/ml Proteinase K/PBT for five to 10 min. (5 min. for stage E8.0-E9.5 and 10 min. for stage E10-E12.5). After stopping of the Proteinase K reaction (by washing 5 min. in Glycine buffer), the embryos were washed twice in PBS for 5 min. Postfixation was then performed in 0.2% Glutaraldehyde/4% PFA/PBT for 20 min. After removing the fixative by washing in PBT, the embryos were prehybridized for 90 min. at 70°C in Prehybridization solution by using a preheated water bath. The hybridization of sections with riboprobes (approx. 1μg/ml in prehybridization solution) was done overnight at 70°C in a water bath. Prior to adding probes to the prehybridization mix, they were denaturated for 3 min. on an 80°C heat block.

5.5.2.2 Post hybridization washes

The hybridization mix was removed and the samples washed in Sol I for 30 min. at 70°C. Further, they were washed for 10 min. in Sol I/Sol II (1:1) at 70°C and three times in Sol II for 5 min. at RT. The unspecific binding of mRNA probes was removed by incubating the embryos for 30 min. in 100μg/mlRNAse A/Sol II at 37°C. The reaction was then stopped by washing in SolI I, then in Sol III for 5 min. at RT, followed by two washing steps in Sol III for 5 min. at RT alone. Excessive formamide in the samples was removed by washing three times in TBST (5 min. at RT).

Afterwards, the tissues were blocked in 10% FCS/TBST for 90 min. at RT. During the washing procedures, the AP-tagged DIG antibody (Roche) was diluted 1:2000 and preabsorbed in 5μl FCS/3mg embryo powder/2 ml TBST for several hours by rocking at 4°C. After blocking of the embryos, they were incubated with the preabsorbed antibody, gently shaking overnight at 4°C.

5.5.2.3 Post antibody washes and histochemistry

On the next morning, the antibody solution was removed and the embryos were transferred to screw-capped glass cylinders (4ml volume), filled with MABT. These cylinders were incubated for 3 to 4 days (shaking) at 4°C and changing the MABT twice a day. After these excessive washings, the embryos were transferred to Petri dishes and the brain vesicles were again punctated with a canula. Afterwards, they were washed in NTMT (three times for 10 min.) and the staining reaction developed in NBT/BCIP in NTMT (1:200) at RT. The staining solution was changed every 90 to 120 min. The enzymatic reaction was stopped by incubation in PBT three times for 5 min., therefore changing the pH. Stained embryos were fixed overnight in 4% PFA, washed in PBS and kept in the cold. For imaging, the embryos were incubated in 30% Glycerol/H2O and 50% Glycerol/H2O for 2 hours each step. For sectioning, the embryos were kept in PBS and processed for vibratome sectioning.

5.5.3 ISH on cryo sections (cold *in situs*)

ISH on cryo sections was performed, following the protocol of Moorman et al. (1993).

5.5.3.1 Pretreatment and hybridization

Cryo sections were thawed and allowed to air dry for approximately 20 min. Following, the slides were encircled with a chemical and heat-resistant ImmEdge pen (Vector). The dried slides were then postfixed in PFA for 20 min. and rinsed in PBS twice for 5 min. Proteinase K treatment was done afterwards in Prot K buffer for 4 min. at RT. The

digestion was stopped by incubation of the samples in Glycine buffer and rinsing in PBS twice (each step for 5 min.). Then, the sections were refixed in postfix buffer for 20 min. and washed in PBS for 10 min.
Afterwards, slides were transferred to a humidified chamber and coated with 180μl/slide prehybridization mix, followed by 2 hours of incubation in a hybridization oven at 70°C. Then, (in order to denature the RNA´s) the DIG labeled probe was incubated for 3 min. on a heat block (80°C). The prehybridization mix was further removed from the slides and replaced by 150μl Hybridization mix/slide. The hybridization was done overnight at 70°C.

5.5.3.2 Post hybridization washes and antibody incubation

The next day, all sections were rinsed in 2X SSC (pH4.5) for 5 min. and washed three times under high stringency conditions in 50% Formamide/2X SSC (pH4.5) for 30 min. at 65°C. Subsequently, slides were washed in KTBT for 10 min. twice and blocked in 20% FCS/KTBT blocking solution for 1 hour. The αDIG antibody (coupled to alkaline phosphatase, Roche) was diluted 1:2000 in blocking solution, in which the sections were incubated overnight at 4°C.

5.5.3.3 Post antibody washes and histochemical staining

Excessive and unspecifically bound antibodies were removed by extensive washing. The washing was performed in KTBT six times for 30 min. Afterwards; sections were incubated twice in (alcalic) NTMT for 15 min. The staining was derived by incubation of slides in staining solution, containing NBT/BCIP and NTMT (1:200). The staining reaction was developed at RT protected from light. Approximately every 2 to 3 hours the staining solution was changed. The development of the color strengths was monitored and the staining was typically stopped after 5-8 hours. In the case of only a weak staining of the tissue after several hours, the specimens were further stained overnight at 4°C. The color-reaction was afterwards stopped by washing three times in PBS (neutral pH) for 5 min. Stained sections were mounted with a glass cover slip using Mowiol mounting medium and kept at RT (protected from excessive light).

5.5.4 Radioactive ISH (hot *in situs*)

5.5.4.1 Pretreatment and hybridization

Hot *in situs* were performed on 10μm paraffin sections. First, the slides were dewaxed by washing them twice for 10 min. in Histoclear. Slides were then rehydrated through a descending Ethanol/H2O series and equilibrated for 5 min. in Saline (0.86% NaCl). After washing the specimens for 5 min. in PBS, they were postfixed in 4% PFA for 20 min. The fixative was removed by incubation of the samples in PBS twice (5 min.). Further, the slides were treated with Prot K buffer for 2 min. at 37°C. Refixation was achieved afterwards by incubation of the slides in PFA for 5 min. Slides were then washed in PBS (5 min.) and in Acetylation mix (0.1M Triethylamine/0.25% Acetic acid anhydride, 10 min.). These buffers were removed by washing samples twice in PBS and Saline for 5 min. Afterwards, the sections were dehydrated through an ascending Ethanol series. The dehydrated slides were allowed to air dry for 60 min. at RT.
The [^{35}]S-labeled RNA probes were subsequently diluted in hybridization mix to a final concentration of 5x10^{4}cpm/μl. The probes were then denaturated by incubating them for 3 min. in a heat block at 80°C. Following, the probes were applied on the sections (approx. 4μl/section) and then slides were sealed with a glass cover slip (15x20mm, Menzel). Hybridization of the slides with the labeled probes was incubated overnight in a humidified chamber at 50°C.

5.5.4.2 Post hybridization washes

To get rid of possible unspecific RNA hybrids, the sections were washed twice (gently shaking) in 50% Formamide/2X SSC pH4.5/0.14% Mercaptoethanol; first at 37°C, then at 65°C. The still remaining attached cover slips were then removed and the slides washed for 3 hours in 50% Formamide/2X SSC pH4.5/0.14% Mercaptoethanol at 37°C. Afterwards, the sections were equilibrated by washing them 15 min. in NTE. Unspecifically bound RNA was removed by incubating sections in 20μg/mlRNAse

A/NTE for 15 min. at 37°C. Slides were then washed in NTE (15 min.) and 50% Formamide/2X SSC pH4.5/0.14% Mercaptoethanol (30 min.) at 37°C. Subsequently, formamide was removed by washing the samples twice in 2X SSC and once in 0.1X SSC for 15 min. Sections were then dehydrated through an ascending ethanol series.
To get a first impression about the specificity and the strengths of the signal, slides were transferred to a developing cassette, covered with an autoradiography film (Biomax, Agfa) and the film developed overnight.

5.5.4.3 Dipping

The application of the liquid film emulsion (dipping solution) was performed in complete darkness (no red safety light) in the darkroom. The dipping solution was filled into a dipping cuvette (MPI work shop) and heated to 42°C in a water bath. Slides were then dipped twice for several seconds and air dried for 2 hours at RT. Afterwards, the slides were transferred into a completely photoresistent slide box and exposed for 3 weeks at 4°C.

5.5.4.4 Developing of the slides

The developing of the autoradiography was performed in complete darkness. All solutions were chilled to 18°C and slides were first incubated for 3 min. in 16% D-19 developing solution (Kodak). Slides were then washed in 1% Acetic acid for 1 minute and fixed in 30% Natrium thiosulfate for 3 min. Excessive solutions were removed from sections by washing them three times in H2O at RT, followed by three washing steps at 42°C. To counterstain the tissues, slides were incubated for 30 min. in Giemsa staining solution (4% Giemsa stock-solution/40mM Natrium phosphate buffer pH6). Afterwards, the sections were washed for 30-40 min. in tap water and air dried for several hours. The dried sections were then mounted with Eukitt mounting medium.

5.6 Immunohistochemistry

Immunohistochemistry was performed on 18μm cryo sections or paraffin-embedded sections of 5μm to 10μm thickness. The protein antigens were generally unmasked by boiling sections for 2 min. in citrate buffer (Vector) in a pressure cooker (MPI work shop). The primary antibodies used were as indicated in Table 4. Paraffin sections were dewaxed in Histoclear (Vogel), rehydrated in a descending ethanol series and rinsed in PBS. Cryosections were washed in PBS and afterwards postfixed in 4% PFA/PBS for 10 min. After unmasking of the epitopes by boiling, the sections were blocked in a solution containing PBT (PBS + 0,1% TritonX 100) and 10% FCS for 30 min. The diluted primary antibodies were incubated on the slides for overnight at 4°C in blocking solution. Then, the secondary antibodies were diluted 1:500 in blocking solution and sections incubated for 1-2 hours at room temperature. The secondary antibodies used were Alexa594- or Alexa488-conjugated antibodies raised against mouse-, rabbit- or rat antigens (Molecular Probes). Before mounting, the sections were rinsed three times for 5 min. in PBT and sealed with Vectashield mounting medium containing DAPI or Propidium Iodide (as nuclear counterstain) (Vector). The mounted sections were kept at 4°C protected from light.

Table 4: Primary Antibodies

Name	Host	Marker	Supplier
BrdU	Mouse	S-phase marker	Abcam
BrdU/IdU	Rat	S-phase marker	Caltag
Gap43	Rabbit	Intermediate filament marker	Chemicon
GFAP	Rabbit	Glia cells	Dako
Nestin	Rabbit	Progenitors/Glia	Chemicon
NeuN	Mouse	Neuronal marker	Chemicon
Pax6	Rabbit	Palliial VZ progenitors	Babco
Phospho Histone H3	Mouse	M-phase marker	Abcam
Reelin	Mouse	Cajal-Retzius cells	A. Goffinet
Tbr1	Rabbit	Postmitotic deep-layer neurons	R. Hevner
Tbr2	Rabbit	SVZ-progenitors	R. Hevner
Tuj1	Mouse	Postmitotic neurons	Covance

5.7 ß-Galactosidase staining, using X-Gal substrate

X-Gal staining was performed on whole mount tissues or on 18μm cryo sections. The ß-galactosidase activity was developed in staining solution (PBS, 1mg/ml X-Gal, 2mM $MgCl_2$, 0,01% SDS, 0,02% NP40, 5mM $K_3Fe(CN)_6$, 5mM $K_4Fe(CN)_6$) for several hours to overnight at 37°C protected from light. Specimens were then washed in PBS and postfixed in PFA. X-Gal stained sections were then counterstained for 10 min. in 0.1% Neutral Red (Sigma). After counterstaining was done, the samples were dehydrated in 70% Ethanol and 100% Ethanol for 2 min. Slides were finally processed through Histoclear (Kindler) for 5 min. and then sealed with a glass cover slip using Eukitt (Kindler) mounting medium.

5.8 BrdU/IdU labeling strategies

BrdU and IdU (Sigma) uptake experiments were done by intraperitoneal injection (50 μg/g body weight) of either BrdU or IdU alone, or both nucleotide analogs simultaneously into pregnant mice. For pulse labeling, the injected mice were sacrificed 30 min. after injection. The S-Phase labeling index was subsequently estimated by dividing DAPI+ from BrdU+ cells, counted on complete forebrain sections. For fate mapping analysis, BrdU was injected into pregnant mice on varying time points from E 10.5 to E 16.5 of development. Tissues of injected embryos were then dissected on E14.5, E15.5, E16.5 E18.5 or P10, respectively. The cell cycle lengths were determined, according to Martynoga et al. and Burns and Kuan (2005). The strategy is visualized in the scheme below (Fig. 46). The verification of the cell cycle leaving fraction was performed by dividing the values of counted IdU+/BrdU+ cells from IdU+-only cells on immunolabeled forebrain sections. The samples of injected embryos were in all cases processed for paraffin embedding and subsequently 5μm to 10μm sections were cut and then used for immunohistochemistry.

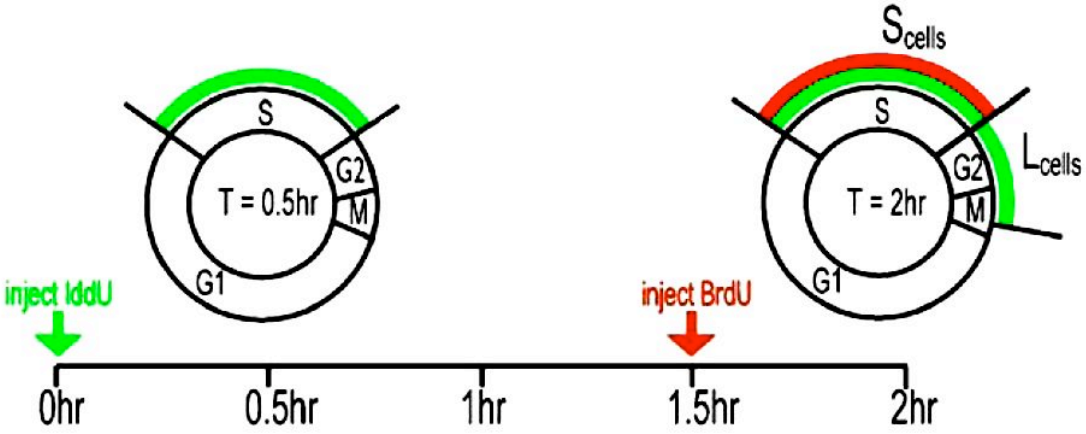

Figure 46: BrdU/IdU double labeling strategy. At time point P0, pregnant mothers were injected with IdU. After 1.5 hours, the same mice were injected with BrdU. After a 30 min. interval, the double injected tissues were dissected sectioned and stained with antibodies for BrdU and IdU. The division of BrdU+/IdU+ (double positive) cells from the BrdU+ cells was used to calculate the cell cycle leaving fraction. (adapted from Martynoga et al., 2005).

5.9 TUNEL staining

TUNEL assay was done on 5μm sections of varying age (E10.5-P5) using ApopTag Red *In Situ* Apoptosis Detection Kit (Chemicon). Experiments were performed, according to manufacturers advice. TUNEL staining visualizes DNA double strand knick-breaks, characteristic for already fragmented genomic DNA of apoptotic cells. The assayed amount of TUNEL+ cells of control specimens of a particular stage was defined as 100% and the resulting amount of TUNEL+ of mutant tissues displayed according to the wild type (100%) value. Apoptotic clusters were only identified in cKO specimens from stage E12.5 to E18.5 and were statistically classified as one TUNEL+ apoptotic cell.

5.10 Cell tracing with lipophylic Dyes

Anterograde or retrograde labeling of axonal processes and neuronal trajectories was performed using the lipophylic dyes DiI and DiO (Molecular Probes). Both lipophylic tracers can diffuse along the cell membrane of axons, therefore the labeling allows the visualization of such treated cells. The two different dyes differ in their emission spectra

Subsequent application of both tracers enabled us to follow the projections of different neuronal populations simultaneously.

For tracing experiments with a single dye, the brains of the desired embryonic stage were dissected from the skull and then fixed for three days in 4% PFA. We performed the dye labeling on E18.5 mostly hemisected brains of cKO and control embryos. The hemi sectioning of the brains was done, by cutting the fixed brains along the midline with a blade (Swann-Morton). Before applying the dyes, the samples were dried with a Kim wipe tissue. For retrograde axon labeling, small crystals of DiI and DiO were placed into the white matter of the somatosensory cortex.

In double labeling experiments, DiI was placed in the visual cortex and DiO into the somatosensory cortex area of the assayed brains, respectively. For an anterograde labeling of the dorsal thalamus/diencephalon afferents, the DiI was inserted into the dorsal thalamus, posterior to the caudal edge of the cortical hemisphere. To label callosal projection neurons anterogradely, the DiI tracer was inserted into the white matter of the rostromedial pallium of the right brain hemisphere of non-hemisected brains and the DiO-crystal into the left hemisphere. In order to document the reproducibility of the injection sites, images were taken. For the diffusion of the injected tracers, treated samples were kept in 4% PFA. The dye-transport developed for 4 weeks at 37°C protected from light.

Afterwards, the fixative was removed from the brains by washing specimens in PBS for 1 hour. Subsequently, brains were embedded in 5% LMP Agarose (Invitrogen). Then, 100μm thick sections were cut with a vibratome, lifted to glass slides and counterstained with mounting medium containing DAPI (Vector). Because of a fast and extensive photo bleaching of the dye-treated tissue sections, images were taken on the same day.

5.11 Molecular biology methods

5.11.1 Commercial kits

The purification of bacterial plasmid DNA was performed using Mini, Midi and Maxi Kits (Qiagen). The purification and the extraction of DNA fragments from agarose gels were done using the Gene Clean DNA gel extraction kit (Q-Bio-Gene). Phenol/Chloroform extraction and DNA precipitation was done, according to standard protocols.

5.11.2 Culturing and handling of bacteria

Handling of the bacteria was always done assuring sterile working equipment and conditions. Bacterial stocks were created by diluting 1ml of an overnight culture to 15% Glycerol and freezing of tubes on dry ice. The bacterial stocks were kept at –80°C.
For the liquid culture of bacteria, 5-200ml standard media was inoculated with the appropriate bacterial stock and adding the required antibiotic (50μg/ml, Ampicillin, Kanamycin), according to standard protocols. After 15 hours of incubation on a rotator at 37°C, cells were sedimented, resuspended and processed for plasmid purification using commercial kits.
Culturing of bacteria on agar plates was performed using a Drygalski spattel or an inoculating loop. Agar plates contained the appropriate antibiotic and were incubated for not longer than 15 hours at 37°C.

5.11.3 Cloning of DNA constructs

The cloning of DNA constructs was done, by sub cloning of DNA fragments into appropriate bacterial vectors (pLCBS, pBSKS+, pGEMt-EASY, pGEX-4T-3, pCMV-TnT, lab stock P. Gruss). The DNA fragments were obtained by restriction digest, followed by the purification of plasmid DNA or the amplification of DNA fragments using PCR primers. The target vector and the DNA fragments were ligated by using T4-

ligase (Promega) and incubation at 16°C overnight (in a vector to fragment ratio of 1:3 to 1:5). The ligated plasmids were transformed into Ca^{2+}-competent *E. coli* as described below.

5.11.4 Chemical-competent bacteria

To create chemical competent cells, 100 ml of standard media was inoculated with *E. coli DH5-α* cells and incubated on a shaker for overnight at 37°C. The culture was then sedimented in a cooled centrifuge (15 min. at 3000rpm) at 4°C. After discarding the supernatant, the cell pellet was resuspended on ice in 10 ml 50mM $CaCl_2$ and further incubated for 30 min. in the cold. Following, cells were sedimented as described above and resuspended in 10 ml $CaCl_2$/10% Glycerol. The cell suspension was split into 100 µl aliquots and frozen on dry ice. Afterwards, the chemical competent cells were kept at –80°C for several month.

5.11.5 Heat-shock transformation of Ca^{2+} competent *E. coli*

For the transformation of circular plasmids into bacterial hosts, aliquoted competent cells were slowly thawn on ice. After adding of 3µl plasmid DNA (in varying concentrations) and incubation on ice for 20 min., the cell suspension was put into a 42°C heat block for 50 seconds (precise). Immediately afterwards, cells were put on ice for 10 min. The bacteria were then diluted with 800µl standard medium and incubated shaking for 30 min. at 37°C. The cells were subsequently sedimented briefly and then resuspended in 100µl media. The transformed cells were then plated on agar plates with a Drygalski spattel. Plates were further incubated overnight at 37°C. Potential positive colonies were analyzed after plasmid purification and analytical digests. In case of transformed pGemT-EASY vectors, positive colonies were identified upon blue/white selection by additionally plating 100µl of X-Tra-Blue (Q-BioGene) reagent per agar plate.

5.11.6 Analytical digests

Analytical digests were performed, by incubating plasmid DNA with appropriate commercial restriction enzymes, supplemented with suitable cutting buffers (according to the manufacturers advice). Double digests were performed using the optimal buffer following the activity chart table (Boehringer). Digests were typically incubated for 1 hour to overnight at 37°C. Digested samples were then run on an analytical agarose gel and photographs taken with a digital camera (BioRad). The analysis of the fragment sizes was done by comparison with the known sequence data by using the Sequencer software (Gene Codes Corporation).

5.11.7 GST-pulldown assay

To evaluate biochemical interactions between Sp8 and Emx2 proteins, Sp8 (MGI clone 2443471) full-length cDNA (i, AA 1-486) and Sp8 lacking Zn-fingers cDNA (ii, Sp8ΔZn, AA 1-355) was PCR-amplified, adding 5´ BamHI and 3´ EcoRI restriction sites using primers indicated in table 5. Synthesized PCR fragments were digested, creating the inserted 5´ and 3´ restriction site overhangs, subcloned into the BamHI and EcoRI restriction sites of the pGEX-4T-3 protein expression vector (Promega), generating in frame GST-Sp8 fusion protein sequences (i and ii), and transformed into *E. coli* BL21 (Promega).

For each construct, a single colony, carrying one of the two GST-Sp8 fusion proteins vectors (i and ii), and the GST vector without fusion partner (iii) as control were picked, 500 ml LB-Amp medium inoculated and cultures incubated at 37°C. At optical density of 0.5, 0.4 mM IPTG was added to the culture media, inducing protein expression. IPTG-induced liquid cultures were then transferred to 30°C and protein expression incubated for 1 hour. Afterwards, cells were sedimented by centrifugation (4000 rpm for 15 min. at 4°C) and washed in ice-cold PBS. The cell extract was harvested by adding 10 ml Lysis buffer and rotating for 30 min at 4°C. Then, the lysate was frozen in liquid nitrogen, thawed on ice and sonicated for 15 seconds (amplitude 15-25 microns) in a tip sonicator (Cell Disruptor B15, Benson). After centrifugation for 20 min at 15.000 rpm in the cold, the supernatant was frozen in dry ice and kept at –80°C until further use.

To purify the GST fusion protein, 1ml of the cell lysate supernatant was incubated with 100μl glutathione sepharose beads (Amersham) and 10 Volumes HEMG 1, rotating 2 hours at 4°C. Afterwards, affinity beads were washed three times 10 minutes in HEMG 1, HEMG 2 and HEMG 3, rotating in the cold, and afterwards kept at 4°C.

To generate *in vitro* translated Emx2 protein, Emx2 (gift from A. Mallamaci) full-length cDNA (i, AA 1-253) and Emx2 lacking the homeobox (ii, Emx2ΔHox, AA 1-144) was PCR-amplified, adding 5´ EcoRI and 3´ NotI restriction sites using primers indicated below in table 5. PCR products were digested and subloned into the EcoRI and NotI restriction sites of the pCMV-TnT vector (Promega) and transformed into *E. coli*.

1μg purified vector, carrying one of the two Emx2 protein sequences (i and ii), was then transcribed *in vitro* using a TNT-Rabbit Reticulocyte lysate protein transcription kit (Promega), adding 2μl/reaction $^{[32]}$S-labeled methionin (Amersham), according to manufacturers recommendations (Promega). After incubating the translation reaction at 30°C for 90 minutes, the lysate was diluted with 210μl HEMG 3 and sedimented for 15 min at 15000 rpm in the cold.

Afterwards, 50μl of the reticulocyte lysate supernatant was mixed with 15μl GST-, GST-Sp8 full-length- and GST-Sp8 lacking Zn-fingers affinity beads and incubated in 10 volumes HEMG 3, rotating 2 hours at 4°C. The beads were then washed five times in HEMG 3, rotating 10 minutes at 4°C. Subsequently, excessive wash buffer was removed and affinity beads were resuspended in 50μl 5X Sample buffer, boiled for 5 minutes in a water bath and immediately analyzed on a 15% SDS-PAGE gel or frozen in liquid nitrogen and kept at –80°C.

Following electrophoresis (described below), the SDS gel was washed three times in H2O, dried in a vacuum dryer (Christ), transferred into a developing cassette and covered with an autoradiography film (Biomax, Agfa). After 3 days exposure time at –70°C, the film was developed in a developing machine (Agfa).

Table 5: Primer sequences for GST-pulldown assay.

(lower case letters highlight base sequences of added restriction sites)

Amplified sequence	Name and Sequence
Sp8 full-length + 5´ BamHI and 3´ EcoRI site	Sp8-full for: G CGC gga tcc ATG CTT GCT GCT ACC TGT AAT AAG ATC Sp8-full rev: G CGC gaa ttc CTC CAG GCC GTT GCG GTG
Sp8 lacking Zn-fingers + 5´ BamHI and 3´ EcoRI site	Sp8-short rev: G CGC gaa ttc CAG CCC TTT GCG ACG CAG GC
Emx2 full-length + 5´ EcoRI and 3´ NotI site	Emx2-full for: G CGC gaa ttc ATG TTT CAG CCG GCG CC Emx2-full rev: GCG Cgc ggc cgc ATC GTC TGA GGT CAC ATC
Emx2 lacking homeobox + 5´ EcoRI and 3´ NotI site	Emx2-short rev: GCG Cgc ggc cgc GCC AGG GGT AGA AGG TGG ACG

5.11.8 SDS-PAGE

For electrophoresis of proteins, a 15% SDS-PAGE running gel was prepared, according to standard procedures, mixing the below indicated ingredients in a falcon tube.

SDS-PAGE (15%):	
H2O:	7.2 ml
1.5M Tris pH 8.8:	7.5 ml
10% SDS:	0.3 ml
30% Acryl amide (Roth):	15 ml
10% Ammonium persulfate:	0.15 ml
TEMED (Sigma):	0.02 ml

The gel was poured immediately in a prepared SDS-PAGE chamber (MiniVE, Hoefler), covered with 1ml Isopropanol, and allowed to polymerize for approximately 30 minutes. Afterwards, 2 ml stacking gel (indicated below) was poured on top of the running gel and a sample comb placed above the stacking gel.

Stacking gel:	
H2O:	3.075 ml
0.5M Tris pH 6.8:	1.25 ml
10% SDS:	0.05 ml
30% Acryl amide (Roth):	0.67 ml
10% Ammonium persulfate:	0.025 ml
TEMED (Sigma):	0.005 ml

After polymerization, the gel chamber was filled with running buffer. Then, samples were boiled for 5 minutes in a water bath and loaded into the pockets, opened by the removed sample comp. Applying 70V for 1 hour first and subsequently applying 120V for two to three hours was performed for gel electrophoresis. Afterwards, the gel was removed from the chamber, washed three times in H2O and processed for further use, according to standard procedures.

5.11.9 Quantitative RT-PCR

Total RNA was extracted from complete E12.5 and E15.5 forebrains of mutant and control specimens. Dissected tissues were collected and stored in RNAlater (Ambion) at –20°C. The homogenization of samples and further the RNA extraction was done using Trizol (Invitrogen) reagent according to manufacturers recommendations with a Polytron PT 1200 homogenizer (Kinematica). The concentration of the extracted RNA was measured with a photometer (Eppendorf). The quality of the RNA was estimated by using a RNA Bio analyzer (Agilent). Total RNA samples were then stored at –20°C. The first strand cDNA was generated with a QuantiTect reverse transcription Kit (Qiagen). RT-PCR was done by using a Realplex Mastercycler (Eppendorf) RT-PCR cycler and the QuantiTect SYBR-Green RT-PCR kit (Qiagen). The used primers for the detection of the target transcripts were specific mouse QuantiTect primer assays (qiagen.com). We used 18s rRNA as housekeeping gene (control) and Sp8, Emx2, Foxg1, Reelin, Cux2 and Hes5 primer assays as unknown targets. The relative quantification of mRNA levels was done by the monoplex method. Monoplex quantitative PCR calculates the unknown relative expression level of the target gene by normalization of its expression to the expression level of the housekeeping gene in different wells. All experiments included the appropriate negative and internal controls according to the manufacturers recommendations. Quantifications were repeated at least three times under equal conditions and analyzed using Excel (Microsoft).

6 LITERATURE

Assimacopoulos, S., Grove, E. A. & Ragsdale, C. W. Identification of a Pax6-dependent epidermal growth factor family signaling source at the lateral edge of the embryonic cerebral cortex. *J Neurosci* **23**, 6399-403 (2003).

Bell, S. M. et al. Sp8 is crucial for limb outgrowth and neuropore closure. *Proc Natl Acad Sci U S A* **100**, 12195-200 (2003).

Bertrand, N., Castro, D. S. & Guillemot, F. Proneural genes and the specification of neural cell types. *Nat Rev Neurosci* **3**, 517-30 (2002).

Bishop, K. M., Goudreau, G. & O'Leary, D. D. Regulation of area identity in the mammalian neocortex by Emx2 and Pax6. *Science* **288**, 344-9 (2000).

Bishop, K. M., Rubenstein, J. L. & O'Leary, D. D. Distinct actions of Emx1, Emx2, and Pax6 in regulating the specification of areas in the developing neocortex. *J Neurosci* **22**, 7627-38 (2002).

Bulchand, S., Subramanian, L. & Tole, S. Dynamic spatiotemporal expression of LIM genes and cofactors in the embryonic and postnatal cerebral cortex. *Dev Dyn* **226**, 460-9 (2003).

Burns, K. A. & Kuan, C. Y. Low doses of bromo- and iododeoxyuridine produce near-saturation labeling of adult proliferative populations in the dentate gyrus. *Eur J Neurosci* **21**, 803-7 (2005).

Campbell, K. & Gotz, M. Radial glia: multi-purpose cells for vertebrate brain development. *Trends Neurosci* **25**, 235-8 (2002).

Casarosa, S., Fode, C. & Guillemot, F. Mash1 regulates neurogenesis in the ventral telencephalon. *Development* **126**, 525-34 (1999).

Cau, E., Gradwohl, G., Fode, C. & Guillemot, F. Mash1 activates a cascade of bHLH regulators in olfactory neuron progenitors. *Development* **124**, 1611-21 (1997).

Chan, W. Y., Lorke, D. E., Tiu, S. C. & Yew, D. T. Proliferation and apoptosis in the developing human neocortex. *Anat Rec* **267**, 261-76 (2002).

Chiang, C. et al. Cyclopia and defective axial patterning in mice lacking Sonic hedgehog gene function. *Nature* **383**, 407-13 (1996).

Collinson, J. M., Quinn, J. C., Hill, R. E. & West, J. D. The roles of Pax6 in the cornea, retina, and olfactory epithelium of the developing mouse embryo. *Dev Biol* **255**, 303-12 (2003).

Corbin, J. G., Rutlin, M., Gaiano, N. & Fishell, G. Combinatorial function of the homeodomain proteins Nkx2.1 and Gsh2 in ventral telencephalic patterning. *Development* **130**, 4895-906 (2003).

Dellovade, T. L., Pfaff, D. W. & Schwanzel-Fukuda, M. Olfactory bulb development is altered in small-eye (Sey) mice. *J Comp Neurol* **402**, 402-18 (1998).

Depaepe, V. et al. Ephrin signalling controls brain size by regulating apoptosis of neural progenitors. *Nature* **435**, 1244-50 (2005).

Dou, C. L., Li, S. & Lai, E. Dual role of brain factor-1 in regulating growth and patterning of the cerebral hemispheres. *Cereb Cortex* **9**, 543-50 (1999).

Dupont, E., Hanganu, I. L., Kilb, W., Hirsch, S. & Luhmann, H. J. Rapid developmental switch in the mechanisms driving early cortical columnar networks. *Nature* **439**, 79-83 (2006).

Eisenstat, D. D. et al. DLX-1, DLX-2, and DLX-5 expression define distinct stages of basal forebrain differentiation. *J Comp Neurol* **414**, 217-37 (1999).

Englund, C. et al. Pax6, Tbr2, and Tbr1 are expressed sequentially by radial glia, intermediate progenitor cells, and postmitotic neurons in developing neocortex. *J Neurosci* **25**, 247-51 (2005).

Estella, C., Rieckhof, G., Calleja, M. & Morata, G. The role of buttonhead and Sp1 in the development of the ventral imaginal discs of Drosophila. *Development* **130**, 5929-41 (2003).

Friocourt, G., Poirier, K., Rakic, S., Parnavelas, J. G. & Chelly, J. The role of ARX in cortical development. *Eur J Neurosci* **23**, 869-76 (2006).

Fukuchi-Shimogori, T. & Grove, E. A. Emx2 patterns the neocortex by regulating FGF positional signaling. *Nat Neurosci* **6**, 825-31 (2003).

Garel, S., Huffman, K. J. & Rubenstein, J. L. Molecular regionalization of the neocortex is disrupted in Fgf8 hypomorphic mutants. *Development* **130**, 1903-14 (2003).

Gong, Q. & Shipley, M. T. Evidence that pioneer olfactory axons regulate telencephalon cell cycle kinetics to induce the formation of the olfactory bulb. *Neuron* **14**, 91-101 (1995).

Gorski, J. A. et al. Cortical excitatory neurons and glia, but not GABAergic neurons, are produced in the Emx1-expressing lineage. *J Neurosci* **22**, 6309-14 (2002).

Griesel, G. et al. Sp8 controls the anteroposterior patterning at the midbrain-hindbrain border. *Development* **133**, 1779-87 (2006).

Griesel, G. Funktionelle Analyse des Zinkfinger-Transkriptionsfaktors Sp8 während der frühen Mittel- und Hinterhirnentwicklung. *Inaguraldissertation Justus-Liebig-Universität Gießen.* (2006).

Grove, E. A., Tole, S., Limon, J., Yip, L. & Ragsdale, C. W. The hem of the embryonic cerebral cortex is defined by the expression of multiple Wnt genes and is compromised in Gli3-deficient mice. *Development* **125**, 2315-25 (1998).

Guillemot, F., Molnar, Z., Tarabykin, V. & Stoykova, A. Molecular mechanisms of cortical differentiation. *Eur J Neurosci* **23**, 857-68 (2006).

Gutin, G. et al. FGF signalling generates ventral telencephalic cells independently of SHH. *Development* **133**, 2937-46 (2006).

Hamasaki, T., Leingartner, A., Ringstedt, T. & O'Leary, D. D. EMX2 regulates sizes and positioning of the primary sensory and motor areas in neocortex by direct specification of cortical progenitors. *Neuron* **43**, 359-72 (2004).

Hebert, J. M. & McConnell, S. K. Targeting of cre to the Foxg1 (BF-1) locus mediates loxP recombination in the telencephalon and other developing head structures. *Dev Biol* **222**, 296-306 (2000).

Hebert, J. M., Lin, M., Partanen, J., Rossant, J. & McConnell, S. K. FGF signaling through FGFR1 is required for olfactory bulb morphogenesis. *Development* **130**, 1101-11 (2003).

Hevner, R. F. et al. Tbr1 regulates differentiation of the preplate and layer 6. *Neuron* **29**, 353-66 (2001).

Hevner, R. F., Hodge, R. D., Daza, R. A. & Englund, C. Transcription factors in glutamatergic neurogenesis: conserved programs in neocortex, cerebellum, and adult hippocampus. *Neurosci Res* **55**, 223-33 (2006).

Jimenez, D. et al. Evidence for intrinsic development of olfactory structures in Pax-6 mutant mice. *J Comp Neurol* **428**, 511-26 (2000).

Kammermeier, L. & Reichert, H. Common developmental genetic mechanisms for patterning invertebrate and vertebrate brains. *Brain Res Bull* **55**, 675-82 (2001).

Kawakami, Y. et al. Sp8 and Sp9, two closely related buttonhead-like transcription factors, regulate Fgf8 expression and limb outgrowth in vertebrate embryos. *Development* **131**, 4763-74 (2004).

Kawauchi, S. et al. Fgf8 expression defines a morphogenetic center required for olfactory neurogenesis and nasal cavity development in the mouse. *Development* **132**, 5211-23 (2005).

Kimura, J. et al. Emx2 and Pax6 function in cooperation with Otx2 and Otx1 to develop caudal forebrain primordium that includes future archipallium. *J Neurosci* **25**, 5097-108 (2005).

Kolk, S. M., Whitman, M. C., Yun, M. E., Shete, P. & Donoghue, M. J. A unique subpopulation of Tbr1-expressing deep layer neurons in the developing cerebral cortex. *Mol Cell Neurosci* **30**, 538-51 (2005).

Kriegstein, A. R. & Noctor, S. C. Patterns of neuronal migration in the embryonic cortex. *Trends Neurosci* **27**, 392-9 (2004).

LaMantia, A. S., Bhasin, N., Rhodes, K. & Heemskerk, J. Mesenchymal/epithelial induction mediates olfactory pathway formation. *Neuron* **28**, 411-25 (2000).

Laub, F., Dragomir, C. & Ramirez, F. Mice without transcription factor KLF7 provide new insight into olfactory bulb development. *Brain Res* **1103**, 108-13 (2006).

Long, J. E., Garel, S., Depew, M. J., Tobet, S. & Rubenstein, J. L. DLX5 regulates development of peripheral and central components of the olfactory system. *J Neurosci* **23**, 568-78 (2003).

Lopez-Mascaraque, L., Garcia, C., Valverde, F. & de Carlos, J. A. Central olfactory structures in Pax-6 mutant mice. *Ann N Y Acad Sci* **855**, 83-94 (1998).

Lopez-Mascaraque, L. & de Castro, F. The olfactory bulb as an independent developmental domain. *Cell Death Differ* **9**, 1279-86 (2002).

Mallamaci, A. et al. EMX2 protein in the developing mouse brain and olfactory area. *Mech Dev* **77**, 165-72 (1998).

Mallamaci, A. & Stoykova, A. Gene networks controlling early cerebral cortex arealization. *Eur J Neurosci* **23**, 847-56 (2006).

Marin, O. & Rubenstein, J. L. Cell migration in the forebrain. *Annu Rev Neurosci* **26**, 441-83 (2003).

Martynoga, B., Morrison, H., Price, D. J. & Mason, J. O. Foxg1 is required for specification of ventral telencephalon and region-specific regulation of dorsal telencephalic precursor proliferation and apoptosis. *Dev Biol* **283**, 113-27 (2005).

Molnar, Z. et al. Comparative aspects of cerebral cortical development. *Eur J Neurosci* **23**, 921-34 (2006).

Monuki, E. S., Porter, F. D. & Walsh, C. A. Patterning of the dorsal telencephalon and cerebral cortex by a roof plate-Lhx2 pathway. *Neuron* **32**, 591-604 (2001).

Moorman, A. F., De Boer, P. A., Vermeulen, J. L. & Lamers, W. H. Practical aspects of radio-isotopic in situ hybridization on RNA. *Histochem J* **25**, 251-66 (1993).

Müller, W.A. und Hassel, M., Entwicklungsbiologie und Reproduktionsbiologie von Mensch und Tier. *Springer Verlag Berlin, Heidelberg*, **2. Auflage** (2002).

Muzio, L. et al. Conversion of cerebral cortex into basal ganglia in Emx2(-/-) Pax6(Sey/Sey) double-mutant mice. *Nat Neurosci* **5**, 737-45 (2002a).

Muzio, L. et al. Emx2 and Pax6 control regionalization of the pre-neuronogenic cortical primordium. *Cereb Cortex* **12**, 129-39 (2002b).

Muzio, L. & Mallamaci, A. Foxg1 confines Cajal-Retzius neuronogenesis and hippocampal morphogenesis to the dorsomedial pallium. *J Neurosci* **25**, 4435-41 (2005a).

Muzio, L., Soria, J. M., Pannese, M., Piccolo, S. & Mallamaci, A. A mutually stimulating loop involving emx2 and canonical wnt signalling specifically promotes expansion of occipital cortex and hippocampus. *Cereb Cortex* **15**, 2021-8 (2005b).

Nakagawa, Y., Johnson, J. E. & O'Leary, D. D. Graded and areal expression patterns of regulatory genes and cadherins in embryonic neocortex independent of thalamocortical input. *J Neurosci* **19**, 10877-85 (1999).

Nakamura, M., Runko, A. P. & Sagerstrom, C. G. A novel subfamily of zinc finger genes involved in embryonic development. *J Cell Biochem* **93**, 887-95 (2004).

Nieto, M. et al. Expression of Cux-1 and Cux-2 in the subventricular zone and upper layers II-IV of the cerebral cortex. *J Comp Neurol* **479**, 168-80 (2004).

Noctor, S. C., Martinez-Cerdeno, V., Ivic, L. & Kriegstein, A. R. Cortical neurons arise in symmetric and asymmetric division zones and migrate through specific phases. *Nat Neurosci* **7**, 136-44 (2004).

O'Leary, D. D. & Nakagawa, Y. Patterning centers, regulatory genes and extrinsic mechanisms controlling arealization of the neocortex. *Curr Opin Neurobiol* **12**, 14-25 (2002).

Panganiban, G. & Rubenstein, J. L. Developmental functions of the Distal-less/Dlx homeobox genes. *Development* **129**, 4371-86 (2002).

Parras, C. M. et al. Divergent functions of the proneural genes Mash1 and Ngn2 in the specification of neuronal subtype identity. *Genes Dev* **16**, 324-38 (2002).

Pellegrini, M., Mansouri, A., Simeone, A., Boncinelli, E. & Gruss, P. Dentate gyrus formation requires Emx2. *Development* **122**, 3893-8 (1996).

Putz, U., Harwell, C. & Nedivi, E. Soluble CPG15 expressed during early development rescues cortical progenitors from apoptosis. *Nat Neurosci* **8**, 322-31 (2005).

Rakic, S., Davis, C., Molnar, Z., Nikolic, M. & Parnavelas, J. G. Role of p35/Cdk5 in preplate splitting in the developing cerebral cortex. *Cereb Cortex* **16 Suppl 1**, i35-45 (2006).

Reichert, H. Conserved genetic mechanisms for embryonic brain patterning. *Int J Dev Biol* **46**, 81-7 (2002).

Rubenstein, J. L., Shimamura, K., Martinez, S. & Puelles, L. Regionalization of the prosencephalic neural plate. *Annu Rev Neurosci* **21**, 445-77 (1998).

Rubenstein, J. L. et al. Genetic control of cortical regionalization and connectivity. *Cereb Cortex* **9**, 524-32 (1999).

Ruest, L. B., Hammer, R. E., Yanagisawa, M. & Clouthier, D. E. Dlx5/6-enhancer directed expression of Cre recombinase in the pharyngeal arches and brain. *Genesis* **37**, 188-94 (2003).

Scardigli, R., Baumer, N., Gruss, P., Guillemot, F. & Le Roux, I. Direct and concentration-dependent regulation of the proneural gene Neurogenin2 by Pax6. *Development* **130**, 3269-81 (2003).

Schock, F., Purnell, B. A., Wimmer, E. A. & Jackle, H. Common and diverged functions of the Drosophila gene pair D-Sp1 and buttonhead. *Mech Dev* **89**, 125-32 (1999).

Schock, F. et al. Phenotypic suppression of empty spiracles is prevented by buttonhead. *Nature* **405**, 351-4 (2000).

Schuurmans, C. et al. Sequential phases of cortical specification involve Neurogenin-dependent and -independent pathways. *Embo J* **23**, 2892-902 (2004).

Shen, Q. et al. The timing of cortical neurogenesis is encoded within lineages of individual progenitor cells. *Nat Neurosci* **9**, 743-51 (2006).

Shimogori, T., Banuchi, V., Ng, H. Y., Strauss, J. B. & Grove, E. A. Embryonic signaling centers expressing BMP, WNT and FGF proteins interact to pattern the cerebral cortex. *Development* **131**, 5639-47 (2004).

Shinozaki, K. et al. Absence of Cajal-Retzius cells and subplate neurons associated with defects of tangential cell migration from ganglionic eminence in Emx1/2 double mutant cerebral cortex. *Development* **129**, 3479-92 (2002).

Shou, J., Rim, P. C. & Calof, A. L. BMPs inhibit neurogenesis by a mechanism involving degradation of a transcription factor. *Nat Neurosci* **2**, 339-45 (1999).

Smith, K. M. et al. Midline radial glia translocation and corpus callosum formation require FGF signaling. *Nat Neurosci* **9**, 787-97 (2006).

Soriano, P. Generalized lacZ expression with the ROSA26 Cre reporter strain. *Nat Genet* **21**, 70-71. (1999).

Storm, E. E. et al. Dose-dependent functions of Fgf8 in regulating telencephalic patterning centers. *Development* **133**, 1831-44 (2006).

Stoykova, A., Hatano, O., Gruss, P. & Gotz, M. Increase in reelin-positive cells in the marginal zone of Pax6 mutant mouse cortex. *Cereb Cortex* **13**, 560-71 (2003).

St-Onge, L., Sosa-Pineda, B., Chowdhury, K., Mansouri, A. & Gruss, P. Pax6 is required for differentiation of glucagon-producing alpha-cells in mouse pancreas. *Nature* **387**, 406-9 (1997).

Sur, M. & Rubenstein, J. L. Patterning and plasticity of the cerebral cortex. *Science* **310**, 805-10 (2005).

Sussel, L., Marin, O., Kimura, S. & Rubenstein, J. L. Loss of Nkx2.1 homeobox gene function results in a ventral to dorsal molecular respecification within the basal telencephalon: evidence for a transformation of the pallidum into the striatum. *Development* **126**, 3359-70 (1999).

Tarabykin, V., Stoykova, A., Usman, N. & Gruss, P. Cortical upper layer neurons derive from the subventricular zone as indicated by Svet1 gene expression. *Development* **128**, 1983-93 (2001).

Theil, T., Aydin, S., Koch, S., Grotewold, L. & Ruther, U. Wnt and Bmp signalling cooperatively regulate graded Emx2 expression in the dorsal telencephalon. *Development* **129**, 3045-54 (2002).

Theil, T. Gli3 is required for the specification and differentiation of preplate neurons. *Dev Biol* **286**, 559-71 (2005).

Tissir, F. & Goffinet, A. M. Reelin and brain development. *Nat Rev Neurosci* **4**, 496-505 (2003).

Tole, S., Gutin, G., Bhatnagar, L., Remedios, R. & Hebert, J. M. Development of midline cell types and commissural axon tracts requires Fgfr1 in the cerebrum. *Dev Biol* **289**, 141-51 (2006).

Toresson, H., Potter, S. S. & Campbell, K. Genetic control of dorsal-ventral identity in the telencephalon: opposing roles for Pax6 and Gsh2. *Development* **127**, 4361-71 (2000).

Treichel, D., Schock, F., Jackle, H., Gruss, P. & Mansouri, A. mBtd is required to maintain signaling during murine limb development. *Genes Dev* **17**, 2630-5 (2003).

Treichel, D. Isolierung, evolutive Einordnung und funktionelle Charakterisierung von Knopfkopf, einem Buttonhead-Ortholog in der Maus. *Dissertation Julius-Maximilian-Universität Würzburg*. (2003).

Veraksa, A., Del Campo, M. & McGinnis, W. Developmental patterning genes and their conserved functions: from model organisms to humans. *Mol Genet Metab* **69**, 85-100 (2000).

Vincent, A., Blankenship, J. T. & Wieschaus, E. Integration of the head and trunk segmentation systems controls cephalic furrow formation in Drosophila. *Development* **124**, 3747-54 (1997).

Waclaw, R. R. et al. The zinc finger transcription factor Sp8 regulates the generation and diversity of olfactory bulb interneurons. *Neuron* **49**, 503-16 (2006).

Wang, X., Gao, C. & Norgren, R. B., Jr. Cellular interactions in the development of the olfactory system: an ablation and homotypic transplantation analysis. *J Neurobiol* **49**, 29-39 (2001).

Wilkinson, D. G. & Nieto, M. A. Detection of messenger RNA by in situ hybridization to tissue sections and whole mounts. *Methods Enzymol* **225**, 361-73 (1993).

Wimmer, E. A., Jackle, H., Pfeifle, C. & Cohen, S. M. A Drosophila homologue of human Sp1 is a head-specific segmentation gene. *Nature* **366**, 690-4 (1993).

Wimmer, E. A., Simpson-Brose, M., Cohen, S. M., Desplan, C. & Jackle, H. Trans- and cis-acting requirements for blastodermal expression of the head gap gene buttonhead. *Mech Dev* **53**, 235-45 (1995).

Xie, Y. et al. Influence of the embryonic preplate on the organization of the cerebral cortex: a targeted ablation model. *J Neurosci* **22**, 8981-91 (2002).

Xu, Q., Wonders, C. P. & Anderson, S. A. Sonic hedgehog maintains the identity of cortical interneuron progenitors in the ventral telencephalon. *Development* **132**, 4987-98 (2005).

Yoshihara, S., Omichi, K., Yanazawa, M., Kitamura, K. & Yoshihara, Y. Arx homeobox gene is essential for development of mouse olfactory system. *Development* **132**, 751-62 (2005).

Younossi-Hartenstein, A. et al. Control of early neurogenesis of the Drosophila brain by the head gap genes tll, otd, ems, and btd. *Dev Biol* **182**, 270-83 (1997).

Yun, K., Garel, S., Fischman, S. & Rubenstein, J. L. Patterning of the lateral ganglionic eminence by the Gsh1 and Gsh2 homeobox genes regulates striatal and olfactory bulb histogenesis and the growth of axons through the basal ganglia. *J Comp Neurol* **461**, 151-65 (2003).

Zaki, P. A., Quinn, J. C. & Price, D. J. Mouse models of telencephalic development. *Curr Opin Genet Dev* **13**, 423-37 (2003).

Zhou, C., Tsai, S. Y. & Tsai, M. J. COUP-TFI: an intrinsic factor for early regionalization of the neocortex. *Genes Dev* **15**, 2054-9 (2001).

Zimmer, C., Tiveron, M. C., Bodmer, R. & Cremer, H. Dynamics of Cux2 expression suggests that an early pool of SVZ precursors is fated to become upper cortical layer neurons. *Cereb Cortex* **14**, 1408-20 (2004).

7 ABBREVATIONS

ACX	Archicortex
AER	Apical Ectodermal Ridge
ANR	Anterior Neural Ridge
BMP	Bone Morphogenetic Protein
BrdU	5´-Bromo-2´-Deoxyuridine
btd	Buttonhead
CC	Corpus Callosum
cDNA	Complementary DNA
CGE	Caudal Ganglionic Eminence
CH, HEM	Cortical Hem
cKO	Foxg1-Cre-driven Sp8 mutant
CNS	Central Nervous System
CP	Cortical Plate
CP, ChP	Choroid Plexus
cpm	Counts Per Minute
CSB	Cortico-striatal Boundary (also PSB)
CTX	Cerebral Cortex
CX	Cortex
DAPI	4',6-Diamidino-2-Phenylindole Dihydrochloride
DEPC	Diethyl Pyrocarbonate
DI	Diencephalon
DIG	Digoxygenin
DiI	1,1'-Dioctadecyl-3,3,3',3'-Tetramethyl-indocarbocyanine Perchlorate
DiO	3,3'-dioctadecyloxacarbocyanine-perchlorate
dLGE	Dorsal Lateral Ganglionic Eminence
dLGN	Dorsal Lateral Geniculate Nucleus
DNA	Desoxy Nucleic Acid
dNTP	Desoxy-ribonukleoside triphosphate
DP	Dorsal Pallium
dRET	Dorsal Retina
DT	Dorsal Thalamus
dTEL	Dorsal Telencephalon
DTT	Dithiothreitol
E	Embryonic Day
EDTA	Ethylen Diamine Tetra-acetate
Emx	Empty Spiracles genes
EPL	External Plexiform Layer of OB
FB	Forebrain
FCS	Fetal Calf Serum
FGF	Fibroblast Growth Factor
Fig.	Figure
FL	Forelimb
GC	Ganglionic Cell Layer of OB
GFAP	Glia Fibrillary Acidic Protein
GFP	Green Fluorescent Protein
H2O	Water
HC	Hippocampus
HT	Hypothalamus
IdU	5´-Iodo-2´-Deoxyuridine
IPC	Intermediate Progeinotor Cell
IPL	Internal Plexiform Layer of OB
ISH	*In Situ* Hybridization
IZ	Intermediate Zone
KO	Knockout
LacZ	ß-Galactosidase
LGE	Lateral Ganglionic Eminence
LP	Lateral Pallium
LT	Lamina Terminalis
M, MB	Midbrain
M1	Primary Motor Cortex
mBtd	Mouse-Buttonhead
MC	Mitral Cell Layer of OB
MGE	Medial Ganglionic Eminence
MHB	Midbrain-Hindbrain Boundary
min.	Minutes
MNP	Medial Nasal Process
MP	Medial Pallium
M-phase	Mitotic Phase of cell cycle

mPSB	Medial Pallial-Subpallial Boundary
MZ	Marginal Zone
NCX	Neocortex
Ngn	Neurogenin
OB	Olfactory Bulb
OBLS	Olfactory Bulb-Like Structure
OC	Optic Chiasm
OE	Olfactory Epithelium
ON	Overnight
ON	Olfactoty Nerve
ONL	Olfactory Nerve Layer of OB
OP	Olfactory Placode
OSN(s)	Olfactory Sensory Neurons(s)
OTV	Otic Vesicle
Otx	Orthodentricle genes
OV	Optic Vesicle
P	Postnatal Day
Pax	Paired-Box Genes
PB(s)	Probst Bundle(s)
PBS	Phosphate Buffered Saline
PCR	Polymerase Chain Reaction
PCX	Paleocortex
PFA	Paraform aldehyde
PG	Periglomerular Layer of OB
PN	Postmitotic Neuron
POA	Preoptic Area
PPL	Preplate
Prop-Iod.	Propidium Iodide
PSB	Lateral Pallial-Subpallial Boundary
RG	Radial Glia
RGC	Radial Glia Cell
RMS	Rostral Migratory Stream
RNA	Ribo Nucleic Acid
rpm	Rounds per minute
RT	Room Temperature
RT-PCR	Reverse Transcription PCR
S1	Primary Somatosensory Cortex
SDS	Sodium Dodecyl sulfate
SE	Septum
SHH	Sonic Hedgehog
SP	Subplate
S-phase	Synthesis Phase of cell cycle
SSC	Sodium-Sodium citrate solution
SVZ	Subventricular Zone
TE	Tris-EDTA
TH	Thalamus
UV	Ultra-Violet
V1	Primary Visual Cortex
VNO	Vomeronasal Organ
VP	Ventroposterior Complex
vTEL	Ventral Telencephalon
VZ	Ventricular Zone
WMISH	Whole Mount *In Situ* Hybridization
WT	Wildtype
X-Gal	5-Brom-4-Chlor-3-Indoxyl-ß-D-Galactopyranoside

8 APPENDIX

8.1 Index of Figures and Tables

9 ACKNOWLEDGEMENT

Mein herzlichster Dank gilt im Besonderen:

Hans-Henning Arnold für die Übernahme der Betreuung meiner Arbeit als Mentor an der Technischen Universität zu Braunschweig.

Martin Korte für den Vorsitz und die Leitung meiner Prüfungskommission an der Technischen Universität zu Braunschweig.

Ahmed Mansouri für das Projekt meiner Doktorarbeit und sein Vertrauen, mich in der Arbeitsgruppe zu integrieren. Darüber hinaus danke ich ihm für die tägliche Unterstützung und spontane Hilfe bei meiner Arbeit sowie dafür, dass er mir/uns das richtige Maß aus Selbstständigkeit und Zusammenarbeit in der Gruppe gelehrt und ermöglicht hat.

Anastassia Stoykova für sehr viel in mein Projekt und meine Ausbildung investierte Zeit und Geduld und dafür, dass ich dadurch so enorm viel dazulernen konnte.

Gundula H Griesel für ein enormes Stück professionelle Zusammenarbeit und darüber hinaus entstandene Freundschaft.

Jens Krull und Patrick Collombat für unendlich viel Hilfe und Unterstützung bei jedem Problemchen im täglichen Laboralltag.

Der Abteilung Molekulare Zellbiologie, besonders aber Boyka, Friederike, Geli, Gundi, Katha, Manuela, Sabine und Michael für eine sehr schöne Zeit, nette Unterhaltungen in der raren Pausenzeit und dafür, dass alles so ist wie es ist.

Julianna Butler und Tanja Vogel für das kritische Lesen der Arbeit und den daraus entstandenen Verfeinerungen dieser Schrift.

Alexandra Driehorst, Heike Fett, Ulrike Teichmann und Christian Dietl sowie dem Rest des BTL-Teams für hervorragende und sehr zuverlässige Arbeit und Hilfe im Maushaus.

Peter Gruss für die Möglichkeit, diese Arbeit in seiner Abteilung anfertigen zu dürfen.

Maike, Nina, Rieke und Thomas für wertvolle Freundschaft und die großartige Atmosphäre in der WG, aber auch für das Verständnis und die Hilfe besonders an schwierigeren Tagen der vergangenen Zeit.

Inge, Juli, Julia, Katha, Alexander, Boris und Rainer für die nötige Ablenkung und neue Energie durch nette Abendgestaltungen und Verständnis für meine chronischen Verspätungen.

Anja für mein Entdecken der besseren Hälfte aller Dinge.

Meinen Geschwistern Bettina, Mark und Stephan, weil sie für mich sehr wichtig sind und vieles ohne sie recht langweilig und undenkbar wäre.

Meinen Eltern Ursula und Heinz-Dieter, die mir mein Studium und meinen bisherigen Lebensweg erst ermöglicht haben. Zudem ganz besonders für die Anleitung, Unterstützung und Rückendeckung in allen Phasen meines bisherigen Lebens.

…vielen Dank!

10 CURRICULUM VITAE

Personal data:

Name:	Andreas Zembrzycki
Date and place of birth:	22nd of April 1978, Gelsenkirchen, Germany

School:

August 1988 – July 1997	Hüffertgymnasium-Warburg, Warburg, Germany, Grade: Allgemeine Hochschulreife (general qualification for university entrance)
August 1984 – July 1988	Primary school Liebenau, Germany

Scientific education:

January 2004 – April 2007	**PhD thesis:** Max-Planck-Institute of Biophysical Chemistry, Goettingen, Germany; Department of Molecular Cell Biology; Peter Gruss, Prof. Dr. Research group Molecular Cell Differentiation; Ahmed Mansouri, Prof. Dr. Thesis Title: “Dissection of the molecular function of the transcription Factor Sp8 during development of the murine telencephalon and olfactory system.”
January 2003 - December 2003	**Diploma thesis:** Max-Planck-Institute of Biophysical Chemistry, Goettingen, Germany; Department of Molecular Cell Biology; Peter Gruss, Prof. Dr. Research group Molecular Cell Differentiation; Ahmed Mansouri, Prof. Dr. Thesis Title: “Funktionelle Analyse des Pax7 Gens im Mittelhirn der Maus”
November 2000 - December 2003	**Undergraduate student:** Georg-August-University Goettingen, Goettingen, Germany Major: Zoology Minors: Microbiology, Pharmacology & Toxicology Grade: Diplom Biologe (Diploma Biologist)
November 1998 - October 2000	**Undergraduate student:** University of Kassel, Kassel, Germany

Publications:

3. **Zembrzycki A.**, Griesel, G., Stoykova, A. and Mansouri, A. (2007). Genetic interplay between the transcription factors Sp8 and Emx2 in the patterning of the forebrain. *Neural Development* 2007, **2**:8.

2. Griesel, G., Treichel, D., Collombat, P., Krull, J., **Zembrzycki A.**, van den Akker, WM., Gruss, P., Simeone, A. and Mansouri, A. (2006). Sp8 controls the anteroposterior patterning at the midbrain-hindbrain border. *Development* **133**, 1779-1787.

1. **Zembrzycki, A.** (2004). Funktionelle Analyse des Pax7 Gens im Mittelhirn der Maus. *Diploma thesis.*